KINETO-ELASTODYNAMIC ANALYSIS OF HIGH-SPEED MECHANISMS

By
PRABIR KUMAR NATH

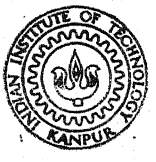

DEPARTMENT OF MECHANICAL ENGINEERING
INDIAN INSTITUTE OF TECHNOLOGY KANPUR

MARCH, 1976

KINETO-ELASTODYNAMIC ANALYSIS OF HIGH-SPEED MECHANISMS

A Thesis Submitted
in partial Fulfilment of the Requirements
for the Degree of
DOCTOR OF PHILOSOPHY

By
PRABIR KUMAR NATH

to the

DEPARTMENT OF MECHANICAL ENGINEERING
INDIAN INSTITUTE OF TECHNOLOGY KANPUR

MARCH, 1976

ME-1976-D-NAT-KIN

To

My Parents

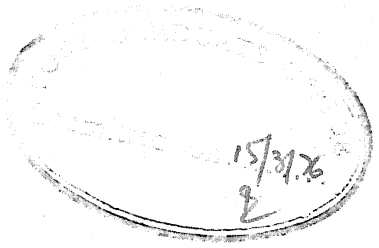

CERTIFICATE

Certified that this work entitled KINETO-ELASTODYNAMIC ANALYSIS OF HIGH-SPEED MECHANISMS has been carried out by Shri Prabir Kumar Nath under my supervision and has not been submitted elsewhere for a degree.

March, 1976

(A. Ghosh)
Professor
Department of Mechanical Engineering
Indian Institute of Technology,
Kanpur.

ACKNOWLEDGEMENT

I acknowledge my great indebtedness to Professor Amitabha Ghosh, an excellent thesis advisor, for his able guidance, help and encouragement in all phases of preparation of this thesis. It was Dr. Ghosh who first introduced to me this fascinating field of research first through a course and then by suggesting the problem for further study. I can not adequately express my deep sense of gratitude for the tender and friendly attitude of Dr. Ghosh which often surpassed his role as a guide.

I take this opportunity to thank Drs. G.N. Sandor, I. Imam and T. Yamamoto for promptly sending the reprints of their papers.

I wish to acknowledge the help from Drs. M. Hariharan and C.P. Vendon of Civil Engineering Department, I.I.T. Kanpur in drawing my attention to some important references.

I also wish to extend my appreciation to Dr. B. Sen, Principal of Jalpaiguri Government Engineering College for kindly granting a leave of absence from my teaching responsibilities.

To Professors V.K. Stokes, J. Chakraborty, A. Mallik, R. Rajagopalan, P.K. Nandi, D. Sengupta and C.P. Reddy go special thanks for their interest in my research work and its early completion.

Thanks are due to Mr. R.N. Srivastava who skillfully typed from an untidy manuscript.

Finally, I must extend my thanks to Mrs. Meena Ghosh who smilingly tolerated my lengthy consultations with Dr. Ghosh even in the late evenings.

TABLE OF CONTENTS

CHAPTER		Page
	LIST OF FIGURES	
	LIST OF IMPORTANT SYMBOLS	
	SYNOPSIS	
I	INTRODUCTION	1
	1.1 Review of Past Works	3
	1.1.1 Deflection analysis	3
	1.1.2 Input torque analysis	10
	1.1.3 Harmonic analysis	12
	1.1.4 Stress analysis	14
	1.1.5 Stability analysis	15
	1.2 Objective of the Present Work	18
II	DEFLECTION AND STRESS ANALYSIS	23
	2.1 Introduction	23
	2.2 Statement of the Problem	24
	2.3 Element Analysis	27
	2.4 Assembly of Element Matrices	37
	2.5 System Analysis	43
	2.5.1 Derivation of the transformation matrix	43
	2.5.2 Elimination of the rigid body degrees of freedom	46
	2.5.3 Variable input forces	49
	2.5.4 Solutions of equations	50
	2.6 Input Forces for Different Conditions	56
	2.6.1 Input forces for 'dynamic' equilibrium	56
	2.6.2 Input forces supplied by motors	58
	2.7 Harmonic Analysis of Rigid Body Forces	65
	2.8 Stress Analysis	75
	2.9 Rigid Body Analysis	80
	2.9.1 Displacement analysis	80
	2.9.2 Velocity and acceleration analysis	85
	2.9.3 Quasi-static analysis	87

CHAPTER		Page
III	DYNAMICS OF AXIALLY LOADED MOVING LINKS	92
	3.1 Introduction	92
	3.2 Derivation of the Equation of Motion	94
	3.3 Solution of Equation of Motion	110
	3.4 Elastic Axial Forces	120
IV	DIRECT STEADY STATE ANALYSIS	124
	4.1 Introduction	124
	4.2 Equations of Motion	126
	4.2.1 Element analysis	126
	4.2.2 Assembly of elements	128
	4.2.3 Constraint equations	132
	4.2.4 Displacements expressed in harmonics	136
	4.3 Displacement and Stress Analysis	140
	4.4 Stability Analysis	144
V	RESULTS AND DISCUSSIONS	151
	5.1 Introduction	151
	5.2 Basic Analysis	153
	5.3 Effects of the Dynamic Factors	164
	5.4 Direct Steady State Solution	179
VI	CONCLUSIONS	192
	REFERENCES	195
Appendix - A.	Description of Computer Programs	203
Appendix - B.	Explicit Expressions of the Element Matrices	212
Appendix - C.	Direct Calculation of the Transformation Matrix	216
Appendix - D.	Rigid Body Analysis	225
Appendix - E.	Expressions for Harmonic Analysis and Constraint Equations	233
Appendix - F.	Solution of Large Eigenvalue Problems	240

LIST OF FIGURES

Figure		Page
2.1	Steps of displacement analysis	26
2.2	Element co-ordinates	28
2.3	System co-ordinates	38
2.4	Restrained structure	77
3.1	Axially loaded moving element	95
3.2	Moving co-ordinate system	96
3.3	Rigid body axial forces	104
4.1	Element oriented system co-ordinates	130
5.1	Follower stress of 'mechanism' and 'structure'	155
5.2	Effect of division on follower stress	156
5.3	Effect of division on coupler stress	157
5.4	Crank and rocker torque	159
5.5a	Effect of crank-shaft inertia on crank displacement	160
5.5b	Effect of crank-shaft inertia on follower stress	161
5.6	Variation of the first natural frequency	163
5.7	Relative magnitudes of σ_I, σ_{II} and σ_{III}	165
5.8	Effect of rigid body axial force on follower stress : 1200 RPM	167
5.9	Effect of rigid body axial force on follower stress : 2400 RPM	168
5.10	Coupler stress for cases 'A', 'B' and 'D'	169

Figure		Page
5.11	Effect of dynamic factors at 600 RPM	170
5.12	Effect of dynamic factors at 1200 RPM	171
5.13	Effect of dynamic factors at 2400 RPM	172
5.14	Variation of coupler stress with crank speed case 'A'	174
5.15	Variation of follower stress with crank speed case 'A'	175
5.16	Variation of coupler stress with crank speed case 'D'	176
5.17	Variation of follower stress with crank speed case 'B'	177
5.18	Connecting rod deflection cases 'B' and 'C'	178
5.19	Deflection of a point on the connecting rod case 'A'	180
5.20	Steady state crank stress of mechanism 3	182
5.21	Steady state coupler stress for 'mechanism' and 'structure'	183
5.22	Steady state follower stress for 'mechanism' and 'structure'	184
5.23	Steady state deflection of the connecting rod	185
5.24	Connecting rod deflection for various speeds	187
5.25	Frequency response of mechanism 2	189
5.26	Phase shift for various crank speeds	190
C-1	Slider crank mechanism	217
C-2	Crank-rocker mechanism	221
D-1	Forces in a slider crank mechanism	227
D-2	Forces in a crank-rocker mechanism	230

List of Important Symbols

A - area of the cross-section of an element

A_{Mx} - absolute acceleration at the left end of an element in its axial direction

A_{My} - absolute acceleration at the left end of an element in its transverse direction

A_{Nx} - absolute acceleration at the right end of an element in its axial direction

A_{Ny} - absolute acceleration at the right end of an element in its transverse direction

A_s - effective shear area of the cross-section of an element

B - body force vector due to the distributed inertia forces within an element

C - damping matrix of the system

E - Young's modulus of elasticity

E' - a representative element

F_x - axial force at a distance x from the left end of an element

G - shear modulus of elasticity

I - second moment of area of the cross-section. Also identity matrix

K - elastic stiffness matrix of the system

K^G - geometric stiffness matrix of the system

M - mass matrix of the system

P - force vector of the system

$\overline{Q}$ - element force vector due to the external forces acting at the nodes

R - rotation matrix

T - rigid body displacement transformation matrix

U - displacement vector of the system

$\dot{U}$ - velocity vector of the system

$\ddot{U}$ - acceleration vector of the system

U^o - initial displacement vector of the system

$\dot{U}^o$ - initial velocity vector of the system

W_f - work function

X - X-axis of the system co-ordinates. Also a general vector

Y - Y-axis of the system co-ordinates

a - shape function of an element

a_1 - first row of the matrix a

a_2 - second row of the matrix a

b - element strain matrix

b_1 - first row of the matrix b

b_2 - second row of the matrix b

e - internal strain vector of an element

e_{xx}, e_1 - normal strain at any point within an element

e_{xy}, e_2 - shear strain at any point within an element

$h_1 - h_3$ - total number of sine (cosine) terms in a harmonic series

k^G - element geometric stiffness matrix

$\bar{k}$ - element oriented element stiffness matrix

$\hat{k}$ - system oriented element stiffness matrix

l - length of an element

m - total number of elastic modes

$\bar{m}^a$ - additional mass matrix

$\bar{m}$ - element oriented element mass matrix

$\hat{m}$ - system oriented element mass matrix

n - total number of constrained co-ordinates of the system

p_e - equivalent element force vector due to the external forces acting within the element

$\bar{p}$ - element oriented element force vector due to the rigid body inertia forces

$\bar{p}_T$ - element oriented total element force vector

$\bar{p}^a$ - additional element oriented element force vector due to the angular acceleration of the element

$\hat{p}$ - system oriented element force vector

u - internal displacement vector in the element oriented element co-ordinate system

u_x - component of u in the x-direction

u_y - component of u in the y-direction

u_x^b - component of u_x due to the transverse forces

u_x^a - component of u_x due to the axial forces

$\bar{u}$ - element oriented element displacement vector

$\bar{u}_1 - \bar{u}_6$ - elements of $\bar{u}$

$\hat{u}$ - system oriented element displacement vector

$\dot{\hat{u}}^o$ - initial velocity vector in the system oriented element co-ordinates

v - volume of an element

w - total number of the rigid body degrees of freedom

x - x-axis of the element co-ordinates of an element along its axis

y - y-axis of the element co-ordinates of an element along its transverse direction

$\Delta\tau$ - prescribed interval of time

$\sum$ - summation symbol

Φ - modal matrix (corresponding to elastic modes)

Ψ - modal matrix corresponding to the rigid body modes

Ω^2 - spectral matrix

$\alpha_{E'}$ - absolute angular acceleration of the element E'

$\frac{\partial}{\partial x}$ - partial derivative with respect to x

δ - small variation

ζ - non-dimensionalised y-co-ordinate

η - displacement vector in the normal co-ordinate system

θ_i - angle made by the i-th link with the X-axis

$\theta_{E'}$ - angle made by the element E' with the X-axis of the system

λ - displacement vector in the normal co-ordinates for rigid body modes

ξ - non-dimensionalized x-co-ordinate

ξ_i - damping ratio corresponding to the i-th normal mode

ρ - density of the material

σ - internal stress vector of an element

σ_{xx}, σ_1 - normal stress at any point within an element

σ_{xy}, σ_2 - shear stress at any point within an element

τ - time

ϕ - a factor to account for the shear effect

χ - a matrix relating the strains of an element with its stresses

ω - natural frequency of the system

$\{\ \}$ - column vector

$[\ ]$ - matrix (or vector)

Subscripts

A - independent system co-ordinates

B - dependent system co-ordinates

X - relating to X-co-ordinate of the system

Y - relating to Y-co-ordinate of the system

i - i-th element of a vector or matrix

j - j-th element of a vector or matrix

ij - an element corresponding to the i-th row and j-th column of a matrix

x - relating to x-co-ordinate of the element E'

y - relating to y-co-ordinate of the element E'

Superscripts

a - relating to the additional acceleration terms

g - generalised co-ordinate system

t - transpose of a matrix

*	- transformed co-ordinate system
-	- element oriented element co-ordinate system when used over a small letter vector or matrix
-	- normal co-ordinate system when used over a capital letter vector or matrix
~	- system oriented element co-ordinate system
o	- corresponding to initial time
$(\dot{})$	- differentiation with respect to time
$(\ddot{})$	- two times differentiation with respect to time

CHAPTER I

INTRODUCTION

Satisfactory performance of the machines can be ensured only through rigorous and accurate analysis and synthesis of mechanisms involved in the system. Improper design of mechanisms may lead to loss of accuracy and also eventual failure of its members. Under normal circumstances, the analysis and synthesis of the mechanisms are done without considering the finite rigidity of the members and the problem is mainly geometric. However, in many cases the design of the members also involves the consideration of the static and dynamic forces acting on the mechanism. When the speed of operation is low, the dynamic forces play a relatively insignificant role. But as the speed of the mechanism increases, the accelerations of the different members of the mechanism and consequently the dynamic forces increase. For sufficiently large speeds, the dynamic forces may play even the predominant role. Under such circumstances, the members are designed from the consideration of the stresses developed due to the dynamic and static forces. The usual practice, until recently, had been to consider the links to be absolutely rigid. This is acceptable so long as the accuracy required in the

relationship between the input and the output is not very high. Apart from this, in high speed mechanisms, the chances of the mechanism being subjected to resonant condition is quite high. In the last decade, machines comprising of high speed mechanisms have been developed to meet the demand of the industry. Moreover, the accuracy requirement of such machines is also having an increasing trend. The elastic displacements, which are the consequences of increased speeds and loads, may cause inaccuracies of position in addition to noise and fatigue. For such cases, the usual design procedures for the mechanism may not yield satisfactory results.

In view of the above facts, the research work in the field of analysis and design of the mechanisms with flexible members is gaining momentum. Already a considerable amount of work in this area has been published. Nevertheless, the extent of research in this field is far from complete and enough scope is present to solve a number of challenging problems.

Introduction of the flexibility of the links complicates the analysis and synthesis of the mechanisms considerably. Analytical treatment of such problems leads to a number of extremely complicated differential equations solution of which, even by numerical methods, requires very

simplifying assumptions. To overcome such difficulties, a number of numerical methods have been proposed by different workers. However, such methods have neglected many important dynamical effects whose contributions may be significant. Therefore it has become necessary to assess the magnitudes of these effects. Moreover, efforts should be made to evolve new techniques to solve such problems with reduced computer time without detoriating the accuracy level. Apart from these, a mechanism with elastic members should be also studied to investigate the stability of the system.

Before starting with the main body of the thesis, it is pertinent to review the extent of research published to date in the fields of the flexible mechanisms studied in the present work. A survey of these investigations (and many others also) is carried out in the two excellent review papers[1,2] published a few years ago. In the next section only the important ones with recent origin are reviewed briefly.

1.1 Review of Past Works

1.1.1 Deflection analysis

In 1965, Kozsevnyikov[3] reported on the flexural vibrations of an elastic coupler of a slider-crank mechanism considering only the effect of the transverse accelerations.

Neubauer, Cohen and Hall[4], in the analysis of the same mechanism, considered the effect of a constant axial force derived from the rigid body analysis. Viscomi and Ayre[5] contributed several improvements on the analysis of the same mechanism. The authors include the Coriolis components of acceleration as well as the additional relative normal and tangential components of accelerations arising from the transverse vibrations of the coupler in an acceleration field. The effect of the axial forces due to the rigid-body normal acceleration as well as due to the foreshortening of the coupler is also taken into account. The further simplification of the differential equations excludes all effects of longitudinal vibrations and retains only the first two modes of the transverse vibrations. Jainiski, Lee and Sandor found out both the steady-state axial and transverse deflections in the analysis of the same mechanism without the piston force[6] and with the piston force[7]. But subsequent linearisation of the differential equations neglects the effect of all axial forces on the bending moment of the coupler. Furthermore, the solution method requires that the obliquity ratio must be small enough to allow an asymptotic expansion of the deflections in terms of this ratio. This restricts the validity of the analysis to limited cases only.

Meyer zur Capellen[8] analysed the transverse vibrations of an elastic coupler of a four-bar mechanism which included the effect of the rigid body axial forces only. But the analysis is made simple by equating the periodic terms of the axial forces to zero and the final solution is rather approximate.

Using a lumped mass model, Sadler and Sandor[9] analysed the slider-crank mechanism and also for the case when the coupler has a concentrated mass at the end of its rigid extension. The method of analysis is later extended to a planar four-bar linkage composed of elastic links[10]. The longitudinal deformations resulting from the axial forces and the foreshortening of the links due to bending are neglected. The investigation is confined to the transverse deflections only by employing D' Alembert's principle for each lumped mass and solving the Euler's equation of the elastic curves by finite difference method. The additional relative normal and tangential accelerations are included and the pin forces are calculated from the force and moment balance of each link at their instantaneous positions. In addition to the gross rigid body motions, the analysis takes into account the additional rigid body motions of the coupler and the follower due to elastic deflections of the crank. Because of the assumption of the inextensibility of the links, the effects of the elastic deformations of each

link on the rigid body motions of the other can not be fully studied by their analysis. It is demonstrated through an example that the rigid body motions of the follower due to the elastic motion of the crank is comparable to its elastic motions and should not be neglected.

Winfrey[11,12] first used a finite element model to analyse the longitudinal, transverse and torsional displacements of a general mechanism. Six elastic and three rigid body co-ordinates are defined for each link (planar). This type of modelling of the links increases the size and complexity of the matrices without any corresponding increase in the accuracy of the displacements. Kinematic analysis is performed by adopting the general iterative procedures of Denavit and his group[13,14]. A connectivity matrix is constructed to assemble the element matrices into the system matrices. Since the connectivity matrix is to be constructed for each problem separately, it is seldom preferred to other techniques of assembly available in the finite elemen method. The author directly applies the principle of the conservation of generalised momentum during the free vibra of the mechanism to form a constraint equation for the elimination of the rigid body degrees of freedom. Here again the connectivity matrix and its derivatives are involved in addition to numerous calculations. Upon

utilisation of this constraint equation in a transformation to the generalised co-ordinates, the stiffness matrix is made non-singular and the eigenvalue problem in the transformed co-ordinates is solved by inverting this non-singular matrix. The final transformation of the original equation of motion to the normal co-ordinate system is achieved by using first the constraint equation and next the modal matrix formed after solving the eigenvalue problem. Since the constraint equation is valid for the free vibration only, the extension of its range of applicability to the equation of forced vibration is unwarranted. The equations in the normal co-ordinate system are made uncoupled by assuming the damping as proportional to the mass matrix and solved by Laplace transform method. The final values of the displacements and the velocities found out in the system co-ordinates of the current interval of time are used as the 'initial conditions' for the system co-ordinates of the next interval. This is justified as the system co-ordinates are located at element positions for each interval.

The formation of the system force vector uses the connectivity matrix and its derivatives alongwith the unknown displacements. Thus the equations of the forced vibrations are to be solved by iterative procedures. In an initial analysis, the author finds that the inertia forces due to

the relative accelerations are only 1% of the inertia forces arising from the rigid body accelerations and these terms are dropped out in the subsequent calculations as their retaintion entails intricate calculations within the iteration loop. This finding may not be true in general. Under another assumption, the force vector term is reduced to its final form which does not take into account the variation of the accelerations along the links. The effect of the axial forces on the transverse vibrations of the links is altogether neglected in the above analysis.

Erdman, Sandor and Oakberg[15] analysed mechanisms by the flexibility approach of the finite element method. Starting from the rigid body inertia forces, the deflections are obtained by an iterative procedure. For this purpose, a kineto-elastodynamic stretch rotation operator (KEDSRO) describing the elastic motions of a single point is used. The crank is treated as a cantilever beam thus reducing the mechanism to a structure and a system flexibility matrix is developed. To avoid excessive computations, Taylor series expansions of the matrices are used. These expansions effectively eliminate the deflections due to the elastic inertia forces. Erdman, Imam and Sandor[16] extended the above analysis by using the method of 'dynamic equivalence system' to include the elastic inertia forces. The authors

show that the elastic accelerations, in some cases, can be of the same order of magnitude as the rigid body accelerations.

Imam, Sandor and Kramer[17] used the stiffness approach of the finite element method to analyse the planar flexible mechanisms. The assembly of the element matrices is done by permutation vector method generally reserved for large systems as it generates the system co-ordinates automatically within the program. It does not offer any special advantage because the system co-ordinates are less in number in case of mechanisms. On the other hand, it limits the flexibility of the program to some extent. The force vectors, calculated by multiplying the mass matrix with the negative of the acceleration vector, is assumed to remain constant during each interval. The errors in the force vectors, formed in this way, vary from 5% to 14.3% (in case of a purely rotating link) even at the element level. Furthermore, these force vectors do not take into account the actual distribution of the rigid body inertia forces. The technique of the rate of change of eigenvalues and eigenvectors[18] is employed for the first time in mechanism analysis and the computation time is reduced by a factor of three. However, it appears[17,18] that the number of the eigenvalues to be taken in a mechanism without any intermediate check and the range of the crank angle up to which the technique can be safely applied is yet

inconclusive in the general case. No system co-ordinate is defined corresponding to the element co-ordinate for rotation at the support-end of the crank. This effectively reduces the crank to a cantilever beam and consequently the mechanism to a structure. Though this procedure by-passes the necessity of eliminating the rigid body degree of freedom, it does not analyse the mechanism with its actual boundary conditions.

1.1.2 Input torque analysis

The fluctuation of the input torque due to the variable inertia forces have interested many researchers. But their investigations are mainly confined to the problem of balancing the shaking forces and moments of the rigid link mechanisms[19,20]. The importance of the fluctuation of the speed of a driving induction motor due to the variable moments exerted by a mechanism is first recognised by Habiger[21], Müller[22] and Houben[23-26] in their investigations of the torsional vibrations of the input shaft. It is shown that in some cases the fluctuation of the motor torque may enhance the instability of the system.

In the areas of the planar rigid link mechanisms, Benedict and Tesar[27,28] found out the angular velocity fluctuations by employing the kinematic influence co-efficients and the following three methods: (i) energy

distribution method, (ii) equivalent mass and force method and (iii) rate of change of energy method. The fluctuating input torque can be next found out from the torque-speed characteristics of the driving motor. Erdman, Sandor and Oakberg[15] extended this approach to the flexible mechanisms by including the rate of change of strain energy of the mechanism in the analysis. However, the accurate determination of the rate of change of strain energy involves extensive computations.

Winfrey[11,12] has not incorporated any input torque in the force vector term of the equation of motion. Thus the unbalanced rigid body inertia forces must be balanced by the additional inertia forces due to the subsequent elastic and rigid body accelerations. As the modal matrix does not include any rigid body mode and a constant input speed is assumed, the subsequent rigid body accelerations during each interval are suppressed and the analysis does not represent the actual situation.

Sadler and Sandor[9,10] assume that the input shaft has a large moment of inertia so that the fluctuation of the moment exerted by the mechanism on the input shaft does not affect the constancy of the crank speed and therefore the crank rotates as a cantilever beam. Imam and his colleagues[17] also consider the crank as a cantilever

beam as previously mentioned. This restriction on the crank obviates the necessity of finding out the variable input torque and its contribution towards the displacements of the mechanism. However, the moment at the cantilever-end may be easily found out by further calculations.

1.1.3 Harmonic analysis

The importance of the harmonic analysis of mechanisms is borne out by the fact that it is the most efficient approach to describe the dynamic behaviour of mechanisms and to find out the characteristics of a motion or the shape of the path in a wide range of the mechanism parameters. It also serves as a powerful tool for the synthesis of mechanisms and enables the designer whether the designed mechanism possesses sizable overtones. However, the complexity involved in the harmonic analysis of the general mechanisms has been acting as an impediment to extensive research works in this area as evident from the scarcity of research papers published on this topic. The development of the harmonic analysis started with the planar slider-crank mechanism[29] and with the mechanisms involving slider pairs[30-32]. Freudenstein[33] performed the harmonic analysis of a rigid link four-bar mechanism and proved that the satisfaction of certain requirements by the link lengths leads to optimisation of the transmission angle and

minimisation of the higher harmonics thereby reducing the accelerations, inertia forces, deflections and the dynamic bearing reactions. Following the publication of Freudenstein's work, a few papers have come out on the harmonic analysis of planar mechanisms[34-36], spatial slider-crank mechanisms[37] and spherical four-bar mechanisms[38,39], all assuming the links to be rigid. Sadler and Sandor[40,41] are the only authors who have attempted to extend the harmonic analysis in the area of the flexible mechanisms. The authors utilise[40] the harmonic analysis of a crank-rocker mechanism[33] to find out the steady-state lateral vibrations of a concentrated mass attached to a flexible extension of the coupler. The crank and the rocker are assumed to be rigid; the coupler and its extension are considered massless elastic springs. Though the equation of motion for the longitudinal deflections of the mass is given, it is dropped out in the subsequent analysis by assuming the longitudinal inextensibility of the springs. The governing equation of motion is a non-homogeneous Hill equation in which the periodicity of the stiffness terms results from the changing geometry only. The unknown displacement is expressed as a Fourier series and the steady-state solution is found out by equating the co-efficients on both sides. Bending resonance (in both undamped and damped conditions) of the

concentrated mass is examined by numerical examples for a special case where the coupler is assumed rigid. This work is later extended[41] to include the centrifugal force of the concentrated mass in the analysis. The analysis is very limited in the sense that the links are too much idealised and the stability analysis is not treated at all.

1.1.4 Stress analysis

When a continuum model is used to study the deflections[3-8], the normal and shear stresses within the links can be obtained without much difficulty from the stress-displacement relationships. Since all the authors using continuum model have concerned themselves with the deflections only, it remains to be seen how the stresses, involving the space-derivatives of the displacements, are affected when the actual displacement function is approximated by one or two mode functions.

In the lumped-mass models of the mechanisms[9,10], the stresses are calculated[42] from the bending moments, axial forces and transverse forces, obtained in the course of deflection analysis. Since these procedures make use of the derivatives of the elastic curves, the stresses, thus calculated, may not yield accurate results[43] when the operating speed is high.

In the area of the finite element method applied to mechanisms, Beggs[44] first found out the stresses in a redundant mechanism for the static forces only. Winfrey[12] does not find the stresses but only mentions about the computational difficulties in calculating the stresses from the deflection analysis. Imam, Sandor and Kramer[17] outline a new procedure for calculating the stresses within the links. This procedure assumes that when the mechanism vibrates in any of its normal modes, each link also vibrates (at least approximately) in one of its natural modes. This is not true in general. Moreover, the procedure requires that the deflections of the mechanism should be calculated and transformed back to the element co-ordinates separately for each normal mode thus entailing complexities in the numerical procedure.

1.1.5 Stability analysis

Seevers and Yang[45,46] studied the stability of the elastic coupler of a slider-crank mechanism. The authors calculate the pin forces from the rigid body analysis only and use only the first mode of deflection in the resulting Hill-type equations.

Houben[47-49] first investigated a four-bar mechanism treating all the moving links as elastic. The author develops nine simultaneous partial differential

equations with periodic co-efficients which describe the bending in the mechanism plane as well as perpendicular to it and torsional vibrations but exclude the longitudinal deformations of the links. In the analysis, the author includes some linear terms coming from the relative tangential and normal components of accelerations, the Coriolis component of accelerations and the axial forces obtained from the rigid body analysis. Since the solution of these simultaneous equations is extremely unwieldy, he assumes the driver and driven links to be rigid and, instead of solving the equations for the displacements, he studies the attendant instabilities by numerical methods. With the aid of an analog computer, the first stability zone is determined.

Witfeld[50] investigated the stability and bending resonances of an elastic coupler of a planar four-bar mechanism for various combinations of linkage parameters. Calculating the pin forces from the rigid body analysis, the author finally forms a linear integro-differential equation with the curvature as the independent variable. Using a digital computer, he furnishes the stability and the resonance curves and discusses about the possibility of combination resonances.

Tobias[51] studied the stability of an elastic coupler of a four-bar mechanism by giving small vibratory

motions to the crank about a rigid body position of the mechanism. The mechanism is idealised by considering the crank and the follower to be rigid. Moreover, the follower is assumed to have a large moment of inertia compared to that of the coupler. Starting with Eringen's nonlinear bending equations[55], the author finds a power series expansion using the ratio of the inertia of the coupler to the inertia of the driven link as a parameter. The zero-th approximation is a four-bar mechanism with a massless but flexible coupler which becomes a spring-mass system with a time varying spring constant. Using Bolotin's results[52] for parametric instabilities of a rod, the critical frequency zones for the axial instabilities are found out from the zero-th approximation. From the zero-th and first order approximations, it is shown that the buckling can occur only when the axial load exceeds Euler's critical load. However, by perturbing the base solution, the critical frequency zones for the bending instabilities are found out. The analysis shows that (i) the axial vibrations of the coupler is of primary importance and (ii) the bending instability occurs either when the axial load becomes sufficiently large to cause the column type buckling or due to the parametric resonance.

It is proved that the bending instability is greatly influenced by the axial vibrations and the author

concludes that the axial vibrations should not be neglected. The similar conclusion has also been drawn in the studies of the parametric vibrations of columns and strings[53,56].

Broniarek and Sandor[57] examined the stability of a parallelogram linkage with massless elastic coupler and rigid cranks, connecting two rotating masses mounted on elastic shafts. Because of these special properties of the links, the stability of the system is easily determined by studying the stability of a simple Hill-type equation.

Some of the authors cited in Section 1.1.1 also discussed briefly in their papers the stability of the mechanisms. Mayer Zur Capellen[8,54] provides some resonance criteria and concludes that several natural modes can occur simultaneously for some input crank-speeds. Jainski, Lee and Sandor[6,7] use the Routh-Hurwitz criterion to find out the stability zones of the coupler. For various frequency ratios, Viscomi and Ayre[5] have plotted the transverse displacements where unbounded regions are shown but have not analysed further to study the stability problem.

1.2 Objective of the Present Work

From a careful study of the past research works cited in the previous section it is found that the solution with the continuum model is almost impossible except for

extremely idealised cases. Such models help only to provide an insight into the general nature of the problem. Several research works have been conducted to obtain a more comprehensive solution for more realistic cases by using numerical methods. The lumped mass model suffers from several drawbacks viz., lack of generality in approach, complexity in the analysis procedure if the axial extensibilities are included and the inaccuracy in the calculated stresses. The above difficulties may be successfully eliminated by using the finite element model. However, several simplifying assumptions have been made in the previous works using the finite element models and till now no effort has been made to study the effects of the additional acceleration terms as well as the axial forces using the finite element models. It is evident that, of all the three models, the finite element model is the most powerful one and its potential can be exploited to obtain a comprehensive analysis of the mechanisms.

The major objectives of the present work may be classified into three groups as follows:

(i) The basic concepts of the finite element techniques will be utilised to provide a firm base for the analysis of mechanisms. The vibrating motions of a completely flexible mechanism will be studied by taking into account the axial vibrations of the links. To achieve this end, an effort will be made to examine the

effects of subdividing the links on the accuracy of the solution. Unlike the previous works, the actual distribution of the rigid body inertia forces will be considered to generate the load vectors. It is also proposed to use a 'code-system' of assembly to generalise the analysis which will be helpful in case of more complex situations. In addition, a general procedure for eliminating the rigid body degrees of freedom will be developed. As a natural extension of the above procedure, a simple equation will be evolved which gives the variable input forces of a general mechanism under certain assumption. With a modified assumption, this equation will be extended to study the vibrations of the flywheel at the crank-shaft. In this connection, a more practical case will be examined without imposing any simplifying assumption on the input forces. To study the dynamic behaviour of the rigid body inertia forces, the harmonic analysis of these forces will be made and their effects on the vibration characteristics of a mechanism will be investigated. A new method of stress analysis will be proposed which requires very little additional computations. It will also be demonstrated how the present procedure for the kineto-elastodynamic

analysis of a mechanism can be very efficiently utilised to obtain the rigid body analysis (viz., the kinematic analysis and the dynamic force analysis) of the mechanism.

(ii) To assess the contributions of the various additional acceleration terms and the rigid body axial forces on the dynamics of the mechanisms, a general equation will be derived from Lagrange's equation of motion by using a moving co-ordinate system. In order to avoid the complexity in the solution of the resulting equation of motion, an approximate method for solving these equations will also be outlined. An attempt will be made to study the effects of the elastic axial forces on the displacements of the flexible mechanisms.

(iii) In the conventional finite element method, the solutions are obtained only for an instantaneous configuration of the mechanism. Consequently, a large number of computations is needed to have a complete picture of the system behaviour. To overcome this difficulty, a new approach will be presented for a restricted class of mechanisms which will incorporate all the dynamic factors and describe the steady state displacements for all configurations of the mechanism by means of a single expression. As a result, the computation time

for finding the steady state solution will be reduced considerably. Since this form of solution is conducive to the stability analysis of mechanisms, the relevant procedures for determining the critical zones of the crank speed will also be described.

The effectiveness of the above studies will be demonstrated by solving several problems and comparing the results with those from the past works whenever possible. However, due to the limitations of time available, the list of the numerically solved examples may not be exhaustive. For the same reason, no numerical example will be furnished corresponding to the following two procedures: for analysing the mechanisms with driving motors and for determining the instability zones of the mechanisms.

CHAPTER II

DEFLECTION AND STRESS ANALYSIS

2.1 Introduction

It is apparent from the review of the past research that the published works on the finite element analysis of the flexible mechanisms lack the generality and rigour. In this chapter an attempt is made to place the basic analysis of the flexible mechanisms in a moderately rigorous and general framework of the finite element method. Section 2.2 contains a precise statement of the problem and the assumptions made in the analysis. Section 2.3 outlines the analysis for each link at the element level. Section 2.4 describes a general method of obtaining the system matrices suitable for mechanisms. In Section 2.5 the solution of the system equations is carried out with a systematic approach to the problem followed by the determination of the deflections within the links. In Section 2.6 the problem of finding the input torque under various conditions is solved. A complete harmonic analysis of the forces for a slider-crank and a four-bar mechanism is performed in Section 2.7. A new and efficient procedure for the calculation of various types of stresses is presented in Section 2.8. The chapter

is concluded in Section 2.9 with a description of a new type of kinematic and force analysis of a rigid link mechanism.

2.2 Statement of the Problem

The problem to be dealt with specifically in the present study is to find out the deflections and stresses of a completely elastic mechanism under pre-assigned external loading conditions. The problem also includes the examination of a flexible mechanism for the limits of critical operating speeds. The major assumptions are: (i) the rigid body motion and the elastic vibrations are separable, (ii) the mean longitudinal vibrations of a link is independent of the transverse vibrations, (iii) the deflections are small so that linear theory can be applied throughout and (iv) the effects of the tolerances, clearances and impact are neglected.

The equations and the method of analysis described in the present study are generally applicable for any mechanism. However, to make the presentation simple, a planar mechanism consisting of straight links with uniform cross-sections will be considered.

To fit in the methodology of the finite element techniques, the following mathematical model of a mechanism is used. At an initial time $\tau = \tau_0$, the rigid body

configuration of the mechanism is considered as an 'instantaneous structure' capable of undergoing both the rigid body and elastic motions. (In case of a four-bar linkage, this position is shown by $O_1A_1B_1O_2$ in Fig. 2.1). The forces acting on this instantaneous structure are the rigid body inertia forces due to the 'gross' rigid-body accelerations of the elements plus the external forces acting on it. The mass and stiffness properties of the mechanism, treated as an elastic structural system, are derived at this position and are assumed to remain unchanged during a chosen interval of time $\Delta\tau$. The displacements, stresses etc. for each element at the end of the interval are determined. From the deflected positions of the ends of the links, the shifted rigid body configuration (position $O_1A_2B_2O_2$) is determined and is allowed to travel for a period of $\Delta\tau$ as a rigid-link mechanism. The configuration thus reached (position $O_1A_3B_3O_2$) is considered as the instantaneous structure for the next interval of time $\Delta\tau$. The displacements and velocities of the elements at the end of this interval are taken as the 'initial conditions' for the next interval. In this way, the entire process is repeated until the steady-state condition is reached.

It is known that in dynamic problems, discretisation of a continuum gives accurate results only when

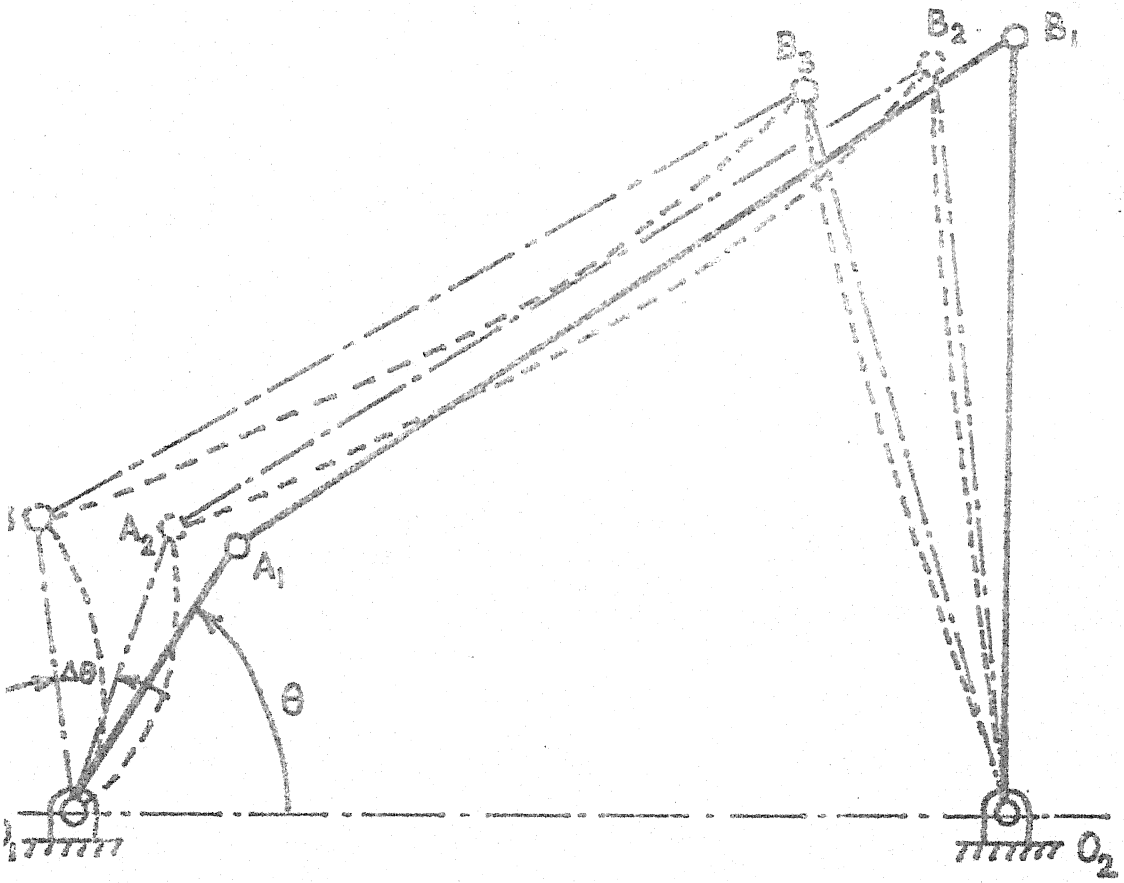

FIG 2.1 STEPS OF DISPLACEMENT ANALYSIS

sufficient numbersof the element co-ordinates are defined. For this reason each link is assumed to be divided into several parts and each part is treated as an element of the mechanism.

2.3 Element Analysis

To start with, the element co-ordinate axes x-y are chosen along the axis of each element and perpendicular to it. Six element co-ordinates $\bar{u}_1(\tau)$ to $\bar{u}_6(\tau)$ are defined at the two ends of each element (denoted by E') along the corresponding element co-ordinate axes (Fig. 2.2) to represent the continuous behaviour of the element in a discretised way. The continuous axial displacement $u_x^a(x, y, \tau)$ due to the axial forces only and the continuous transverse displacement $u_y^b(x, y, \tau)$ due to the bending only can be approximated by the polynomials as expressed in eqs. (2.1 and (2.2).

$$u_x^a = C_1 + C_2 x \tag{2.1}$$

$$u_y^b = C_3 + C_4 x + C_5 x^2 + C_6 x^3 \tag{2.2}$$

where C_1 to C_6 are functions of time τ only.

The above polynomials are used because they relate the continuous displacements u_x^a, u_y^b to the nodal displacements $\bar{u}_1$ to $\bar{u}_6$ (Fig. 2.2) with the accuracy of the

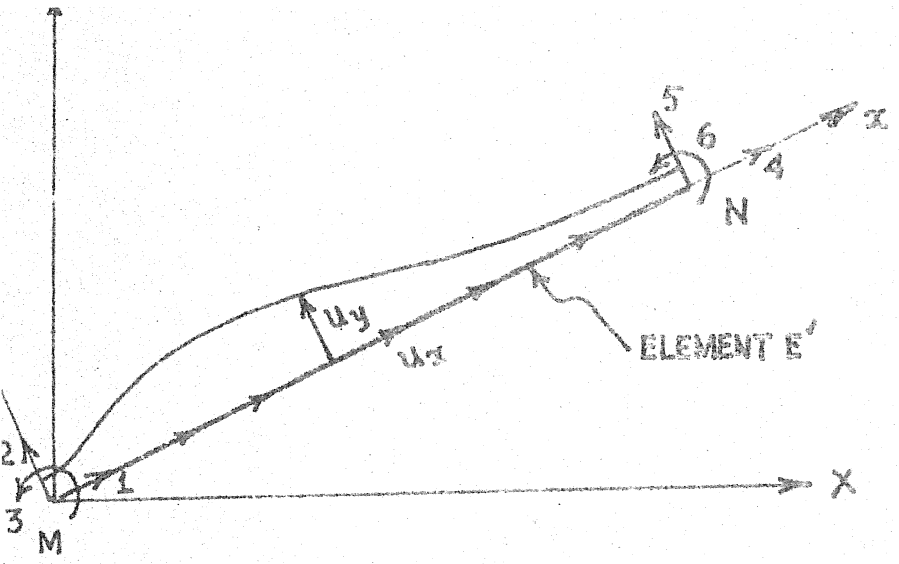

(a)

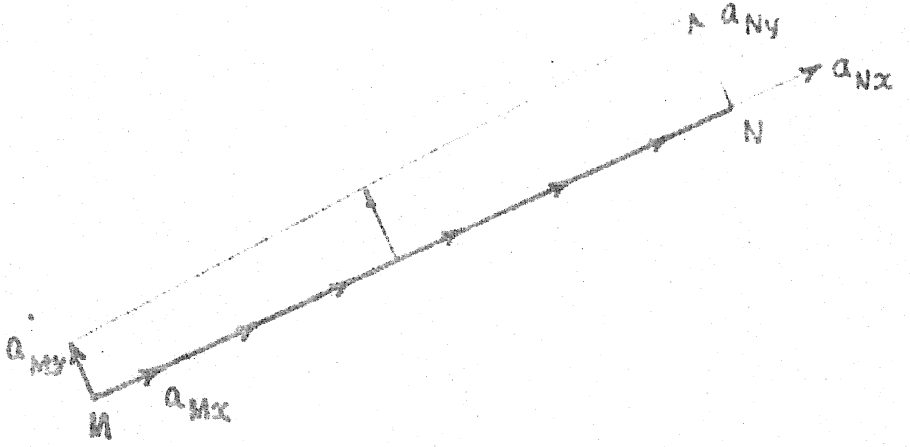

(c)

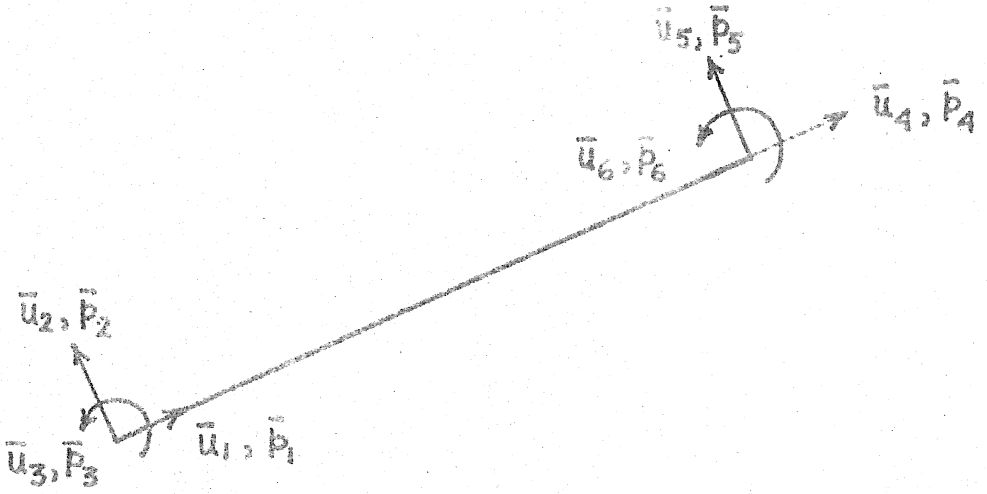

(b)

FIG 2.2 ELEMENT COORDINATES

engineering theory of static bending of beams. In dynamic problems other functions could as well be used and the choice of appropriate functions is a subject of research till now. It may be observed that eqs. (2.1) and (2.2) permit the rigid body motions in addition to the elastic motions.

To include the effect of shear, the following relationships are used.

$$u_y = u_y^b + u_y^s \tag{2.3}$$

$$\frac{\partial u_y^s}{\partial x} = -\frac{S_F}{GA_s} \tag{2.4}$$

$$EI \frac{\partial^3 u_y^b}{\partial x^3} = S_F \tag{2.5}$$

where, u_y^s = the transverse deflection due to shear only

u_y = total transverse displacement

S_F = the shear force acting at a position x of the link

A_s = the effective shear area of the cross-section

G = the shear modulus of elasticity

E = the Young's modulus of elasticity

I = second moment of area of the cross-section

Eliminating S_F from eqs. (2.4) and (2.5), the following equation is obtained:

$$\frac{\partial u_y^s}{\partial x} = \frac{EI}{GA_s} \frac{\partial^3 u_y^b}{\partial x^3} \tag{2.6}$$

Integrating the above equation and using eqs. (2.2) and (2.3), the following relation is obtained

$$u_y = C_3' + C_4 x + C_5(x^2 + \frac{2EI}{GA_s}) + C_6(x^3 + \frac{6EI}{GA_s} x) \tag{2.7}$$

Following boundary conditions are used to determine C_3' to C_6 in terms of $\bar{u}_2$ to $\bar{u}_6$

$$\begin{aligned} &\text{At} \quad x = 0, \quad u_y = \bar{u}_2, \quad \frac{\partial u_y^b}{\partial x} = \bar{u}_3 \\ &\text{At} \quad x = l, \quad u_y = \bar{u}_5, \quad \frac{\partial u_y^b}{\partial x} = \bar{u}_6 \end{aligned} \tag{2.8}$$

Finally,

$$\bar{u}_y = \frac{1}{(1+\varphi)} \begin{bmatrix} 1-3\xi^2+2\xi^3+(1-\xi)\varphi & \xi-2\xi^2+\xi^3+\frac{1}{2}(\xi-\xi^2)\varphi \\ 3\xi^2-2\xi^3+\varphi\xi & -\xi^2+\xi^3-\frac{\varphi}{2}(\xi-\xi^2) \end{bmatrix} \begin{bmatrix} \bar{u}_2 \\ \bar{u}_3 l \\ \bar{u}_5 \\ \bar{u}_6 l \end{bmatrix} \tag{2.9}$$

where, $\varphi = \frac{12EI}{GA_s l^2}$, $\xi = \frac{x}{l}$, l = length of the element.

The longitudinal displacements u_x^b due to the bending is given, in accordance with the engineering bending theory, by eq. (2.10).

$$u_x^b = -\frac{\partial u_y^b}{\partial x}\, y = \frac{1}{1+\phi}[(6\xi-6\xi^2)\,\zeta \;\{-1+4\xi-3\xi^2-(1-\xi)\phi\}\,\zeta$$

$$-(6\xi-6\xi^2)\,\zeta \quad (2\xi-3\xi^2-\xi\phi)\,\zeta] \begin{bmatrix} \bar{u}_2 \\ \bar{u}_3 l \\ \bar{u}_5 \\ \bar{u}_6 l \end{bmatrix} \qquad (2.10)$$

with $\zeta = y/l$

Using the boundary conditions $u_x^a(0,\tau) = \bar{u}_1$, $u_x^a(l,\tau) = \bar{u}_4$, C_1 and C_2 are determined from eq. (2.1). The total displacement u_x in the x direction is

$$u_x(x,y,\tau) = u_x^a(x,\tau) + u_x^b(x,y,\tau) \qquad (2.11)$$

Thus, the continuous displacement $u = \{u_x, u_y\}$ is expressed in terms of the nodal displacements $u = \{u_1, \ldots, u_6\}$ in eq. (2.12a).

$$u = a\,\bar{u} \qquad (2.12a)$$

Consequently, $\dot{u} = a\,\dot{\bar{u}}$; $\ddot{u} = a\,\ddot{\bar{u}}$ (2.12b)

where the shape function a is given by eq. (2.13).

$$a = \frac{1}{(1+\phi)} \begin{bmatrix} (1+\phi)(1-\xi) & 6(\xi-\xi^2)\,\zeta & & \\ 0 & 1-3\xi^2+2\xi^3+(1-\xi)\,\phi & & \\ [-1+4\xi-3\xi^2-(1-\xi)\,\phi]l\zeta & (1+\phi)\xi & 6(-\xi+\xi^2)\,\zeta & (2\xi-3\xi^2-\xi\phi)l\zeta \\ [\xi-2\xi^2+\xi^3+\tfrac{1}{2}(\xi-\xi^2)\,\phi]l & 0 & 3\xi^2-2\xi^3+\xi\phi & [-\xi^2+\xi^3-\tfrac{1}{2}(\xi-\xi^2)\,\phi]l \end{bmatrix}$$

(2.13)

with $\zeta = y/l$.

The normal strain $e_{xx}(x, y, \tau)$ and the shearing strain $e_{xy}(x, y, \tau)$ at any point of the link E' are given by the following equations:

$$e_{xx} = \frac{\partial u_x}{\partial x} \tag{2.14}$$

$$e_{xy} = \frac{\partial u_y}{\partial x} + \frac{\partial u_x}{\partial y} \tag{2.15}$$

Introduction of eq. (2.12) in eqs. (2.14), (2.15) gives the continuous element strains $e = \{e_{xx}, e_{xy}\}$ within the element E' in terms of u as shown below:

$$e = b\,u \tag{2.16}$$

where the element strain matrix b is

$$b = \frac{b_1}{b_2}$$

$$= \frac{1}{(1+\varphi)l}\begin{bmatrix} -(1+\varphi) & 6(1-2\xi)\zeta & (4-6\xi+\varphi)l\zeta & (1+\varphi) & 6(-1+2\xi)\zeta & (2-6\xi-\varphi)l\zeta \\ 0 & -\varphi & -\frac{\varphi l}{2} & 0 & \varphi & -\frac{\varphi l}{2} \end{bmatrix} \tag{2.17}$$

Expressions for normal stress $\sigma_{xx}(x, y, \tau)$ and nominal shear stress $\sigma_{xy}(x, y, \tau)$ at any point of the element E' are given by eqs. (2.18) and (2.19) respectively.

$$\sigma_{xx} = E\, e_{xx} \tag{2.18}$$

$$\sigma_{xy} = \frac{GA_s}{A}\, e_{xy} \tag{2.19}$$

Using eq. (2.12) in eqs. (2.16) to (2.19). continuous element stresses $\sigma = \{\sigma_{xx}, \sigma_{xy}\}$ within the element E' are obtained in terms of $\bar{u}$ as follows:

$$\sigma = \chi\, b\, \bar{u} \tag{2.20}$$

where

$$\chi = \begin{bmatrix} E & 0 \\ 0 & \frac{GA_s}{A} \end{bmatrix} \tag{2.21}$$

The kinematic analysis for a rigid link mechanism can be performed either by iterative procedures[13,14] or by the method described in Section 2.9. For illustrative purposes, direct kinematic analysis for two planar mechanisms is given in Appendix D.

From the kinematic analysis, the absolute rigid body normal accelerations A_{Mx}, A_{Nx} and tangential accelerations A_{My}, A_{Ny} at the end points M and N respectively of the element E' are determined. The components of the corresponding body forces $B(\xi, \tau)$, varying linearly within the element, are given by eq. (2.22).

$$B(\xi, \tau) = -\rho \begin{bmatrix} A_{Mx} + (A_{Nx} - A_{Mx})\xi \\ A_{My} + (A_{Ny} - A_{My})\xi \end{bmatrix} \tag{2.22}$$

where ρ = density of the material.

From the principle of virtual work,[58] the element oriented element stiffness matrix $\bar{k}$, the element mass-matrix $\bar{m}$ and the element load-vector $\bar{p}$ are obtained as shown below:

$$\bar{k} = \int_v b^t \times b \, dv \tag{2.23}$$

$$\bar{m} = \int_v \rho a^t a \, dv \tag{2.24}$$

$$\bar{p} = \int_v a^t B \, dv$$

$$= - \int_v \rho \, a^t \begin{bmatrix} A_{Mx} + (A_{Nx} - A_{Mx}) \\ A_{My} + (A_{Ny} - A_{My}) \end{bmatrix} dv \tag{2.25}$$

where t denotes the transpose of a matrix and v implies that the integrations are carried over the whole volume of the element.

Derivation of these matrices and their explicit expressions are included in Appendix B.

To define the properties of the element E' in a common co-ordinate system, a datum (or system or global) co-ordinate system X-Y is chosen and a rotation matrix R is used for the transformation of the element oriented element co-ordinates into the system oriented element co-ordinates. The matrix R can be expressed as follows:

$$R = \left[\begin{array}{c|c} R_1 & 0 \\ \hline 0 & R_1 \end{array}\right] \tag{2.26}$$

where R_1 is the rotation matrix for each end and is given by the following equation (for plane mechanisms):

$$R_1 = \begin{bmatrix} \cos\theta_{E'} & \sin\theta_{E'} & 0 \\ -\sin\theta_{E'} & \cos\theta_{E'} & 0 \\ 0 & 0 & 1 \end{bmatrix} \tag{2.27}$$

By virtue of the co-ordinate transformation defined by eq. (2.28), the load vector $\hat{\bar{p}}$, the stiffness matrix $\hat{\bar{k}}$ and the mass matrix $\hat{\bar{m}}$ in the system oriented element co-ordinates are obtained, from the contragradient law of transformation, in eqs. (2.29) to (2.31).

$$\bar{u} = R\,\hat{u} \tag{2.28}$$

$$\hat{\bar{k}} = R^t\,\bar{k}\,R \tag{2.29}$$

$$\hat{\bar{m}} = R^t\,\bar{m}\,R \tag{2.30}$$

$$\hat{\bar{p}} = R^t\,\bar{p} \tag{2.31}$$

where $\hat{u}$ is the nodal displacement vector in the system oriented element co-ordinates. The initial displacement $\hat{u}(\tau_o) = \hat{u}^o$ and initial velocity $\dot{\hat{u}}(\tau_o) = \dot{\hat{u}}^o$ in the system oriented element co-ordinates are obtained in eqs. (2.32) and (2.33) from the corresponding terms $\bar{u}(\tau_o) = \bar{u}^o$ and $\dot{\bar{u}}(\tau_o) = \dot{\bar{u}}^o$ in the element oriented element co-ordinates.

$$\hat{u}^o = R^t \bar{u}^o \tag{2.32}$$

$$\dot{\hat{u}}^o = R^t \dot{\bar{u}}^o \tag{2.33}$$

since $R^t R = I$, the identity matrix.

If there is any external distributed or concentrated force acting on the element, it must be converted into an equivalent element force vector p_e, derived from the equivalence of virtual work[58]. For example, if a surface load p_s acts on the element over a length extending from $x = s_1$ to $x = s_2$, the equivalent element force vector p_e is given by eq. (2.33a).

$$p_e = \int_{s_1}^{s_2} a^t p_s \, ds \tag{2.33a}$$

In case of the concentrated forces p_c, s_1 in eq. (2.33a) approaches to s_2 and $p_s ds$ becomes equal to p_c in the limit.

The equivalent force vector p_e found out by eq. (2.33a) is conveniently added either with $\bar{p}$ or with $\hat{p}$ depending on its direction.

The above element analysis is carried out for all the elements present in the mechanism and the element analysis is completed.

2.4 Assembly of Element Matrices

The assembly of the element matrices (found out in the last section) into system matrices for the whole mechanism is carried out by 'code-system' method[59].

To explain the method, identification numbers (encircled in Fig. 2.3) are alloted to each element of the mechanism at the outset. An integer matrix NS is defined such that its columns contain the system co-ordinates associated with the system-oriented element co-ordinates of an element whose identification number matches with the row number of these columns. For example, NS for the mechanism shown in Fig. 2.3a is given by eq. (2.34).

$$NS = \begin{bmatrix} 11 & 12 & 10 & 1 & 2 & 9 \\ 1 & 2 & 3 & 4 & 5 & 6 \\ 5 & 6 & 7 & 13 & 14 & 8 \end{bmatrix} \quad (2.34)$$

Let the element number 1 in Fig. 2.3a be assumed rigid but allowed to rotate while in Fig. 2.3b, the element number 1 be assumed not only rigid but temporarily fixed in space during each interval. For that purpose, the total number of the degrees of freedom for these mechanisms are specified as 8 and 6 respectively and the system co-ordinates are numbered accordingly as shown. When no information like the reactions etc. at the co-ordinates with zero displacements (Fig. 2.3c and Fig. 2.3d, for illustrative purposes) are

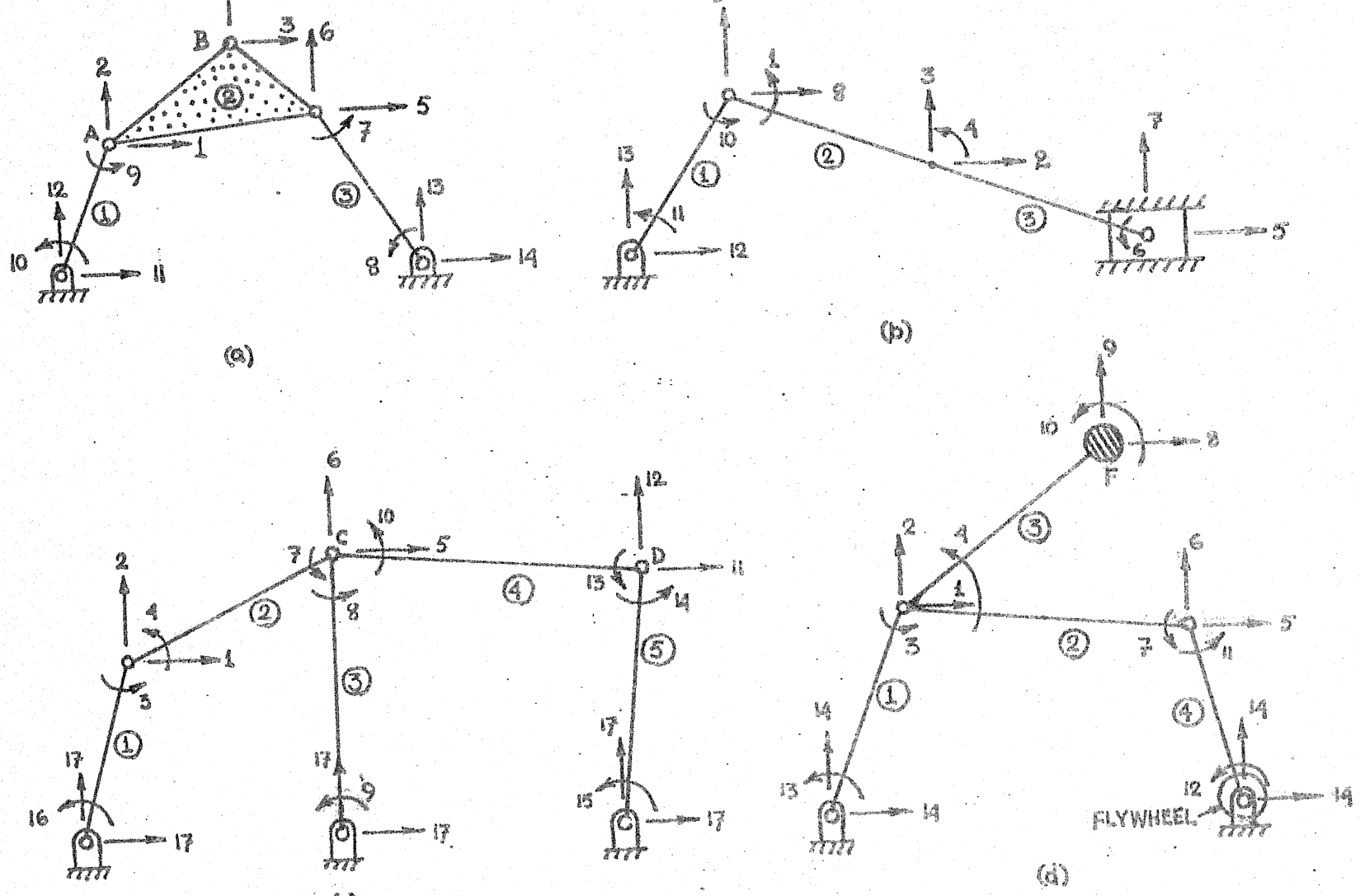

FIG 2.3 SYSTEM CO ORDINATES

required, these co-ordinates can be alloted the same number to reduce the size of the matrices.

In this method of assembly, the number of the element co-ordinates and the system co-ordinates at any type of joints need not follow a regular order. For example, joint C (Fig. 2.3c) having three branches and element 2 (Fig. 2.3a) having 3 nodes but no moment co-ordinate can be handled without any difficulty. Moreover, the dependent co-ordinates (defined afterwards) can be grouped together as the last set among the generalised system co-ordinates and the advantage of this type of flexibility in numbering the co-ordinates is manifested in a later section. As the association of the system co-ordinates with any element can be readily established by simply referring to NS, the special features of a particular mechanism, viz., the mass and the centrifugal effect of the concentrated weight at F in Fig. 2.3d, the gas force, the piston mass and its inertia in Fig. 2.3b, the input and output torques etc. can be directly incorporated to the system even when the division of the links are made arbitrarily. The basic difference between the conventional method[60,17] and this method of assembly is that in the former case the system co-ordinates are numbered automatically inside the program thus imposing certain restrictions in its use while in the later case it

is done through the input data rendering complete freedom in its application. Unlike other structures, the total number of the elements and joints in a mechanism is small; so the automatic numbering does not offer any special advantage over the little disadvantage of using a relatively bigger matrix NS. On the contrary, it is rather advantageous to feed the boundary conditions, regarding the types of the joints, in the program directly through a single matrix NS. In view of the above, the code-system seems to be more general and efficient compared to other methods of assembly like connectivity matrix[43,11], permutation vector method[60,17] etc. used in the earlier works.

A sample program to perform the assembly in case of a flexible mechanism is given in Table 2.1 where the links can be subdivided arbitrarily.

Using the code-system as described above, the system matrices are generated from the corresponding matrices in the system oriented element co-ordinates as indicated in Table 2.1. Having done this, the special features of the mechanism under consideration are incorporated in the system matrices. For example, the inertia of the flywheel at the rocker end (Fig. 2.3d) should be added to a diagonal element of the system mass matrix. The row (or column) number of this diagonal element corresponds to the number of the

Table 2.1: Sample program for assembly

```
      MDS = 0
      DO 1 I = 1,M
      IDIV = DIV(I)
      CALL ESEM(I,ES,EM,EP)
      DO 1 NDIV = IDIV
      MDS = MDS + 1
      DO 1 J = 1,MEC
      IROW = NS(MDS,J)
      SP(IROW) = SP(IROW) + EP(J)
      SUO(IROW) = EUO(J)
      SVO(IROW) = EVO(J)
      DO 1 K = 1,MEC
      ICOL = NS(MDS,K)
      SS(IROW,ICOL) = SS(IROW,ICOL) + ES(J,K)
    1 SM(IROW,ICOL) = SM(IROW, ICOL) + EM(J,K)
```

M = Number of links; DIV(I) = number of divisions for the i-th link; MEC = maximum number of element co-ordinates used. ES, EM, EP, EUO, EVO and SS, SM, SP, SUO, SVO are system oriented element matrices and system matrices for stiffness, mass, load, initial displacement and initial velocity respectively. It is assumed that the elements of a link are numbered sequentially.

system co-ordinate associated with the rotation of that rocker end. Similarly, the centrifugal force and the dead weight of the concentrated mass at F (Fig. 2.3d) should be added to the elements of the system's force vector whose row numbers correspond to the numbers of the horizontal and vertical system co-ordinates respectively at the point F, while its mass should be added to the two corresponding diagonal elements of the system mass matrix. Also the forces or torques exerted by the input shafts (determination of these input forces is discussed in Section 2.5.3) are added to the corresponding elements of the force vector of the system.

When the special features of the mechanism are incorporated, the final equation of motion for the whole mechanism is given by eqs. (2.35) and (2.35a) respectively.

$$M\ddot{U} + C\dot{U} + K\,U = P \qquad (2.35)$$

$$\text{for } \tau_o < \tau < \tau_o + \Delta\tau.$$

subject to the initial conditions:

$$U(\tau_o) = U^o \quad \text{and} \quad \dot{U}(\tau_o) = \dot{U}^o \qquad (2.35a)$$

where M, C, K, P, $U(\tau)$, U^o and $\dot{U}^o$ are the mass matrix, damping matrix, stiffness matrix, force-vector, displacement vector, initial displacement vector and initial velocity vector respectively for the whole mechanism expressed in

the system co-ordinates. Determination of the damping matrix C is deferred to Section 2.5.4.

2.5 System Analysis

2.5.1 Derivation of the transformation matrix

To solve eq. (2.35) by normal mode method for the first few modes, it is necessary to solve the corresponding eigenvalue problem as defined by eq. (2.36)

$$M \ddot{X} + K X = 0. \qquad (2.36)$$

The solution of eq. (2.36) by Power method[61,43] requires the inversion of K. For mechanisms, the stiffness matrix K is singular[43] and the degree of singularity (or nullity) of the matrix K is equal to the number of the rigid body degrees of freedom present in the mechanism. A general method to render K non-singular by removing its rigid body degrees of freedom is presented below.

From the total set of the co-ordinates X of eq. (2.36), any subset of the dependent co-ordinates X_B is chosen in such a way that no rigid body displacement in the mechanism is possible through the remaining independent co-ordinates X_A. It is clear that the total number of the co-ordinates present in X_B must be equal to the number of the rigid body degrees of freedom of the mechanism and

many combinations are possible to form the set of co-ordinates X_B. However, it is convenient to choose the co-ordinates corresponding to the input forces as dependent co-ordinates and the advantage of it will be apparent in Section 2.5.3. Accordingly eq. (2.36) is rewritten in partitioned form as shown below.

$$\begin{bmatrix} M_{AA} & M_{AB} \\ M_{BA} & M_{BB} \end{bmatrix} \begin{bmatrix} \ddot{X}_A \\ \ddot{X}_B \end{bmatrix} + \begin{bmatrix} K_{AA} & K_{AB} \\ K_{BA} & K_{BB} \end{bmatrix} \begin{bmatrix} X_A \\ X_B \end{bmatrix} = 0 \qquad (2.37)$$

If any arbitrary small rigid body displacement dX_B is given to the dependent co-ordinates, the resulting rigid body displacements dX_A at the independent co-ordinates may be expressed in terms of dX_B in the following form.

$$dX_A = T\, dX_B \qquad (2.38)$$

T in eq. (2.38) is called the displacement transformation matrix[58] and depends only on the geometry of the mechanism. The procedure of determining T directly from the geometry in case of simple mechanisms is exemplified in Appendix C. A general procedure for the determination of T in case of any mechanism is outlined next.

Since a mechanism does not produce any elastic force due to the rigid body displacements, eqs. (2.39) and (2.40) immediately follow.

$$\begin{bmatrix} K_{AA} & K_{AB} \\ K_{BA} & K_{BB} \end{bmatrix} \begin{bmatrix} dX_A \\ dX_B \end{bmatrix} = 0 \qquad (2.39)$$

That is,

$$\begin{aligned} K_{AA}\, d_{XA} + K_{AB}\, d_{XB} &= 0 \\ K_{BA}\, d_{XA} + K_{BB}\, dX_B &= 0 \end{aligned} \qquad (2.40)$$

Introduction of eq. (2.38) into eq. (2.40) yields the following useful relations:

$$T = - K_{AA}^{-1} K_{AB} \qquad (2.41)$$

and

$$K_{BA}\, T + K_{BB} = 0 \qquad (2.42)$$

Equation (2.41) offers a most general method for finding T and eq. (2.42) can be used for checking purposes. It is interesting to note that though material and cross-sectional properties are involved in K_{AA} and K_{AB}, the final expression of T solely depends on the geometry of the mechanism. Eq. (2.41) is most efficiently exploited if the inversion of K_{AA} is utilised in the solution of the eigenvalue problem defined by eq. (2.36). For this purpose, a new procedure is described below which requires the inversion of K_{AA} only.

2.5.2 Elimination of the rigid body degrees of freedom

Let any virtual rigid body displacements δX_B be given at the dependent co-ordinates of the system defined by the equilibrium equation (2.37). The resulting virtual rigid body displacements δX_A at the independent co-ordinates follow from eq. (2.38) and is expressed in eq. (2.43).

$$\delta X_A = T\, \delta X_B \tag{2.43}$$

Since the restoring forces do not produce any work on the rigid body displacements, work is done by the inertia forces only. Thus, the following equation is obtained from the principle of virtual work when applied to the equilibrium equation (2.37).

$$\delta X_A{}^t (M_{AA} X_A + M_{AB} X_B) + \delta X_B{}^t (M_{BA} X_A + M_{BB} X_B) = 0 \tag{2.44}$$

Use of eq. (2.43) and the fact that δX_B is arbitrary, yield eq. (2.45) relating X_B with X_A.

$$X_B = T^* X_A \tag{2.45}$$

where $$T^* = - (T^t M_{AB} + M_{BB})^{-1} (T^t M_{AA} + M_{BA}) \tag{2.46}$$

For small displacements, X_A can be resolved into two parts[58] as shown in eq. (2.47).

$$X_A = X_{Ae} + T X_B \tag{2.47}$$

In eq. (2.47) X_{Ae} denotes the displacements at the independent co-ordinates relative to the rigid body configuration corresponding to $X_B = 0$. Direct use of eq. (2.45) in eq. (2.47) to eliminate X_B yields the following equation relating X_A with X_{Ae}.

$$X_A = (I - T\,T^*)^{-1}\,X_{Ae} \tag{2.48}$$

The matrix $I - T\,T^*$ is usually large and therefore its inversion is time consuming. Alternatively, eq. (2.45) can be used in eq. (2.47) to relate X_B with X_{Ae}, after the elimination of X_A, resulting in the following equation.

$$X_B = (I - T^*T)^{-1}\,T^*X_{Ae} \tag{2.49}$$

The size of the matrix $I - T^*T$ is equal to the total number of the rigid body degrees of freedom and its inversion is much simpler than that of $I - T\,T^*$.

X_A is eliminated from eq. (2.37) with the help of eq. (2.47) and from the resulting equation, X_B is eliminated by using eqs. (2.41) and (2.49) to form the following eigenvalue problem expressed in the co-ordinates of X_{Ae}.

$$(-\omega^2 M' + K_{AA})X_{Ae} = 0 \tag{2.50}$$

where,

ω = natural frequency of vibration of the system

M' = effective mass matrix in the free-vibration of the mechanism

$$= M_{AA} + (M_{AA}T + M_{AB})(I - T^*T)^{-1} T^* \qquad (2.51)$$

If n and w be the total number of the system co-ordinates and the rigid body degrees of freedom of the mechanism respectively, the size of the matrices K_{AA} and M' is $(n-w)X(n-w)$.

For single degree of freedom systems, $I - T^*T$ is scalar and M' is symmetric. Since K_{AA} is non-singular, eq. (2.50) is solved by Power method[61] for the first few (say **m** in number) natural frequencies and natural modes. The modal matrix Φ' corresponding to eq. (2.50) is thus found out. Using eqs. (2.47) and (2.49), the modal matrix Φ corresponding to eq. (2.37) is found out as follows:

$$\Phi = \begin{bmatrix} \Phi_A \\ \Phi_B \end{bmatrix} \qquad (2.52)$$

where,

$$\Phi_B = (I - T^*T)^{-1} T^* \Phi' \qquad (2.53)$$

and

$$\Phi_A = \Phi' + T \Phi_B \qquad (2.54)$$

Besides the utilisation of K_{AA}^{-1}, the above eigenvalue formulation in the co-ordinates of X_{Ae} requires

lesser amount of computations compared to similar formulations with respect to X_A [58] or in a sub-space of X_A and X_B [43,11].

2.5.3 Variable input forces

Since the inertia forces arising from the gross rigid body movements of the mechanism vary at every position, the input shafts must exert variable reactive forces (which may include torques also) to maintain the stipulated input conditions at different positions of the mechanism. The problem of finding these variable input forces in a practical operating condition is examined in Section 2.6.2. For the time being, it is assumed that the input shafts exert forces T_B at the dependent co-ordinates of the mechanism in such a way that the rigid body inertia forces together with the external forces acting on the 'instantaneous structure' are in 'static' equilibrium in the rigid body degrees of freedom.

If F_A and F_B are the total forces (the rigid body inertia forces plus other external forces except T_B) acting at the independent and dependent co-ordinates of the mechanism respectively, the corresponding force-displacement relationship can be expressed by eq. (2.55) in partitioned form.

$$\begin{bmatrix} K_{AA} & K_{AB} \\ K_{BA} & K_{BB} \end{bmatrix} \begin{bmatrix} U_A \\ U_B \end{bmatrix} = \begin{bmatrix} F_A \\ F_B + T_B \end{bmatrix} \qquad (2.55)$$

If any virtual rigid body displacements δX_B be given at the dependent co-ordinates, the resulting virtual rigid body displacements δX_A at the independent co-ordinates are obtained as before from eq. (2.43). As mentioned earlier, the elastic forces do not produce any work in this case and eq. (2.56) follows from the principle of virtual work.

$$\delta X_A{}^t F_A + \delta X_B{}^t (F_B + T_B) = 0 \qquad (2.56)$$

Eliminating δX_A from eqs. (2.43) and (2.56) and noting that δX_B is arbitrary, the following equation is obtained:

$$T_B + F_B + T^t F_A = 0 \qquad (2.57)$$

Eq. (2.57) expresses the equilibrium equations (total number of these equations being equal to the total number of the rigid body degrees of freedom) which are satisfied by the self-equilibriating forces acting on the mechanism.

Input forces, thus found out from eq. (2.57), are added to the corresponding elements of P in eq. (2.35).

2.5.4 Solution of equations

Though the displacement vector U in eq. (2.35) is capable of executing the rigid-body motions as well as the elastic motions (by virtue of the polynomials in eqs. (2.1) and (2.2)), the modal matrix Φ contains only the

elastic modes and no rigid body modes. However, it was assumed in Section 2.5.3 that the rigid body forces including the input forces acting on the 'instantaneous structure' balance among themselves. Under this assumption, it is shown in Section 2.6.2 that no rigid body motion is possible for the 'instantaneous structure' during the interval $\Delta\tau$. Therefore the modal matrix Φ, as determined in eq. (2.52), is used for the solution of eq. (2.35). A case where it is necessary to include the rigid body motions in Φ is examined in Section 2.6.2.

To solve the equation of motion (2.35) by the normal mode method, the system co-ordinates of U are transformed to m numbers of normal co-ordinates as shown by eq. (2.58a).

$$U = \Phi\eta \tag{2.58a}$$

where $\eta(\tau)$ is the displacement vector in the normal co-ordinate system.

Noting that Φ is constant during the interval $\Delta\tau$, successive differentiations of eq. (2.58a) with respect to time τ yield

$$\dot{U} = \Phi\dot{\eta} \tag{2.58b}$$

and

$$\ddot{U} = \Phi\ddot{\eta} \tag{2.58c}$$

where $\dot{\eta}$ and $\ddot{\eta}$ are the velocity and acceleration vectors in the normal co-ordinate system.

Substituting eqs. (2.58) in eq. (2.35) and pre-multiplying it by Φ^t, eq. (2.59) is obtained.

$$\overline{M}\ddot{\eta} + \overline{C}\dot{\eta} + \overline{K}\eta = \overline{P} \tag{2.59}$$

where,

$$\begin{aligned} \overline{M} &= \Phi^t M \Phi \quad ; & \overline{C} &= \Phi^t C \Phi \\ \overline{K} &= \Phi^t K \Phi \quad ; & \overline{P} &= \Phi^t P \end{aligned} \tag{2.60}$$

Employing eqs. (2.58), the initial conditions for eq. (2.59) are expressed in the following form.

$$\eta^o = (\Phi^t \Phi)^{-1} \Phi^t U^o \tag{2.61}$$

$$\dot{\eta}^o = (\Phi^t \Phi)^{-1} \Phi^t \dot{U}^o \tag{2.62}$$

Because of the orthogonality of the modes in Φ, $\overline{M}$ and $\overline{K}$ are diagonal matrices. Obviously, the matrix $\overline{C}$ is also diagonal if the damping matrix C is taken as proportional to either M or K or a linear combination of them. But the use of a single constant (proportionality constant) to represent the damping characteristics of the systems with multiple degrees of freedom is not realistic. For this reason, the standard practice is to consider $\overline{C}$ as proportional to the critical damping of the system at the normal modes.[58] For this

case also, $\bar{C}$ becomes diagonal and equation (2.59) become uncoupled. These uncoupled equations assume the following form

$$m_i \ddot{\eta}_i + 2\omega_i \xi_i m_i \dot{\eta}_i + k_i \eta_i = p_i \qquad (2.63)$$

$$i = 1, 2, \ldots, m.$$

where,

η_i = displacement at the i-th normal co-ordinate

$\dot{\eta}_i$ = velocity at the i-th normal co-ordinate

$\ddot{\eta}_i$ = acceleration at the i-th normal co-ordinate

m_i = i-th diagonal of $\bar{M}$

k_i = i-th diagonal of $\bar{K}$

p_i = i-th element of $\bar{P}$

ω_i = i-th natural frequency

$2m_i\omega_i$ = critical damping at the i-th normal mode

ξ_i = damping ratio $(\frac{\text{actual damping}}{\text{critical damping}})$ at the i-th normal mode

As the damping present in a system tends to suppress the higher modes, it is desirable to take the higher values of ξ_i for the successively higher modes.

For the choice of the damping shown in eq. (2.63), the damping matrix $\bar{C}$ is given by eq. (2.64).

$$\bar{C} = 2 \begin{bmatrix} \omega_1 \xi_1 & & \\ & \ddots & \\ & & \omega_m \xi_m \end{bmatrix} \bar{M} \qquad (2.64)$$

Therefore, the system damping matrix C is eventually obtained from eq. (2.60) as

$$C = (\Phi \Phi^t)^{-1} \Phi \bar{C} \Phi^t (\Phi \Phi^t)^{-1} \qquad (2.65)$$

As the damping is chosen to be proportional to the critical damping, the full forms of the damping matrices C and $\bar{C}$ as shown by eqs. (2.64) and (2.65) are never required in actual computations.

Section 2.7 describes the solution procedure when P in eq. (2.35) varies with time. However, in this Section P (and therefore $\bar{P}$) is assumed to remain constant during the interval $\Delta\tau$. For this case, the solution of eq. (2.63) is given by eq. (2.66).

$$\eta_i(\tau) = e^{-\sigma_i \tau'} (I_i \cos\mu_i \tau' + J_i \sin\mu_i \tau') + \frac{P_i}{m_i \omega_i^2} \qquad (2.66)$$

Consequently,

$$\dot{\eta}_i(\tau) = e^{-\sigma_i \tau'} [(-\sigma_i I_i + \mu_i J_i)\cos\mu_i \tau' - (\sigma_i J_i + \mu_i I_i)\sin \mu_i \tau'] \qquad (2.67)$$

$$\text{and} \quad \ddot{\eta}_i(\tau) = \frac{p_i}{m_i} - \omega_i^2 \eta_i - 2\omega_i \xi_i \dot{\eta}_i \tag{2.68}$$

$$\text{for} \quad \tau_o < \tau < \tau + \Delta\tau$$

$$i = 1, \ldots, m$$

where,

$$\tau' = \tau - \tau_o$$

$$\sigma_i = \xi_i \omega_i$$

$$\mu_i = \sqrt{1 - \xi_i^2}\ \omega_i$$

$$I_i = \eta_i^o - \frac{p_i}{m_i \omega_i^2} \tag{2.69}$$

$$J_i = \dot{\eta}_i^o + \xi_i \omega_i I_i$$

η_i^o = i-th element of the vector η^o in eq. (2.61)

$\dot{\eta}_i^o$ = i-th element of the vector $\dot{\eta}^o$ in eq. (2.62)

The displacement η, velocity $\dot{\eta}$ and acceleration $\ddot{\eta}$, determined from eqs. (2.66) to (2.68), are transformed back first to the system co-ordinates with the aid of eq. (2.58) and then to the system oriented element co-ordinates for each element by using the integer matrix NS (as discussed in Section 2.4). These are finally transformed to the element oriented element co-ordinates by using the transformation given by eq. (2.28). The accelerations, transformed in this way, are used in Section 2.8 for the stress analysis of the mechanism.

It may be noted that the element oriented element displacements $\bar{u}(\tau_o + \Delta\tau)$ and element velocities $\dot{\bar{u}}(\tau_o + \Delta\tau)$, thus found out, are measured in the element oriented element co-ordinates and they are the only co-ordinate systems which maintain a time-invariant relation with the corresponding rigid elements. For this reason, $\bar{u}$ and $\dot{\bar{u}}$, as determined above, for each element are used as the 'initial conditions' $\bar{u}^o$ and $\dot{\bar{u}}^o$ in the eqs. (2.32) and (2.33) respectively for the next interval of time $\Delta\tau$. Next, starting from eq. (2.26), the whole procedure is repeated for the next interval after updating the initial time τ_o by $\tau_o + \Delta\tau$.

2.6 Input Forces for Different Conditions

2.6.1 Input forces for 'dynamic' equilibrium

In this section, the analysis described in Section 2.5.2 is modified by making the following assumption: the variable input forces T_B balance the rigid body forces (inertia and externally applied) together with all elastic inertia forces acting on the instantaneous structure, i.e., the instantaneous structure remains in 'dynamic' equilibrium for the rigid body degrees of freedom.

The equation of motion (2.35) for the whole mechanism is rewritten in partitioned form in eq. (2.70) where T_B is shown separately as an unknown quantity in the force vector P.

$$\begin{bmatrix} M_{AA} & M_{AB} \\ M_{BA} & M_{BB} \end{bmatrix} \begin{bmatrix} \ddot{U}_A \\ \ddot{U}_B \end{bmatrix} + \begin{bmatrix} C_{AA} & C_{AB} \\ C_{BA} & C_{BB} \end{bmatrix} \begin{bmatrix} \dot{U}_A \\ \dot{U}_B \end{bmatrix}$$

$$+ \begin{bmatrix} K_{AA} & K_{AB} \\ K_{BA} & K_{BB} \end{bmatrix} \begin{bmatrix} U_A \\ U_B \end{bmatrix} = \begin{bmatrix} P_A \\ P_B + T_B \end{bmatrix} \qquad (2.70)$$

Since the mechanism acted upon by the inertia forces $-M\ddot{U}$, viscous forces $-C\dot{U}$ and rigid body forces P in eq. (2.70) is assumed to be in equilibrium, these forces must satisfy eq. (2.57). Hence,

$$P_B + T_B - M_{BA}\ddot{U}_A - M_{BB}\ddot{U}_B - C_{BA}\dot{U}_A - C_{BB}\dot{U}_B + T^t(-M_{AA}\ddot{U}_A - M_{AB}\ddot{U}_B - C_{AA}\dot{U}_A - C_{AB}\dot{U}_B + P_A) = 0 \qquad (2.71)$$

$$\text{or,} \quad T_B = -T^t P_A - P_B + (M_{BA} + T^t M_{AA})\ddot{U}_A + (M_{BB} + T^t M_{AB})\ddot{U}_B + (C_{BA} + T^t C_{AA})\dot{U}_A + (C_{BB} + T^t C_{AB})\dot{U}_B \qquad (2.72)$$

Upon substituting eq. (2.72) in eq. (2.70), the following equation of motion in modified form is obtained:

$$\begin{bmatrix} M_{AA} & M_{AB} \\ -T^t M_{AA} & -T^t M_{AB} \end{bmatrix} \begin{bmatrix} \ddot{U}_A \\ \ddot{U}_B \end{bmatrix} + \begin{bmatrix} C_{AA} & C_{AB} \\ -T^t C_{AA} & -T^t C_{AB} \end{bmatrix} \begin{bmatrix} \dot{U}_A \\ \dot{U}_B \end{bmatrix}$$

$$+ \begin{bmatrix} K_{BA} & K_{AB} \\ K_{BA} & K_{BB} \end{bmatrix} \begin{bmatrix} U_A \\ U_B \end{bmatrix} = \begin{bmatrix} P_A \\ -T^t P_A \end{bmatrix} \qquad (2.73)$$

It may be noted that in this case also the special form of the force vector in the right side of eq. (2.73) obviates the necessity (explained in Section 2.6.2) to include the rigid body modes in the solution of eq. (2.73). Therefore eq. (2.73) can be solved in a manner similar to that used for eq. (2.35) in the Sections 2.5.3 and 2.5.4.

2.6.2 Input forces supplied by motors

In this section a more practical case is considered where the input forces are given beforehand (and therefore not to be determined from the equilibrium considerations). Though the procedure presented here is quite general, only a particular case is treated for the clarity of presentation.

Let the power to drive the mechanism be supplied by induction motors attached to the massless rigid input shafts. For the known speeds of the input shafts, the torques exerted by the motors at that instant are known from their torque-speed characteristics. As these torques in general do not balance the total moment exerted by the rigid body forces acting on the instantaneous structure, the rigid body motions (in addition to the elastic motions) take place during the interval $\Delta\tau$ caused by the net unbalanced moments. Thus, it is necessary in this case to include the rigid body modes in the modal matrix Φ in eq. (2.58) to allow

the rigid body motions during the solution of equation of motion (2.35).

It is assumed that the torques exerted by the motors (determined from the speeds of the input shafts at the beginning of the present interval $\Delta\tau$) remain constant during the interval and are added to the elements in the appropriate rows of the system force vector P in eq. (2.35). Also it is assumed that the polar moments of inertia of the rotors are added to the appropriate diagonal elements (corresponding to the rotational co-ordinates of the input ends of the cranks) of the system mass matrix.

It is clear that the modal matrix Ψ corresponding to the rigid body modes of the instantaneous structure is given by the following relation:

$$\Psi = \begin{bmatrix} T \\ I \end{bmatrix} \tag{2.74}$$

Replacing $\{X_A, X_B\}$ and $\{\delta X_A, \delta X_B\}$ in eq. (2.44) by Φ and Ψ respectively, equation (2.44) is rewritten in the form shown below:

$$\Psi^t M \Phi = 0 \tag{2.75}$$

Noting that the elastic forces do not produce any work on the rigid body modes, eq. (2.76) follows.

$$\Psi^t K \Phi = 0 \tag{2.76}$$

Eqs. (2.75) and (2.76) express the orthogonality conditions between Φ and Ψ with respect to the mass matrix M and stiffness matrix K respectively. Since dX_A, dX_B in eq. (2.39) is any rigid body mode, the following equation is obtained:

$$K \Psi = 0 \tag{2.77}$$

In general, the rigid body modes in Ψ are not orthogonal to each other with respect to the mass matrix, i.e.,

$$\Psi^t M \Psi = M^o \tag{2.78}$$

where M^o is a w X w matrix (non-diagonal in general).

In contrast to the relations among the elastic eigenmodes (i.e., they are orthogonal to each other with respect to both the stiffness and mass matrix), each of the rigid body modes are orthogonal to each row of the stiffness matrix, as seen from eq. (2.77), while they are not in general orthogonal to each other with respect to the mass matrix as shown by eq. (2.78).

Recalling the special advantage of the normal mode method of analysis (i.e., the final solution being the superposition of the individual solutions obtained for each mode), the solution of eq. (2.35) is shown below for the rigid body modes only as the solution for elastic modes has already been described in Section 2.5.4.

Let w numbers of the rigid body displacements in the normal co-ordinates corresponding to w numbers of the rigid body modes be denoted by the vector $\lambda(\tau)$. The following transformation of the co-ordinates is used to describe the rigid body modes of motion by the normal co-ordinates.

$$U = \Psi\lambda \tag{2.79}$$

Upon substitution of eq. (2.79) in eq. (2.35) and premultiplying it by Ψ^t, the following equation is obtained.

$$\Psi^t M \Psi \ddot{\lambda} + \Psi^t K \Psi \lambda = \Psi^t P \tag{2.80}$$

As the material damping does not occur in the rigid body modes, the damping term drops out from eq. (2.80).

By virtue of eqs. (2.77) and (2.78), eq. (2.80) reduces to

$$\ddot{\lambda} = (M^o)^{-1} \Psi^t P \tag{2.81}$$

Assuming that P is independent of time, the solution of eq. (2.81) is easily obtained as follows:

$$\lambda(\tau) = \frac{1}{2}(M^o)^{-1} \Psi^t P \tau^2 + A\tau + B \tag{2.82}$$

where the constants of integration A and B are to be determined from the initial displacement vector $\lambda(\tau_o)$ and initial velocity vector $\dot{\lambda}(\tau_o)$.

The concept of the instantaneous structure is introduced in the present study (explained in Section 2.2) to perform a step by step analysis of the mechanism by dividing its continuous motion into numerous successive intervals of time. At the beginning of each interval, the total motion, inherited from the previous time history, is separated into two parts: (i) the rigid body motions (represented in the form of the rigid body inertia forces) constituting a part of the force vector P in eq. (2.35) and (ii) the elastic motions represented by the initial elastic displacement U^o and the initial velocity $\dot{U}^o$ constituting the 'initial conditions' of eq. (2.35a). The current rigid body configuration of the mechanism (it is rotating with respect to the fixed frame of reference) is taken as the datum position and during the interval under consideration, the mechanism is allowed to execute the rigid body motions as well as the elastic motions, both measured from this datum position. Thus the rigid body components of the initial displacement U^o in eq. (2.35a) and consequently $\lambda(\tau_o)$ is zero. Let the rigid body velocities in the system co-ordinates, determined from the kinematic analysis, be denoted by the vector V^o. Then using a transformation analogous to eq. (2.79), the initial velocity vector $\dot{\lambda}(\tau_o) = \dot{\lambda}^o$ is given by eq. (2.83)

$$\dot{\lambda}^o = (\Psi^t \Psi)^{-1} \Psi^t V^o \qquad (2.83)$$

After introducing these initial conditions, eq. (2.82) reduces to:

$$\lambda(\tau) = \frac{1}{2}(M^o)^{-1}\ \Psi^t\ P\ \tau^2 + \dot{\lambda}^o\tau \qquad (2.84)$$

and

$$\dot{\lambda}(\tau) = (M^o)^{-1}\ \Psi^t\ P\ \tau + \dot{\lambda}^o \qquad (2.84a)$$

By back substitution of eq. (2.84) into eq. (2.79), the rigid body displacements at the system co-ordinates at the end of the interval $\Delta\tau$ is found out. Similarly, the rigid body velocities at the system co-ordinates are obtained by back substitution of eq. (2.84a) in an equation obtained by differentiating eq. (2.79) with respect to time.

These rigid body displacements, velocities given by eqs. (2.84) and (2.84a) are finally transformed into the element oriented element co-ordinates following the same procedure as described in Section 2.5.4, i.e., by integer matrix NS and eq. (2.28). The rigid body displacements and velocities so obtained at the input shafts are next added to the 'gross' rigid body displacements and speeds of the input shafts prevailing at the beginning of the interval. The total velocities of the input shafts, thus determined, are used to find out the input torques for the next interval. Similarly the total rigid body displacements at the input shafts, as determined above, are used for the rigid body kinematic analysis for the next interval.

In some positions of the mechanism, the variable rigid body moments exerted by the mechanism may differ considerably from the torques exerted by the motors and may, in turn, produce relatively large rigid body accelerations at those positions. It may be noted, however, that the theory of the finite elements described here is valid for small displacements only and, therefore, proper care should be taken to choose $\Delta\tau$ sufficiently small at these positions so that the rigid body motions produced in these intervals remain within limits.

As λ in eq. (2.84) represents only the small rigid body motions with respect to rigid frame of reference, the 'gross' rigid body displacements must be found out each time separately from the rigid body kinematic analysis. The rigid body velocities V^o can be merged with elastic velocities $\dot{U}^o$ to form a total initial velocity vector. Because of the orthogonality relations between the rigid body modes and the elastic modes with respect to the mass matrix M, the respective components of this total initial velocity vector can be isolated by the matrix operations[58]. However, the modes, determined by the numerical procedures, are orthogonal to each other only within a certain degree of accuracy. Therefore the isolation process will involve some inaccuracy. This inaccuracy may accumulate in the successive intervals

and may cause substantial error in the final results. Moreover, the rigid body velocities may vary considerably from the elastic velocities and even slight inaccuracy in the modes will affect the separation process adversely. Therefore it is better to treat V^o separately from U^o as described above.

It is seen that if the force vector P is self-equilibriating, the first terms in the right side of eqs. (2.81), (2.84) and (2.84a) become zero by virtue of eq. (2.74). Therefore no rigid body acceleration is possible during the interval of time. Therefore it is evident from eqs. (2.84) and (2.84a) that the rigid body displacements and velocities at the end of the interval may be obtained by simply allowing the instantaneous structure to continue the rigid body motions existing at the beginning of the interval. For this reason, it was not necessary to include the rigid body modes in the modal matrix in Sections 2.5.2 and 2.6.1.

2.7 Harmonic Analysis of Rigid Body Forces

In the above sections, the force vector P in eq. (2.35) was treated as constant during the interval $\Delta\tau$. Strictly speaking, the rigid body inertia forces vary with time even within the interval $\Delta\tau$. These time dependent forces can be decomposed into several harmonics with various

amplitudes. Evidently, an improvement in the accuracy of the previous analysis can be achieved if the time varying forces are treated in their actual form specially when the amplitudes of the first few harmonics are high. Moreover, when the operating speed becomes near to the frequency of any of these harmonics, large vibrations take place due to the 'resonance' condition corresponding to that harmonic. Such critical situations can not be easily detected if the force vector is treated as constant during the interval.

Unfortunately, the harmonic analysis of the mechanisms is still in its infancy. As mentioned in Section 1.1.3, harmonic analysis is available in the literature only for those mechanisms which have one input crank rotating at constant speed. Consequently, the following analysis is applicable only to that restricted class of mechanisms. Though the analysis may be extended to other cases, only planar mechanisms consisting of straight links with constant cross-section are considered in the following discussion.

In this section, harmonic analysis will be done only for the rigid body inertia forces. The rigid body configuration of the instantaneous structure is considered as a fixed frame of reference to describe the small motion of the mechanism during the current interval of time $\Delta\tau$. Therefore, the rotation matrix R in eq. (2.26), the transformation matrix T in eq. (2.38) and the matrices K, C and

M in eq. (2.35) are considered as time independent though, in a strict sense, they are also composed of several harmonics of the input angle.

When the input crank rotates with a constant speed, the sine and cosine of the angles of the links can be expressed in the form of Fourier series. For illustrative purposes, such expressions for slider-crank and four-bar mechanisms are derived in Appendix E. Thus for any element E' shown in Fig. 2.2, the sine and cosine of the angle $\theta_{E'}$ can be expressed as follows:

$$\cos\theta_{E'} = \sum_{j=1}^{h_1} [cc_j \cos(j-1)\,\omega\tau + cs_j \sin j\,\omega\tau] \qquad (2.85)$$

$$\sin\theta_{E'} = \sum_{j=1}^{h_1} [sc_j \cos(j-1)\,\omega\tau + ss_j \sin j\,\omega\tau] \qquad (2.86)$$

where,

h_1 = total number of sine/cosine terms taken in each series.

cc_j, cs_j, sc_j, ss_j = deterministic Fourier coefficients (2.87)

ω = constant input speed

τ = time

cc_j, cs_j, sc_j, ss_j = 0 for $j > h_1$.

The following trigonometrical relation is used to find the angular velocity $\omega_{E'}$ of the element in the form of Fourier series.

$$\omega_{E'} = \frac{d\theta_{E'}}{d\tau} = \cos\theta_{E'} \frac{d}{d\tau}(\sin\theta_{E'}) - \sin\theta_{E'} \frac{d}{d\tau}(\cos\theta_{E'}) \tag{2.88}$$

As the series in eqs. (2.85) and (2.86) are absolutely and uniformly convergent, term by term differentiation is permissible. After substituting eqs. (2.85) and (2.86) in eq. (2.88), performing the differentiations and retaining terms up to h_1-th harmonic in the series multiplications, the following relation is finally arrived at.

$$\omega_{E'} = \omega \sum_{j=1}^{h_1} [vc_j \cos(j-1)\omega\tau + vs_j \sin j\omega\tau] \tag{2.89}$$

where vc_j, vs_j are known co-efficients.

Squaring both sides of eq. (2.89), the series expression for $\omega_{E'}^2$ is obtained in eq. (2.90) where h_1 numbers of cosine/sine terms only are retained.

$$\omega_{E'}^2 = \omega^2 \sum_{j=1}^{h_1} [nc_j \cos(j-1)\omega\tau + ns_j \sin j\omega\tau] \tag{2.90}$$

where nc_j, ns_j are known co-efficients.

The angular acceleration $\alpha_{E'}$ is found out from the differentiation of eq. (2.89) as follows:

$$\alpha_{E'} = \frac{d}{d\tau}(\omega_{E'}) = \omega^2 \sum_{j=1}^{h_1} [tc_j \cos(j-1)\omega\tau + ts_j \sin j\omega\tau] \qquad (2.91)$$

where,

$$tc_1 = 0$$

$$tc_j = j\ vs_{j-1}\ , \qquad j = 2, \ldots, h_1$$

$$ts_j = -j\ vc_{j+1}\ , \qquad j = 1, \ldots, h_1-1 \qquad (2.92)$$

and $ts_{h_1} = 0$ by virtue of eq. (2.87).

The absolute normal acceleration A_{Mx} and the absolute tangential acceleration A_{My} of the left end M of the element along its axis and perpendicular to it respectively can be similarly expressed in Fourier series by taking projections of the accelerations of the right end of the adjacent element. (For elements generated from the same link, projections are only formal). These accelerations finally take the following form:

$$A_{Mx} = \omega^2 \sum_{j=1}^{h_1} [ac_j \cos(j-1)\omega\tau + as_j \sin j\omega\tau] \qquad (2.93)$$

$$A_{My} = \omega^2 \sum_{j=1}^{h_1} [bc_j \cos(j-1)\omega\tau + bs_j \sin j\omega\tau] \qquad (2.94)$$

where ac_j, as_j, bc_j and bs_j are known constants.

The normal acceleration A_{Nx} and the tangential acceleration A_{Ny} of the right end N of the element along its axis and perpendicular to it respectively are given by eqs. (2.95) and (2.96).

$$A_{Nx} = A_{Mx} - \omega_E^2 . 1 \tag{2.95}$$

$$A_{Ny} = A_{My} + \alpha_E . 1 \tag{2.96}$$

Upon substitution of eqs. (2.90), (2.91), (2.93) and (2.94) in eqs. (2.95) and (2.96), the following series result :

$$A_{Nx} = \omega^2 \sum_{j=1}^{h_1} [dc_j \cos(j-1)\,\omega\tau + ds_j \sin j\,\omega\tau] \tag{2.97}$$

$$A_{Ny} = \omega^2 \sum_{j=1}^{h_1} [ec_j \cos(j-1)\,\omega\tau + es_j \sin j\,\omega\tau] \tag{2.98}$$

where,

$$\begin{aligned} dc_j &= ac_j - nc_j . 1 \\ ds_j &= as_j - ns_j . 1 \\ ec_j &= bc_j + tc_j . 1 \\ es_j &= bs_j + ts_j . 1 \end{aligned} \tag{2.99}$$

Use of eqs. (2.93) to (2.98) in eq. (2.22) yield the series expressions for the body forces of the element. On substitution of these expressions in eq. (2.25) for the body forces, the element oriented element load vector $\bar{p}$ in the form of Fourier series is obtained in eq. (2.100).

$$\bar{p} = \sum_{j=1}^{h_1} [\bar{p}_j^1 \cos(j-1)\,\omega\tau + \bar{p}_j^2 \sin j\,\omega\tau] \qquad (2.100)$$

where $\bar{p}_j^1$, $\bar{p}_j^2$ etc. are known constants.

There may exist a special kind of external forces (i.e., the centrifugal forces of a concentrated weight, the inertia of a flywheel etc.) which have a fundamental frequency equal to the angular speed of the crank. These forces may be expressed in series of harmonics of the input angle and using these expressions in eq. (2.33a), the element oriented element force vector p_e due to the external forces may be found out in the form of a series. Clearly, the forces like gravity etc. will contribute only to the first term of the series. These series expressions should be added to the series of $\bar{p}$ in eq. (2.100). Other types of external forces may also be present whose fundamental frequencies do not coincide with the speed of the crank. These forces, forming a separate group of series, may be similarly treated. However, these forces are not included in this section.

Employing the series expression eq. (2.100) of $\bar{p}$ in eq. (2.31) and noting that the rotation matrix R is considered as constant during the interval, the series expression for the system oriented element load vector $\hat{p}$ is obtained as follows.

$$\hat{p} = \sum_{j=1}^{h_1} [\hat{p}_j^1 \cos(j-1)\omega\tau + \hat{p}_j^2 \sin j\omega\tau] \qquad (2.101)$$

where,

$$\hat{p}_j^1 = R^t \bar{p}_j^1 \; ; \qquad \hat{p}_j^2 = R^t \bar{p}_j^2 \qquad (2.102)$$

The terms $\hat{p}_j^1$, $\hat{p}_j^2$, ($j = 1, \ldots, h_1$) for all elements are separately assembled for each harmonic as described in Section 2.4 and the system force vector P of eq. (2.35) is formed as shown in eq. (2.103).

$$P = \sum_{j=1}^{h_1} [P_j^1 \cos(j-1)\omega\tau + P_j^2 \sin j\omega\tau] \qquad (2.103)$$

where P_j^1 and P_j^2 are the assembled form of $\hat{p}_j^1$ and $\hat{p}_j^2$ respectively.

As the transformation matrix T is considered constant during the interval, each harmonic of the input torque maintaining the 'static' equilibrium of the instantaneous structure may be found out by applying eq. (2.57) for the corresponding harmonics of the elements of the system force vector P. These harmonics of the input torque are to be added to the corresponding elements of P in eq. (2.103).

Corresponding to P in eq. (2.103), $\bar{P}$ in eq. (2.60) assumes the following form:

$$\bar{P} = \sum_{j=1}^{h_1} [\Phi^t P_j^1 \cos(j-1)\omega\tau + \Phi^t P_j^2 \sin j\omega\tau] \qquad (2.104)$$

The i-th element $\bar{P}_i$ of $\bar{P}$ may be written as follows:

$$\bar{P}_i = \sum_{j=1}^{h_1} [e_{ij} \cos(j-1)\omega\tau + f_{ij} \sin j\omega\tau] \qquad (2.105)$$

$$i = 1, \ldots, m$$

where e_{ij} and f_{ij} are the i-th elements of $\Phi^t P_j^1$ and $\Phi^t P_j^2$ respectively.

When $\bar{P}_i$, given by eq. (2.105), is used in eq. (2.63), the complete solution is given by eq. (2.106).

$$\eta_i(\tau) = e^{-\sigma_i\tau'} [W_i \cos \mu_i\tau' + Z_i \sin \mu_i\tau'] + \sum_{j=1}^{h_1} [d_{ij}^1 \cos(j-1)\omega\tau + d_{ij}^2 \sin j\omega\tau] \qquad (2.106)$$

Consequently,

$$\dot{\eta}_i(\tau) = e^{-\sigma_i\tau'} [(-\sigma_i W_i + \mu_i Z_i)\cos \mu_i\tau' - (\sigma_i Z_i + \mu_i W_i)\sin \mu_i\tau'] + \sum_{j=1}^{h_1} [d_{ij}^3 \cos(j-1)\omega\tau + d_{ij}^4 \sin j\omega\tau] \qquad (2.107)$$

and $$\ddot{\eta}_i(\tau) = \frac{\bar{P}_i}{m_i} - \omega_i^2\eta_i - 2\xi_i\omega_i\dot{\eta}_i \qquad (2.108)$$

where,

$$W_i = \eta_i^o - \sum_{j=1}^{h_1} [\, d_{ij}^1 \cos(j-1)\omega\tau_o + d_{ij}^2 \sin j\omega\tau_o]$$

$$Z_i = \frac{1}{\mu_i}[\dot{\eta}_i^o + \sigma_i W_i - \sum_{j=1}^{h_1} \{ d_{ij}^3 \cos(j-1)\omega\tau_o + d_{ij}^4 \sin j\omega\tau_o \}]$$

$$d_{ij}^1 = [1 - \frac{(j-1)^2\omega^2}{\omega_i^2}]\, d_{ij}^5\, e_{ij} - \frac{2j\,\omega\,\xi_i d_{ij}^6}{\omega_i}\, f_{ij}$$

$$d_{ij}^2 = \frac{2(j-1)\,\omega\xi_i\, d_{ij}^5}{\omega_i}\, e_{ij} + (1 - \frac{j^2\omega^2}{\omega_i^2})\, d_{ij}^6\, f_{ij} \qquad (2.109)$$

$$d_{ij}^3 = (j-1)d_{i,j-1}^2 , \qquad d_{i,1}^3 = 0$$

$$d_{ij}^4 = -\, j\, d_{i,j+1}^1 , \qquad d_{i,h_1}^4 = 0$$

$$d_{ij}^5 = \frac{\omega_i^2}{[\omega_i^2 - (j-1)\omega^2]^2 + 4(j-1)^2\omega^2\omega_i^2\xi_i^2}$$

$$d_{ij}^6 = \frac{\omega_i^2}{(\omega_i^2 - j^2\omega^2)^2 + 4j^2\omega^2\omega_i^2\xi_i^2}$$

and $\dot{\eta}_i$, $\ddot{\eta}_i$, τ', σ_i, μ_i, η_i^o, $\dot{\eta}_i^o$, ω_i and ξ_i are already defined in eqs. (2.63) and (2.69).

It is evident from eq. (2.109) that if the crank speed ω becomes nearly equal to some sub-multiple of any of the natural modes of vibration, sub-harmonic oscillations of large amplitudes take place, especially when the damping term is small. Of course, sub-harmonic 'resonance' conditions of higher order are not important because the corresponding amplitudes of the force vector are usually small. Consequently, the amplitudes of vibration are not high in the presence of damping.

2.8 Stress Analysis

The dynamic equilibrium equation for each element may be written in the following form:

$$\bar{k}\bar{u} = \bar{p} + (-\bar{m}\ddot{\bar{u}}) \qquad (2.110)$$

The above equation may be considered as a force-displacement relationship for an element where the forcing terms are kept at the right side. In the finite element method of analysis, the continuous material properties and the distributed forces are idealised for some selected node points and then the analysis for these node points are carried out as evident from the nature of eq. (2.35). Thus, it finally yields the displacements, velocities and accelerations of the mechanism only at the nodes of the elements, those being

again due to the nodal forces only. If the stresses at the nodal points only are desired, use of eq. (2.20) is sufficient for that purpose. However, for any point within the element, the stresses are due to: (i) the actual distribution of the external forces acting over the length of the element, (ii) the nodal displacements of the element and (iii) the actual distribution of the vibratory inertia forces acting over the length of the element. To find out the exclusive contributions of each one of these factors, the principle of superposition is used in the following manner.

If all the nodal displacements of the mechanism are made equal to zero, the resulting configuration is known as restrained structure in the literature of structural analysis. The restrained structure for a slider crank mechanism with two divisions of the connecting rod is shown in Fig. 2.4. When only the external forces in their actual distributed condition are allowed to act on this restrained structure, it may be termed as 'static' restrained structure. The stresses σ_I at any point within the element may then be calculated from the elementary analysis.

Next, all the external forces acting over the elements are converted into statically equivalent nodal forces (from the principle of virtual work) by using eqs. (2.25) and (2.33a). After solving eq. (2.35), the nodal displacements of the elements are found out as described

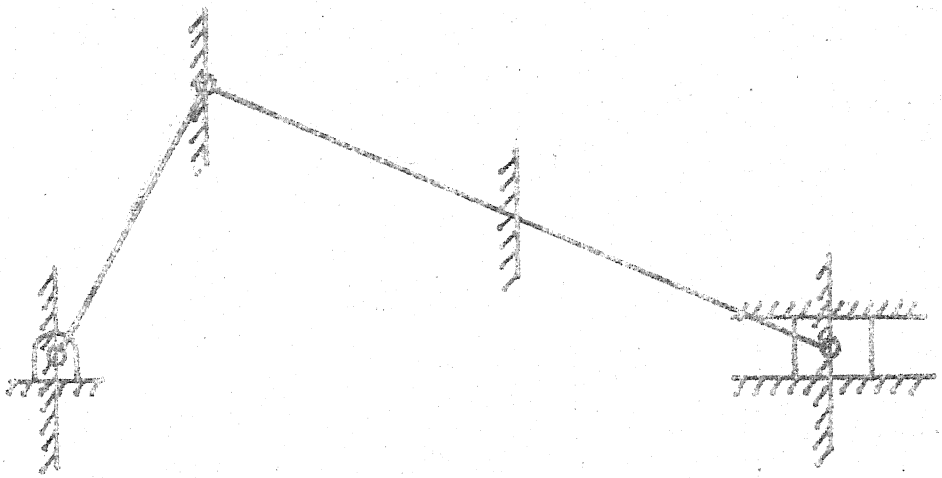

FIG 2.4 RESTRAINED STRUCTURE

in Section 2.5.4. The stresses σ_{II} within the elements due to these displacements alone are given by eq. (2.20).

At the end of each interval of time, the accelerations $\ddot{u}$ at the element oriented element co-ordinates are known. Consequently, the distribution of the vibratory inertia forces may be approximately obtained from eq. (2.12b) as follows:

$$- \rho A\ddot{u} = - \rho Aa\ddot{\bar{u}} \qquad (2.111)$$

where the left side represents the vibratory inertia forces at any point within the element.

The distributed inertia forces ($- \rho A\ddot{u}$), as found out from eq. (2.111), are then allowed to act over the restrained structure. The stresses σ_{III} at any point within the element due to these distributed inertia forces alone may again be found out from the elementary analysis. Thus, the total stress σ_T at any point within the element is given by eq. (2.112).

$$\sigma_T = \sigma_I + \sigma_{II} + \sigma_{III} \qquad (2.112)$$

If desired, the contribution from the distributed element viscous forces acting on the restrained structure towards σ_T may be easily found out by forming an equation similar to eq. (2.111). The restrained structure under the action of the vibratory inertia forces and viscous forces is termed as 'dynamic' restrained structure.

Since the shape function a is exact for beams in static problems only, σ_I gives exact values. The accuracy of σ_{II} and σ_{III} depends on the accuracy of the modelling for the actual dynamic displacements, as done in eq. (2.12).

Most of the loadings in the mechanism are distributed and therefore σ_I and σ_{III} should be included in the stress analysis. However, with the increase in the number of divisions of the links, the actual dynamic displacements are more accurately modelled by eq. (2.12) and both σ_I and σ_{III} decrease progressively as the restrained structure becomes more stiff. The displacements within the elements, if desired, may be obtained by the above procedure by using relations for the displacements in place of the stresses.

In the present method, the internal stresses (and deflections) are calculated by completely isolating the contributions due to the deflections, the distribution of the rigid body inertia forces and the distribution of the vibratory inertia forces from each other. Thus, only a few divisions of the links and elastic modes are necessary if the present method of stress analysis is adopted. Of all available techniques, this method of the stress analysis requires minimum additional computations.

2.9 Rigid Body Analysis

2.9.1 Displacement analysis

The kinematic analysis of a general rigid link mechanism may be carried out following the iterative procedure described in Reference (13). However, use of the transformation matrix T developed in Section 2.5.1 may also be extended further for the same purpose. As the analysis of the rigid link mechanisms does not strictly come within the perview of the present study, mechanisms with revolute pairs only are considered here. The same analysis may be easily extended to mechanisms with prismatic pairs if minor modifications are made.

For a rigid link mechanism with revolute joints, the displacement analysis implies the determination of the angles made by the links with respect to a fixed line i.e., X-axis of the system corresponding to a specified position of the input links. To make the discussion simple, the same system co-ordinates are assumed at present for both the rigid body and kineto-elastodynamic analysis of a mechanism. An efficient choice of the element (and system) co-ordinates for the rigid body analysis is mentioned in Section 2.9.3.

Before explaining the procedure, it may be pointed out that eqs. (2.41) and (2.42) are valid for any combination of the link angles (i.e., for any distorted

position of the links) as long as the boundary conditions at the joints of the mechanism allow the rigid body motions (these motions are possible for any distorted shapes of the links) corresponding to the rigid body degrees of freedom of the mechanism. Thus for the improvement of some guess values for the link angles, eqs. (2.41) and (2.42) can not be utilized. Since eqs. (2.41) and (2.42) are based on the compatibility of the displacements, velocities etc. at the joints, conditions like constancy of the velocities of the joints in a given direction are always maintained by these two equations and the values of dX_A obtained from eq. (2.38) for a given value of dX_B are always exact relative to the values of the link angles used in arriving at eq. (2.41).

Thus, the equation for improving the guess values of the link angles must be rought from such conditions which are valid only for a rigid link mechanism (i.e., necessary conditions). One of such conditions is the closure of the loops of a mechanism.

To describe the procedure in a very simple way, let a planar four-bar mechanism be taken as an example. Starting with some guess values θ_3' and θ_4' for the angles of the coupler and the follower corresponding to a given angle θ_2 of the crank, the system stiffness matrix K is constructed and eq. (2.41) is solved for the transformation matrix T. For a planar four-bar mechanism, the closure

equations may be written as follows:

$$L_2 \cos\theta_2 + L_3 \cos\theta_3 + L_4 \cos\theta_4 + L_1 = 0 \qquad (2.113)$$

and $$L_2 \sin\theta_2 + L_3 \sin\theta_3 + L_4 \sin\theta_4 = 0 \qquad (2.114)$$

where the subscripts 1 to 4 stand for the fixed link, crank, coupler and follower respectively, L denotes the length and θ denotes the exact angle (with the axis of the fixed link) of a link. The errors $d\theta_3'$ and $d\theta_4'$ in the guess values are given by eqs. (2.115) and (2.116).

$$\theta_3 = \theta_3' + d\theta_3' \qquad (2.115)$$

$$\theta_4 = \theta_4' + d\theta_4' \qquad (2.116)$$

With the help of eq. (2.38), the errors $d\theta_3'$ and $d\theta_4'$ may be expressed in terms of a fictitious error $d\theta_2'$ (all measured at the level of the guess values θ_3' and θ_4') in the crank angle θ_2 as shown below.

$$d\theta_3' = T_{\theta_3} d\theta_2' \qquad (2.117)$$

$$d\theta_4' = T_{\theta_4} d\theta_2' \qquad (2.118)$$

where T_{θ_3} and T_{θ_4} are the elements of T corresponding to the rotational co-ordinates (for each link, any one of its two rotational co-ordinates may be used) of the coupler and follower respectively. Using eqs. (2.115) to (2.118) in

eqs. (2.113), (2.114) and solving for $d\theta_2$, the following relations result (assuming $d\theta_2'$, $d\theta_3'$ and $d\theta_4'$ small):

$$d\theta_2' = \frac{L_2 \cos\theta_2 + L_3 \cos\theta_3' + L_4 \cos\theta_4' - L_1}{L_3 T_{\theta_3} \sin\theta_3' + L_4 T_{\theta_4} \sin\theta_4'} \tag{2.119}$$

$$d\theta_2' = -\frac{L_2 \sin\theta_2 + L_3 \sin\theta_3' + L_4 \sin\theta_4'}{L_3 T_{\theta_3} \cos\theta_3' + L_4 T_{\theta_4} \cos\theta_4'} \tag{2.120}$$

Since both eqs. (2.119) and (2.120) give the same quantity $d\theta_2'$, any one of them may be used.

As the term $d\theta_2'$ plays a key role in the present iteration process, it should be calculated as accurately as possible. For this reason, the term $d\theta_2'$ should be evaluated from eq. (2.119) or eq. (2.120) by using double precision arithmetic (i.e., sixteen significant digits) of a computer. However, it may be mentioned that the computations involving double precision arithmetic are slightly slower than calculations using single precision arithmetic (i.e., eight significant digits).

The term $d\theta_2'$, obtained from eqs. (2.119) or (2.120), may be interpreted as the error accumulated at one angle (here the crank angle) due to the incorrect guess values for the other angles. Upon back substitution of

this common error $d\theta_2'$ in eqs. (2.117) and (2.118), the errors $d\theta_3'$ and $d\theta_4'$ are obtained. Thus, the new guess values θ_3'' and θ_4'' for the angles may be obtained by adding the errors to the existing guess values as shown in eqs. (2.121) and (2.122).

$$\theta_3'' = \theta_3' + d\theta_3' \tag{2.121}$$

$$\theta_4'' = \theta_4' + d\theta_4' \tag{2.122}$$

The above process is repeated until the differences (or the relative differences) between the values of $d\theta_3'$ and $d\theta_4'$ (or $d\theta_2'$) obtained from two successive iterations satisfy the pre-assigned convergence criterion. It may be noted that the iteration procedure is carried out for a fixed value of θ_2 and therefore $d\theta_2'$ obtained from eqs. (2.119), (2.120) must not be added to θ_2 during the iteration process.

Equation (2.38) not only plays a key role in the above iteration procedure, but also provides a good estimate for the angles to be used as guess values during the next interval of time. These estimates are obtained from the left side of eqs. (2.117) and (2.118) when the increment in the crank angle (i.e., difference between the crank angles of the current configuration and the next instantaneous structure) is substituted for $d\theta_2'$ in the right side of these equations.

Role of eqs. (2.117), (2.118) is to transfer the errors in the guess values of the angles to the crank angle and redistribute again this accumulated error at the crank angle back to the angles of the respective links.

2.9.2 Velocity and acceleration analysis

Once the accurate positions of the links are known from the procedure described in Section 2.9.1, the absolute velocities at the system co-ordinates corresponding to the given velocities at the dependent co-ordinates are immediately obtained from eq. (2.38) by dividing its both sides by $d\tau$ as shown in eq. (2.123).

$$\dot{X}_A = T\dot{X}_B \tag{2.123}$$

where $\dot{X}_A$ and $\dot{X}_B$ are the absolute velocities at the independent and the dependent system co-ordinates respectively. Thus, the absolute translational velocities at the end points and the absolute angular velocity of each link are obtained from the appropriate elements of the vector $\dot{X}_A$. Since T has been obtained in the displacement analysis, the velocity analysis requires the trivial computations of multiplying a matrix by a vector as indicated by eq. (2.123).

Upon differentiation of eq. (2.123) with respect to time, eq. (2.124) is obtained.

$$\ddot{X}_A = \dot{T}\,\dot{X}_B + T\,\ddot{X}_B \qquad (2.124)$$

where $\ddot{X}_A$ and $\ddot{X}_B$ are the absolute accelerations at the independent and dependent system co-ordinates respectively. The term $\dot{T}$ may be obtained by differentiating eq. (2.41) with respect to time as follows:

$$\dot{T} = -K_{AA}^{-1}\,(\dot{K}_{AA}\,T + \dot{K}_{AB}) \qquad (2.125)$$

Replacement of $\dot{T}$ from eqs. (2.124) and (2.125) yields eq. (2.126)

$$\ddot{X}_A = -K_{AA}^{-1}(\dot{K}_{AA}T + \dot{K}_{AB})\dot{X}_B + T\ddot{X}_B \qquad (2.126)$$

Since element oriented element stiffness matrix $\bar{k}$ for each element is independent of the position of the elements with respect to the fixed frame of reference, the matrix $\dot{\bar{k}}$ for each element are obtained by differentiating eq. (2.29) with respect to time as is shown in eq. (2.127).

$$\dot{\bar{k}} = \dot{R}^t\,\bar{k}\,R + R^t\,\bar{k}\,\dot{R} \qquad (2.127)$$

where R is the rotation matrix for the element. In case of a planar mechanism, $\dot{R}$ for an element E' (making an angle $\theta_{E'}$ with the X-axis of the system co-ordinates) is obtained from eq. (2.26) as

$$\dot{R} = \left[\begin{array}{c|c} \dot{R}_1 & 0 \\ \hline 0 & \dot{R}_1 \end{array}\right] \qquad (2.128)$$

where

$$\dot{R}_1 = \begin{bmatrix} -\sin\theta_{E'} & \cos\theta_{E'} & 0 \\ -\cos\theta_{E'} & -\sin\theta_{E'} & 0 \\ 0 & 0 & 0 \end{bmatrix} \dot{\theta}_{E'} \qquad (2.129)$$

Since the absolute angular velocity of each link is known from eq. (2.123), the matrices $\dot{k}$ for each element is known from eqs. (2.23), (2.127) and (2.128). Assembly of the matrices $\dot{k}$ for each element may be done by using the integer matrix NS as described in Section 2.4 to form the system matrix $\dot{K}$ and consequently the submatrices $\dot{K}_{AA}$ and $\dot{K}_{AB}$. Using the matrices $\dot{K}_{AA}$, $\dot{K}_{AB}$ and the given values of $\dot{X}_B$, $\ddot{X}_B$ in eq. (2.126), the vector $\ddot{X}_A$ is obtained. The absolute angular acceleration and the absolute translational accelerations at the end points of each element are known from the appropriate elements of the vector $\ddot{X}_A$. The absolute velocities and accelerations of each element in its axial and transverse directions may then be easily found out since the angles of the links are also known.

2.9.3 Quasi-static analysis

To apply the method of analysis described below, it is necessary to define separate system co-ordinates (as shown in Fig. 2.3a and Fig. 2.3b) along the directions of the bearing reactions with numbers following that of

the last dependent system co-ordinate. Let the combined group of the dependent co-ordinates and the co-ordinates corresponding to the bearing reactions be denoted by the subscript C. The group of co-ordinates corresponding to the independent co-ordinates is denoted by the subscript A as was done in Section 2.5.1.

The instantaneous structure of a rigid link mechanism is in equilibrium under the actions of the external forces, the rigid body inertia forces, the variable input forces (calculated from eq. (2.57)) and the bearing reactions. Since each co-ordinate corresponding to the bearing reactions represent an additional rigid body degree of freedom (which is suppressed, in actual case, due to zero displacements at these co-ordinates), the force equilibrium equation for the rigid link mechanism given by eq. (2.57) may be extended to find the bearing reactions as follows:

$$T_C + F_C + T_r^t F_A = 0 \qquad (2.130)$$

where the vector T_C contains the variable input forces and the bearing reactions, F_C and F_A are the rigid body forces (external forces and the rigid body inertia forces) at the group of co-ordinates C and A respectively. The matrix T_r in eq. (2.130) is found out from eq. (2.131) which is an extension of eq. (2.41).

$$T_r = - K_{AA}^{-1} K_{AC} \tag{2.131}$$

It may be noted that the first set of the columns of T_r contains the matrix T defined by eq. (2.41) and the first set of the elements of the vector T_C contains the variable input forces. Thus, elimination of T_r from eqs. (2.130) and (2.131) yields the variable input forces and the bearing reactions, contained in the vector T_C, as shown in eq. (2.132).

$$T_C = - F_C + K_{AC}^{t} K_{AA}^{-1} F_A \tag{2.132}$$

It may be noted that the static deflections $K_{AA}^{-1}F_A$ of the mechanism due to the rigid body forces F_A are obtained from eq. (2.132) as an intermediate product. Equation (2.132) may also be derived from the force-displacement relationship of the mechanism.

Once the bearing reactions are obtained from eq. (2.132), the rigid body pin forces at the moving ends of the input links may be obtained from the equilibrium of forces acting on the input links. From the compatibility of the internal forces acting at these moving ends, the pin forces at the same ends of the next links connected with these joints are found out. In this way, the pin forces acting at all the joints of the mechanism may be easily found out by successive applications of the equilibrium equations for the links and the compatibility equations for the joints.

When more than two links are joined in several pin-connections, the number of simultaneous equations to be solved may be considerably reduced if the above process is initiated from all support-ends at a time and if provisions are kept within the computer program to choose the successive links and joints judiciously.

As mentioned in the beginning of this section, it is not necessary to use the same system co-ordinates for the rigid body analysis and the kineto-elastodynamic analysis. For example, divisions of the links are not necessary for the rigid body analysis and also for determining the quasi-static deflections. Moreover, for a link with hinged joints at both ends (i.e., a truss), only translational co-ordinates (two co-ordinates at each joint for a planar link) are needed to describe its rigid body as well as elastic behaviour. Therefore these types of co-ordinates should be used for the rigid body analysis and quasi-static deflections of the mechanism to minimize computations. The shape function and the generation of the rigid body forces for these type of co-ordinates are given in Appendix D. This shape function is exact for the quasi-static analysis; therefore the nodal deflections obtained from eq. (2.132) are also exact. The quasi-static deflections within the links may be calculated following the procedure of Section 2.8 which are exact for an exact shape function. One difficulty in using this type

of co-ordinates lies in the calculation of the errors in the angles (eqs. (2.117) to (2.120)), to be calculated indirectly from the errors in the translational co-ordinates. To circumvent this difficulty, one additional co-ordinate may be used for rotation of each link and the associated shape function may be easily determined following the procedure described in Section 2.3.

For a planar four-bar mechanism, the rigid body displacements, velocities, accelerations, pin forces, variable input torque and quasi-static deflections have been found out (using shape function of eq. (2.13)) for a complete cycle by means of the present procedure with an increment of 4 degrees in the crank angle and a convergence criterion of 10^{-5}. The entire analysis takes only 0.1 min. in IBM 7044 and the iteration process converges in three iterations (on the average) using single precision arithmetic. This computer time is much less compared to the existing matrix analysis procedure[13,14,62].

Like the existing matrix procedure, the analysis procedure described above is completely general and is ideally suited for a digital computer. In addition, its main advantages are: (i) number of computations is less by an order of magnitude, (ii) gives quasi-static deflections (and therefore stresses) as an intermediate product, (iii) may be applied to mechanisms with multi-degrees of freedom, and (iv) simple dimensions of the curved links are needed.

CHAPTER III

DYNAMICS OF AXIALLY LOADED MOVING LINKS

3.1 Introduction

When a mechanism operates, all links of the mechanism experience varying translational as well as angular accelerations. Moreover, the axial accelerations and the interactions between the links transmitted through the joints generate space dependent and time dependent axial forces within the links. At low operating speeds, the effects of these accelerations on the vibrations of the links are not significant. However, even in this case the axial forces transmitted through the pins and their effect on the dynamics of the links may be considerable if the magnitudes of the external forces acting on the mechanism are high. Since the accelerations on the links increase approximately with the square of the input speed, their role on the motion of the links becomes increasingly significant at higher speeds. In the previous analysis described in Chapter II, these accelerations and the external forces were considered to contribute towards the mechanism behaviour exclusively in the form of rigid body forces. Once the force vector was formed, these accelerations were considered to be temporarily

absent and the vibration of the instantaneous structure due to this force vector only was analysed during each interval. In addition, the effect of the axial forces of any kind on the transverse vibration of the links was not included.

The axial forces acting on a link may arise due to the following reasons: (i) rigid body axial accelerations within the link, (ii) the pin forces transmitted by the other links through the joints, (iii) the elastic axial accelerations within the link, and (iv) the elastic forces generated from its axial shortening. The axial shortening of a link may be due to the axial forces or the transverse forces or both acting on it. In this chapter, the accelerations of the links are considered to be active during the interval of time $\Delta\tau$ and the vibrations of the links in these acceleration fields are analysed. In addition to this, the effect of the axial forces on the transverse vibrations of the links, which is essentially non-linear in character, is also included in an otherwise linear analysis. To achieve this objective, the equation of motion is derived in Section 3.2 for a general case by first using a rotating co-ordinate system and then Lagrange's equation of motion. The inclusion of the effect of the acceleration field and the axial forces on the vibrations of the links results in an antisymmetric secondary mass matrix and a symmetric geometric stiffness

matrix respectively. The solution of the equation of motion, with these antisymmetric matrices as coefficients, by the normal mode method requires the use of the complex eigenvalues and eigenvectors. To avoid the complex arithmetic and the accompanying excessive computations, an approximate method is outlined in Section 3.3 which solves the equation of motion with sufficient accuracy but using lesser amount of computations. When the elastic axial forces are considered, the geometric stiffness matrix becomes non-linear. For this case an iterative procedure is presented in Section 3.4, at the end of this chapter.

3.2 Derivation of the Equation of Motion

In this section, the equation of motion will be derived for an element E' in a more general situation, i.e., when the element is axially loaded and is subjected to the longitudinal and transverse vibrations in an acceleration field as shown in Fig. 3.1. Choosing a fixed co-ordinate system X-Y, let the co-ordinates of the left end M of the element E' at any instant be X, Y and its inclination with the X-axis be $\theta_{E'}$ as shown in Fig. 3.2.

At this instant, the absolute rigid body angular velocity and angular acceleration are $\omega_{E'}$ and $\alpha_{E'}$,

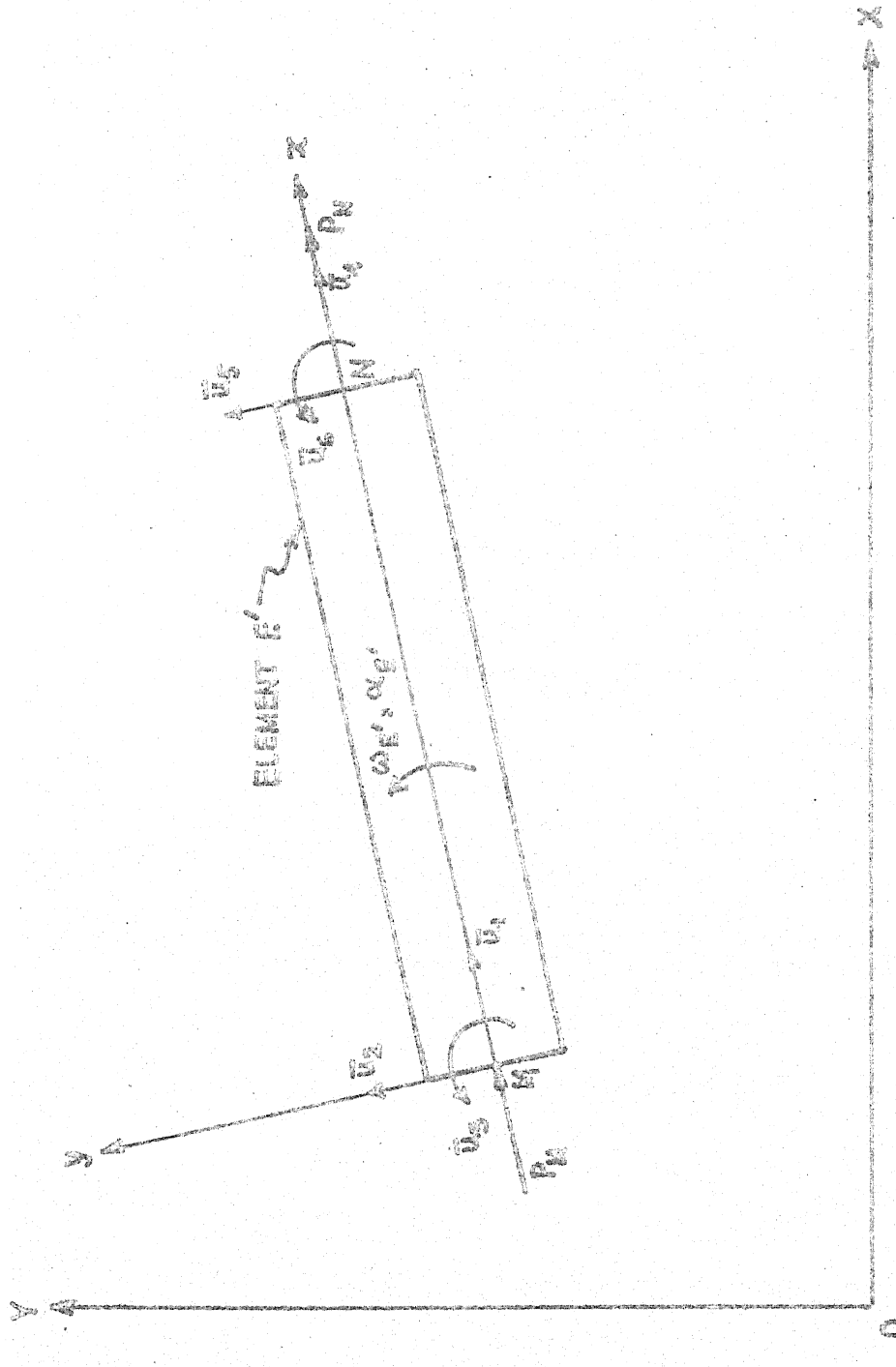

FIG 5.1 AXIALLY LOADED MOVING ELEMENT

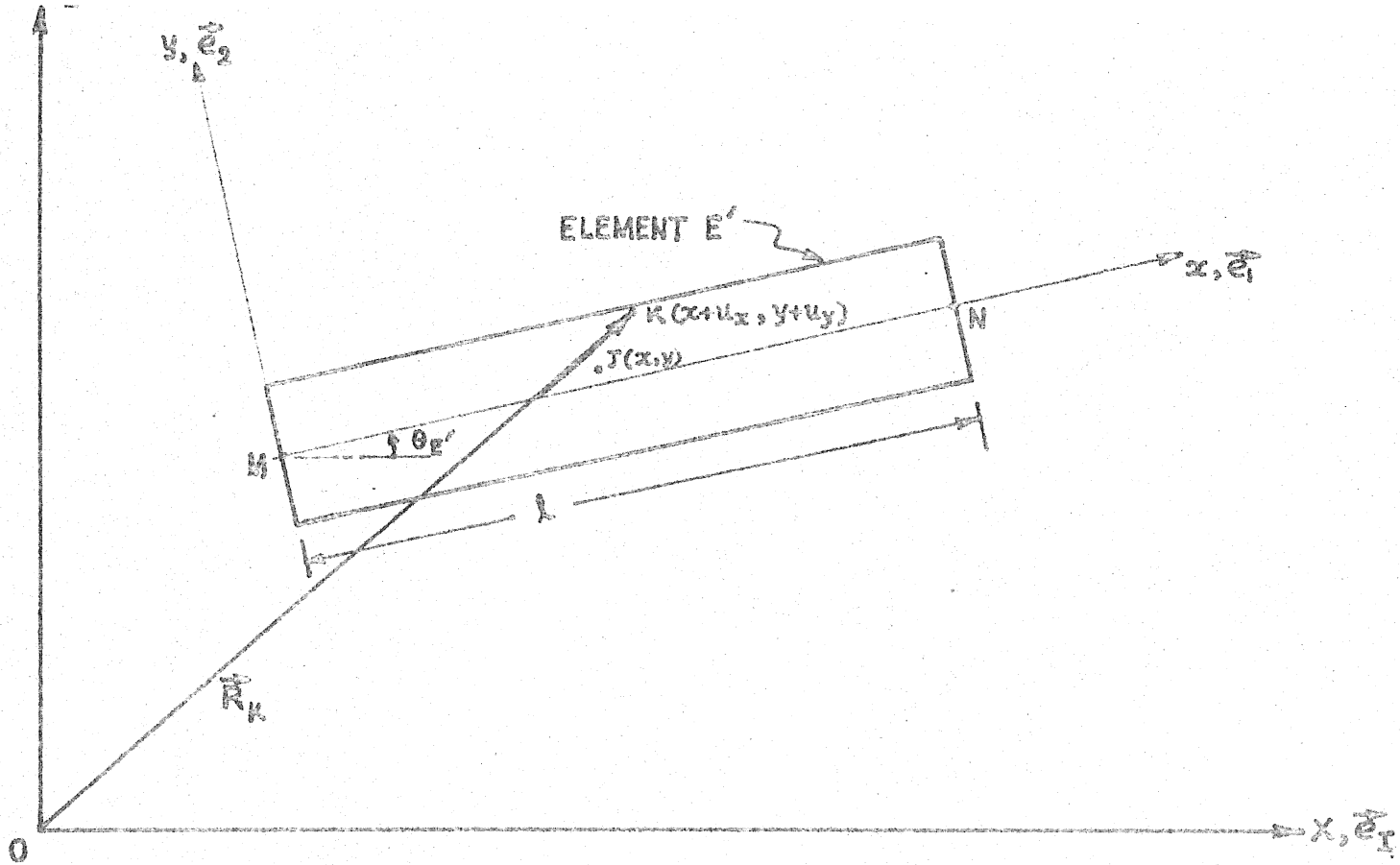

FIG 3.2 MOVING COORDINATE SYSTEM

respectively and the axial forces at the left end M and right end N are P_M and P_N respectively. A rotating co-ordinate system x-y is chosen along the axial of the element and perpendicular to it which remain fixed with the element and rotates along with the element. $\vec{e}_1$, $\vec{e}_2$ and $\vec{e}_I$, $\vec{e}_{II}$ are the unit vectors in the x-y and X-Y co-ordinate systems respectively (Fig. 3.2) satisfying the following relations:

$$\vec{e}_1 \cdot \vec{e}_1 = \vec{e}_2 \cdot \vec{e}_2 = \vec{e}_I \cdot \vec{e}_I = \vec{e}_{II} \cdot \vec{e}_{II} = 1 \qquad (3.1)$$

$$\vec{e}_1 \cdot \vec{e}_2 = \vec{e}_2 \cdot \vec{e}_1 = \vec{e}_I \cdot \vec{e}_{II} = \vec{e}_{II} \cdot \vec{e}_I = 0 \qquad (3.2)$$

$$\vec{e}_I = \vec{e}_1 \cos\theta_{E'} - \vec{e}_2 \sin\theta_{E'} \qquad (3.3)$$

$$\vec{e}_{II} = \vec{e}_1 \sin\theta_{E'} + \vec{e}_2 \cos\theta_{E'} \qquad (3.4)$$

$$\dot{\vec{e}}_1 = \omega_{E'} \vec{e}_2 \; ; \quad \dot{\vec{e}}_2 = -\omega_{E'} \vec{e}_1 \qquad (3.5)$$

$$\vec{e}_I = \vec{e}_{II} = \dot{\vec{e}}_I = \dot{\vec{e}}_{II} = 0 \qquad (3.6)$$

$$\dot{x} = \ddot{x} = \dot{y} = \ddot{y} = 0 \qquad (3.7)$$

Let any point within the element, initially at the position J with co-ordinates x, y, take the position K with co-ordinates $x + u_x$, $y + u_y$ (all measured in x-y system) due to the longitudinal and transverse vibrations of the link. The final position vector $\vec{R}_K$ is given by the following equation:

$$\vec{R}_K = X\,\vec{e}_I + Y\,\vec{e}_{II} + (x + u_x)\,\vec{e}_1 + (y + u_y)\,\vec{e}_2 \qquad (3.8)$$

Differentiating eq. (3.8) with respect to time and using the relations given by eqs. (3.3) to (3.7), eq. (3.9) is obtained.

$$\dot{\vec{R}}_K = \left[\dot{X}\cos\theta_{E'} + \dot{Y}\sin\theta_{E'} + \dot{u}_x - \omega_{E'}(y + u_y)\right]\vec{e}_1 + \left[-\dot{X}\sin\theta_{E'} + \dot{Y}\cos\theta_{E'} + \dot{u}_y + \omega_{E'}(x + u_x)\right]\vec{e}_2 \qquad (3.9)$$

The kinetic energy K_e of the element is:

$$K_e = \frac{1}{2}\int_v \rho\,\dot{\vec{R}}_K.\dot{\vec{R}}_K\,dv \qquad (3.10)$$

where ρ is the mass density of the link and the integration is carried over the whole volume v of the element.

Introducing eq. (3.9) in eq. (3.10) and utilising eqs. (3.1) and (3.2), the following relation results.

$$\begin{aligned} K_e = \frac{1}{2}\int_v \rho\,\Big[&(\dot{X}\cos\theta_{E'} + \dot{Y}\sin\theta_{E'} - \omega_{E'}y)^2 + (\dot{u}_y + \omega_{E'}u_x)^2 \\ &+ (-\dot{X}\sin\theta_{E'} + \dot{Y}\cos\theta_{E'} + \omega_{E'}x)^2 + (\dot{u}_x - \omega_{E'}u_y)^2 \\ &+ 2(\dot{X}\cos\theta_{E'} + \dot{Y}\sin\theta_{E'} - \omega_{E'}y)(\dot{u}_x - \omega_{E'}u_y) \\ &+ 2(-\dot{X}\sin\theta_{E'} + \dot{Y}\cos\theta_{E'} + \omega_{E'}x)(\dot{u}_y + \omega_{E'}u_x)\Big]dv \end{aligned} \qquad (3.11)$$

The continuous displacements $u_x(x, y, \tau)$ and $u_y(x, y, \tau)$ may be replaced by the nodal displacements $\bar{u}_1$ to $\bar{u}_6$ (Fig. 3.1) in the element oriented element co-ordinates

x-y with the aid of the shape function a defined by a 2x6 matrix in eq. (2.13) and is rewritten in expanded form as follows:

$$u_x = \sum_{j=1}^{6} a_{1j}\,\bar{u}_j \tag{3.12}$$

$$u_y = \sum_{j=1}^{6} a_{2j}\,\bar{u}_j \tag{3.13}$$

Employing eqs. (3.12) and (3.13) in eq. (3.11), the following terms are found out.

$$\frac{\partial K_e}{\partial \bar{u}_j} = \int_V \rho\,[(-\dot{X}\sin\theta_{E'} + \dot{Y}\cos\theta_{E'} + \omega_{E',x})\omega_{E'}a_{1j} - (\dot{X}\cos\theta_{E'} + \dot{Y}\sin\theta_{E'} - \omega_{E',y})\omega_{E'}a_{2j} - (\dot{u}_x - \omega_{E',u_y})\omega_{E'}a_{2j} + (\dot{u}_y + \omega_{E',u_x})\omega_{E'}a_{1j}]dv \tag{3.14}$$

and

$$\frac{\partial K_e}{\partial \dot{\bar{u}}_j} = \int_V \rho\,[(\dot{X}\cos\theta_{E'} + \dot{Y}\sin\theta_{E'} - \omega_{E',y})a_{1j} + (-\dot{X}\sin\theta_{E'} + \dot{Y}\cos\theta_{E'} + \omega_{E',x})a_{2j} + (\dot{u}_x - \omega_{E',u_y})a_{1j} + (\dot{u}_y + \omega_{E',u_x})a_{2j}]\,dv \tag{3.15}$$

The following relation is derived from eqs. (3.7), (3.14) and (3.15) for further use.

$$\frac{d}{dt}\left(\frac{\partial K_e}{\partial \dot{\bar{u}}_j}\right) - \frac{\partial K_e}{\partial \bar{u}_j} = \int_V \rho \begin{bmatrix} a_{1j} & a_{2j} \end{bmatrix} \begin{bmatrix} A_{Mx} - \omega_{E'}^2, x - \alpha_{E'}, y \\ A_{My} + \omega_{E'}^2, y + \alpha_{E'}, x \end{bmatrix} dv$$

$$+ \int_V \rho \begin{bmatrix} a_{1j} & a_{2j} \end{bmatrix} \begin{bmatrix} \ddot{u}_x \\ \ddot{u}_y \end{bmatrix} dv + \int_V \rho \begin{bmatrix} a_{1j} & a_{2j} \end{bmatrix} \begin{bmatrix} -\omega_{E'}^2, u_x \\ -\omega_{E'}^2, u_y \end{bmatrix} dv$$

$$+ \int_V \rho \begin{bmatrix} a_{2j} & -a_{1j} \end{bmatrix} \begin{bmatrix} 2\omega_{E'}, \dot{u}_x \\ 2\omega_{E'}, \dot{u}_y \end{bmatrix} dy$$

$$+ \int_V \rho \begin{bmatrix} a_{2j} & -a_{1j} \end{bmatrix} \begin{bmatrix} \alpha_{E'}, u_x \\ \alpha_{E'}, u_y \end{bmatrix} dv \qquad (3.16)$$

where,

$A_{Mx} = \ddot{X} \cos\theta_{E'} + \ddot{Y} \sin\theta_{E'}$ = Acceleration of the point M in the x-direction (3.17)

$A_{My} = -\ddot{X} \sin\theta_{E'} + \ddot{Y} \cos\theta_{E'}$ = Acceleration of the point M in the y-direction (3.18)

$$\omega_{E'} = \dot{\theta}_{E'} \qquad (3.19)$$

and $$\alpha_{E'} = \dot{\omega}_{E'} = \ddot{\theta}_{E'} \qquad (3.20)$$

The potential energy P_e stored in the link E' (neglecting the gravity) is the strain energy of the link and is given by eq. (3.21).

$$P_e = \frac{1}{2} \int_V \sigma^t e \, dv \qquad (3.21)$$

where $\sigma(x, y, \tau)$ and $e(x, y, \tau)$ are the stress and strain at any point of the link.

Continuous functions σ and e can be expressed in terms of $\bar{u}$ as shown in eqs. (2.20) and (2.16) and are rewritten here in the following expanded form.

$$e = \begin{bmatrix} e_1 \\ e_2 \end{bmatrix} \quad ; \qquad \sigma = \begin{bmatrix} \sigma_1 \\ \sigma_2 \end{bmatrix} \tag{3.22}$$

where,

$$e_1 = \sum_{j=1}^{6} b_{1j}\, \bar{u}_j \quad ; \quad e_2 = \sum_{j=1}^{6} b_{2j}\, \bar{u}_j \tag{3.23}$$

$$\sigma_1 = E\, e_1 \quad ; \quad \sigma_2 = \frac{GA_s}{A}\, e_2 \tag{3.24}$$

(b, E, G, A_s and A are defined in Section 2.3).

From eqs. (3.21) and (3.22),

$$P_e = \frac{1}{2} \int_v (\sigma_1 e_1 + \sigma_2 e_2)dv \tag{3.25}$$

Using eqs. (3.23) and (3.24) in eq. (3.25) and differentiating P_e with respect to $\bar{u}_j$,

$$\frac{\partial P_e}{\partial \bar{u}_j} = \frac{1}{2} \int_v (\sigma_1 b_{1j} + E\, b_{1j} e_1 + \sigma_2 b_{2j} + \frac{GA_s}{A}\, b_{2j}\, e_2)dv$$

$$= \int_v (E\, b_{1j} e_1 + \frac{GA_s}{A}\, b_{2j} e_2)dv$$

$$= \int_v [b_{1j} \quad b_{2j}] \begin{bmatrix} E & 0 \\ 0 & \frac{GA_s}{A} \end{bmatrix} \begin{bmatrix} e_1 \\ e_2 \end{bmatrix} dv \tag{3.26}$$

The strain energy P_e given by eq. (3.21), when used along with equation (2.17) for strains, does not take into account the additional work done by the axial forces on the foreshortening of the link due to the transverse displacements, i.e., the buckling effect of the axial forces. For the time being, it is assumed that these axial forces come from the rigid body forces (i.e., the rigid body axial accelerations of the link under consideration and the rigid body pin forces exerted by the other links on it) alone and therefore have known values. The additional axial forces generated due to the elastic deformations of the links are considered later in Section 3.4.

To include the buckling effect in the finite element method of analysis, the conventional procedure[58] is to use the higher order terms in the expression for the strains in eq. (3.21). But this procedure is unable to take into account the variation of the rigid body forces along the link, For this reason a special work function[63] is introduced below.

The displacement ΔL^b of the point of application of the axial force acting on the element (+ve in the +ve x-direction) due to the transverse displacement u_y alone is approximately given by eq. (3.27).

$$\Delta L^b \approx \frac{1}{2} \left(\frac{\partial u_y}{\partial x}\right)^2 dx \qquad (3.27)$$

Denoting the rigid body axial force at any point x by F_x, the work done by the foreshortening of the element due to the bending is given by eq. (3.28)

$$W_f = \frac{1}{2} \int_0^l F_x \left(\frac{\partial u_y}{\partial x}\right)^2 dx \qquad (3.28)$$

where,

W_f = the work done

and F_x = the rigid body axial force acting at the left end of the element dx (considered +ve in the +ve x-direction).

The axial force F_x, shown in Fig. 3.3, is:

$$F_x = P_M - \int_0^x \rho \, A(A_{Mx} - \omega_E^2, \xi) \, d\xi \qquad (3.29)$$

The rigid body pin force P_M may be obtained either by direct analysis of the rigid link mechanism (as described in Appendix D) or by the general method presented in Section 2.9. From eq. (3.13), $\frac{\partial u_y}{\partial x}$ can be written as

$$\frac{\partial u_y}{\partial x} = \sum_{j=1}^{6} a'_{2j} \bar{u}_j \qquad (3.30)$$

where $a'_{2j} = \frac{\partial a_{2j}}{\partial x}$; $j = 1, \ldots, 6$ (3.31)

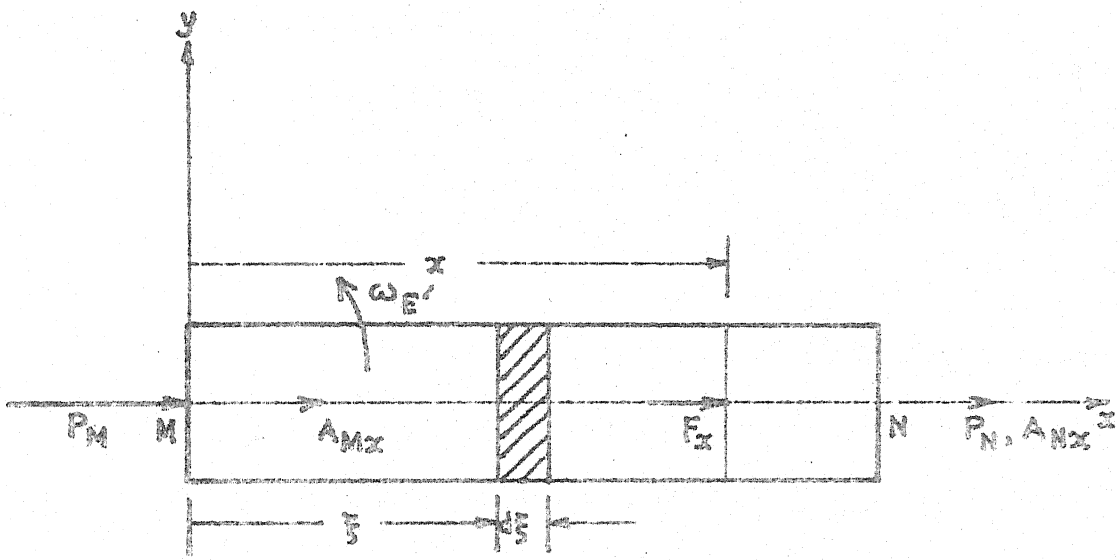

FIG 3.3 RIGID BODY AXIAL FORCES

Introducing eq. (3.30) in eq. (3.28) for $\frac{\partial u_y}{\partial x}$, eq. (3.32) is obtained.

$$\frac{\partial W_f}{\partial \bar{u}_j} = \int_0^l F_x \, a'_{2j} \, \frac{\partial u_y}{\partial x} \, dx \tag{3.32}$$

The Lagrange's equations of motion for the link can be written in the following form:

$$\frac{d}{dt}\left(\frac{\partial K_e}{\partial \dot{\bar{u}}_j}\right) - \frac{\partial K_e}{\partial \bar{u}_j} + \frac{\partial P_e}{\partial \bar{u}_j} - \frac{\partial W_f}{\partial \bar{u}_j} = \bar{Q}_j \tag{3.33}$$

$$j = 1, \ldots, 6$$

where $\bar{Q}_j$ is the external force (if any) acting at the j-th element co-ordinate.

Writing eqs. (3.16), (3.26) and (3.32) for j = 1, 2, ... 6, introducing them into the set of equations given by eq. (3.33) and using eqs. (3.12), (3.13), (3.23), (3.24) and (3.29), the following equation of motion in matrix form is finally arrived at.

$$\int_v \rho a^t \begin{bmatrix} A_{Mx} - \omega_{E,x}^2 - \alpha_{E,y} \\ A_{My} + \omega_{E,y}^2 + \alpha_{E,x} \end{bmatrix} dv + \bar{m}\,\ddot{\bar{u}} - \omega_{E,\bar{m}}^2\,\bar{u} + 2\bar{m}^a\,\omega_{E,}\,\dot{\bar{u}}$$

$$+ \alpha_{E,}\,\bar{m}^a\,\bar{u} + \bar{K}\,\bar{u} + \bar{K}^G\,\bar{u} = \bar{Q} \tag{3.34}$$

where,

$$\bar{m} = \int_v \rho a^t \, a \, dv \tag{2.24}$$

$$[\bar{m}^a_{ij}] = \int_v \rho (a_{2i}a_{1j} - a_{1i}a_{2j}) dv \tag{3.35}$$

$$\bar{k} = \int_v b^t \chi b \, dv \tag{2.23}$$

$$[\bar{k}^G_{ij}] = -\int_v F_x \, a'_{2i} \, a'_{2j} \, dv \tag{3.36}$$

$$\bar{Q} = \{ \bar{Q}_1, \ldots, \bar{Q}_6 \} \tag{3.37}$$

The matrices $\bar{m}^a$ and $\bar{k}^G$ in final form are given in Appendix B.

If the x-axis passes through the centroid of the cross-section of a straight link, the following relation holds.

$$\int_v y \, dv = 0 \tag{3.38}$$

Noting that the second row of the shape function does not contain y, the first term becomes equal to

$$- \bar{p} - \bar{p}^a$$

where,

$$\bar{p} = -\int_v \rho a^t \begin{bmatrix} A_{Mx} - \omega^2_{E',x} \\ A_{My} + \alpha_{E',y} \end{bmatrix} dv \tag{3.39}$$

and

$$\bar{p}^a = -\int_v \rho \, a^t \begin{bmatrix} \alpha_{E',y} \\ 0 \end{bmatrix} dv \tag{3.40}$$

It may be noted that $\bar{p}$ in eq. (3.39) is same as that given by eq. (2.25) differing only in notations and $\bar{p}^a$ is the additional rigid body force due to the effect of the angular acceleration $\alpha_{E'}$. This term is small when either $\alpha_{E'}$ or the second moment of area of the cross-section is small.

Thus the general equation of motion (3.34) is rewritten as follows:

$$\bar{m}\,\ddot{\bar{u}} + 2\omega_{E'}\bar{m}^a\,\dot{\bar{u}} + (\bar{k} - \omega_{E'}^2\bar{m} + \bar{k}^G + \alpha_{E'}\bar{m}^a)\bar{u} = \bar{p} + \bar{p}^a + \bar{Q} = \bar{p}_T \tag{3.41}$$

The terms $\bar{m}\,\ddot{\bar{u}}$, $\bar{k}\,\bar{u}$ and $\bar{p}$ were also previously obtained from the conventional procedure used in Chapter II. The term $2\omega_{E'}\bar{m}^a\dot{\bar{u}}$ comes due to the Coriolis component of the elastic longitudinal and transverse acceleration of the link in a rotational velocity field. The term $-\omega_{E'}^2\bar{m}\,\bar{u}$ takes into account the centrifugal effect of the elastic motions (in both directions) in a rotational velocity field. The additional acceleration term arising due to the longitudinal and transverse vibrations in a rotational acceleration field is given by $\alpha_{E'}\bar{m}^a\bar{u}$. The term $\bar{k}^G\,\bar{u}$ includes the buckling effect of the rigid body forces as explained earlier. It is interesting to note that the secondary mass matrix $\bar{m}^a$, given by eq. (3.35), is antisymmetric while the other matrices $\bar{m}$, $\bar{k}$ and $\bar{k}^G$ are symmetric.

For the reasons explained in the next sections, the element matrices and the force vector in eq. (3.41) are divided into five groups, i.e., (i) $\bar{m}$, (ii) $2\omega_E, \bar{m}^a$, (iii) $(\bar{k} - \omega_E^2, \bar{m} + \bar{k}^G)$, (iv) $\alpha_E, \bar{m}^a$ and (v) the vector $\bar{p}_T = \bar{p} + \bar{p}^a + \bar{Q}$. The first four groups of the matrices for all elements are transformed into the system oriented element co-ordinates and next are assembled to form four system matrices, following the procedure described in Sections 2.3 and 2.4. It may be noted that the pin forces P_M are the internal forces and therefore need not be included in the force vector because the stiffness (or displacement) method of finite element analysis automatically satisfies the compatibility of the internal forces whenever the compatibility of the displacements are satisfied.

When the links of the mechanism are subdivided into several elements, equation of motion for each element is evidently given by eq. (3.41) where the matrices of eq. (3.41) are to be formed for each element. For a link with constant cross-section, the terms $\bar{m}$, $2\omega_E$, $\bar{m}^a$, $\bar{k}$, $-\omega^2_E$, $\bar{m}$, α_E, $\bar{m}^a$ and $\bar{p}^a$ are identical for all the elements generated from that link and are to be calculated only once. However, the terms $\bar{k}^G$, $\bar{p}$ and $\bar{Q}$ are different even for these elements and therefore have to be calculated separately.

The assembly of the element matrices and the incorporation of the special conditions of the mechanism into the system matrices are carried out as described in Section 2.4. The general equation of motion in the system co-ordinates finally assumes the following form:

$$M\ddot{U} + (C + C^a)\dot{U} + (K + K^N + K^G) + K^T \; U = P \qquad (3.42)$$

where,

M = mass matrix

C = damping matrix

C^a = apparent damping matrix due to the additional Coriolis components of accelerations

K = elastic stiffness matrix

K^N = apparent stiffness matrix due to the additional normal components of accelerations

K^G = geometric stiffness matrix

K^T = apparent stiffness matrix due to the additional tangential components of accelerations

P = force vector

and $U(\tau)$ = displacement vector in the system co-ordinates.

The matrices M, C^a, K, K^N, K^G and K^T are formed from the assembly of the element matrices $\bar{m}$, $2\omega_E, \bar{m}^a$, $\bar{k}$, $-\omega^2_E, \bar{m}$, $\bar{k}^G$ and $\alpha_E, \bar{m}^a$ of eq. (3.41). Similarly, the force vector P results from the assembly of the element force

vectors $\bar{p}_T$ of eq. (3.41). The matrix C is the damping matrix of the system and may be taken (as was done in Section 2.5.4) to be proportional to the critical damping at the normal modes of the mechanism. Though associated with the damping term, the matrix C^a is not dissipative because the contribution of this term towards the total amount of work done by the individual normal modes of the system is zero. The conservative nature of C^a follows from its antisymmetry.

3.3 Solution of Equation of Motion

The undamped eigenvalue problem for equation (3.42) may be formulated in the form of eq. (3.43).

$$M\ddot{X} + C^a\dot{X} + K^oX = 0 \qquad (3.43)$$

The eigenvectors (or eigenmodes) obtained from the solution of eq. (3.43) will form a system of uncoupled equations in the normal co-ordinates. But these eigenvectors and the corresponding eigenvalues are complex quantities and excessive computations are involved with their use.

Alternatively, the eigenvalue problem may be formulated in the following way:

$$M\ddot{X} + K^oX = 0 \qquad (3.44a)$$

where $$K^o = K + K^N + K^G + K^T \qquad (3.44b)$$

Because of the antisymmetry of K^T, the eigenvectors of eq. (3.44a) are mutually independent but not orthogonal to each other with respect to either M or K^o. For this reason, the solution of eq. (3.44a) by Power method to find the sub-dominant eigenvalues and vectors requires[64] either the right-hand and left-hand eigenvectors simultaneously or the matrix deflation procedure. Either of these two techniques increases the volume of computation. Moreover, the eigenvectors obtained from eq. (3.44a) can not diagonalise the matrix C^a and so the resulting equations in the normal co-ordinates still remain coupled.

In view of the above, the following simple formulation of the eigenvalue problem is adopted for subsequent use.

$$M\ddot{X} + K^S X = 0 \qquad (3.45a)$$

where $K^S = K + K^N + K^G$, the symmetric part of K^o (3.45b)

As both M and K^S are real and symmetric, the eigenvalues and eigenvectors of eq. (3.45a) are real and orthogonal to each other with respect to M or K^S. But these eigenvectors do not diagonalise K^a or C^a. To overcome this difficulty, an approximate method is developed below for solving the coupled equations in the normal co-ordinates.

Two assumptions are made in the following approximate method. The first of them may be stated as

follows: the eigenvalues and eigenmodes obtained from eq. (3.45) represent the actual behaviour of the system (in its free vibration) with reasonable degree of accuracy. The second assumption will be mentioned in due course. Though the approximate method described below is equally applicable to all situations treated in Chapter II, it is assumed, to simplify the presentation, that the rigid body forces remain constant during the interval of time $\Delta\tau$ and satisfy the static equilibrium equation for the rigid body degrees of freedom (so that only the elastic modes may be used).

The eigenvalues and eigenvectors of eq. (3.45) are found out following the procedure described in Section 2.5.2 and the modal matrix Φ' is formed. Employing this modal matrix Φ', the following transformation of co-ordinates is defined.

$$U = \Phi'\eta \tag{3.46a}$$

where $\eta(\tau)$ is the displacement vector in the normal co-ordinate system. As Φ' is independent of time (during the current interval), the following equations result from the differentiation of eq. (3.46a) with respect to time τ.

$$\dot{U} = \Phi'\dot{\eta} \tag{3.46b}$$

and

$$\ddot{U} = \Phi'\ddot{\eta} \tag{3.46c}$$

Substitution of eqs. (3.46) in eq. (3.42) and pre-multiplication by Φ'^{t}, yield the following equation of motion in the normal co-ordinates.

$$\overline{M}\ddot{\eta} + (\overline{C} + \overline{C^a})\dot{\eta} + (\overline{K^S} + \overline{K^a})\eta = \overline{P} \tag{3.47}$$

where,

$$\begin{aligned}
\overline{M} &= \Phi'^{t}\, M\, \Phi' \\
\overline{C} &= \Phi'^{t}\, C\, \Phi' \\
\overline{C^a} &= \Phi'^{t}\, C^a\, \Phi' \\
\overline{K^S} &= \Phi'^{t}\, K^S\, \Phi' \\
\overline{K^a} &= \Phi'^{t}\, K^a\, \Phi'
\end{aligned} \tag{3.48}$$

and $\overline{P} = \Phi'^{t}\, P$

As explained in Chapter II, $\overline{M}$, $\overline{C}$ and $\overline{K^S}$ are diagonal matrices. Consequently, the i-th equation of eq. (3.47) may be written as:

$$\ddot{\eta}_i + 2\xi_i \omega_i \dot{\eta}_i + \omega_i^2 \eta_i + \sum_{j=1}^{m} \varepsilon_{ij}\dot{\eta}_j + \sum_{j=1}^{m} \nu_{ij}\eta_j = p_i \tag{3.49}$$

$$i = 1, \ldots, m.$$

where p_i is the i-th element of $\overline{M}^{-1}\,\overline{P}$, ω_i is the i-th natural frequency found out from eq. (3.45), η_i is the i-th element of η, ξ_i is the damping ratio at the i-th mode, and ε_{ij}, ν_{ij} are the (i,j)-th element of $\overline{M}^{-1}\,\overline{C^a}$ and $\overline{M}^{-1}\overline{K^a}$ respectively.

Since $\bar{C}^a$, $\overline{K^a}$ are antisymmetric,

$$\varepsilon_{ii} = \nu_{ii} = 0 \tag{3.50}$$

Consequently, it is convenient to rewrite eq. (3.49) in a rearranged form as shown in eq. (3.51)

$$\ddot{\eta}_i + 2\xi_i\omega_i\dot{\eta} + \omega_i^2\eta_i = p_i - \sum_{\substack{j=1 \\ j\neq i}}^{m} \varepsilon_{ij}\dot{\eta}_j - \sum_{\substack{j=1 \\ j\neq i}}^{m} \nu_{ij}\eta_j \tag{3.51}$$

$$i = 1, \ldots, m.$$

In view of eq. (3.50), the left side of eq. (3.51) still maintains the standard form of eq. (2.63) and shows that the coupling terms affect the forcing terms p_i more significantly than the natural frequency ω_i. Thus, the first assumption stated above can be further reinforced by adding very few additional modes in Φ'.

The complete solution of eq. (3.51) can be divided into three parts: i) the homogeneous solution η_i^h, ii) the particular solution η_i^f due to the forcing term p_i only and iii) particular solution η_i^a due to the additional terms $-\sum_{j=1}^{m}(\varepsilon_{ij}\dot{\eta}_j - \nu_{ij}\eta_j)$. Thus, the complete solution η_i is given by the following relation:

$$\eta_i(\tau) = \eta_i^h(\tau) + \eta_i^f(\tau) + \eta_i^a(\tau) \tag{3.52}$$

$$\tau_o < \tau < \tau_o + \Delta\tau$$

where,

$$\eta_i^h = e^{-\sigma_i \tau'} (I_i^1 \cos\mu_i \tau' + I_i^2 \sin\mu_i \tau')$$

$$\eta_i^f = \frac{p_i}{m_i \omega_i^2}$$

$$\tau' = \tau - \tau_o \qquad (3.53)$$

$$\sigma_i = \xi_i \omega_i$$

$$\mu_i = (1 - \xi_i^2)^{\frac{1}{2}} \omega_i$$

ξ_i = damping ratio at the i-th normal mode

I_i^1, I_i^2 = constants of integration

and η_i^a is given by the particular solution of the following equation:

$$\ddot{\eta}_i^a + 2\xi_i \omega_i \dot{\eta}_i^a + \omega_i^2 \eta_i^a = - \sum_{j=1}^{m} (\varepsilon_{ij} \dot{\eta}_j + \nu_{ij} \eta_j) \qquad (3.54)$$

(the restriction $j \neq i$ is removed in view of eq. (3.50)).

Since the right side of eq. (3.54) contains various functions of time τ, the functional nature of the actual η_i^a is very much involved. Therefore, instead of finding the actual η_i^a (which satisfies eq. (3.54) identically), an approximate expression for η_i^a is sought which satisfies eq. (3.54) only at some specified instants of time. The second assumption is now made as follows: the actual η_i^a satisfying eq. (3.54) can be adequately described by a parabolic expression (given by eq. (3.55)) during a small interval of time $\Delta\tau$.

$$\eta_i^a(\tau) = H_{3i-2} + H_{3i-1}(\tau - \tau_o) + H_{3i}(\tau - \tau_o)^2 \qquad (3.55)$$

where the unknown constants H_{3i-2}, H_{3i-1} and H_{3i} are to be determined.

As $\tau = \tau - \tau_o$ is small and η_i^a is not expected to vary widely in this small interval $\Delta\tau$, the second assumption seems to be justified.

Eq. (3.52) can now be rewritten in eq. (3.56) as

$$\eta_i(\tau) = I_i^1 f_i^1(\tau) + I_i^2 f_i^2(\tau) + \frac{p_i}{m_i \omega_i^2} + H_{3i-2} + H_{3i-1}(\tau - \tau_o) + H_{3i}(\tau - \tau_o)^2 \qquad (3.56)$$

consequently,

$$\dot{\eta}_i(\tau) = I_i^1 f_i^3(\tau) + I_i^2 f_i^4(\tau) + H_{3i-1} + 2H_{3i}(\tau - \tau_o) \qquad (3.57)$$

where,

$$f_i^1(\tau) = e^{-\sigma_i \tau'} \cos \mu_i \tau'$$

$$f_i^2(\tau) = e^{-\sigma_i \tau'} \sin \mu_i \tau'$$

$$f_i^3(\tau) = \frac{d}{d\tau}(f_i^1(\tau)) = e^{-\sigma_i \tau'}(-\sigma_i \cos \mu_i \tau' - \mu_i \sin \mu_i \tau') \qquad (3.58)$$

and $$f_i^4(\tau) = \frac{d}{d\tau}(f_i^2(\tau)) = e^{-\sigma_i \tau'}(-\sigma_i \sin \mu_i \tau' + \mu_i \cos \mu_i \tau')$$

Using the initial conditions

$$\begin{aligned} \eta_i(\tau_o) &= \eta_i^o \\ \dot{\eta}_i(\tau_o) &= \dot{\eta}_i^o \end{aligned} \tag{3.59}$$

the constants of integration I_i^1, I_i^2 are found out from eqs. (3.56) and (3.57) as

$$\begin{aligned} I_i^1 &= (\eta_i^o - \frac{p_i}{m_i \omega_i^2} - H_{3i-2}) \\ I_i^2 &= \frac{\dot{\eta}_i^o - I_i^4 + \sigma_i I_i^1}{\mu_i} \end{aligned} \tag{3.60}$$

Eliminating I_i^1 and I_i^2 from eqs. (3.56) and (3.57) by eq. (3.60), $\eta_i(\tau)$ and $\dot{\eta}_i(\tau)$ are reduced to

$$\eta_i(\tau) = \beta_i(\tau) + \gamma_{3i-2}(\tau)\, H_{3i-2} + \gamma_{3i-1}(\tau)\, H_{3i-1} + \gamma_{3i}(\tau)\, H_{3i} \tag{3.61}$$

$$\dot{\eta}_i(\tau) = \varphi_i(\tau) + \psi_{3i-2}(\tau)\, H_{3i-2} + \psi_{3i-1}(\tau)\, H_{3i-1} + \psi_{3i}(\tau)\, H_{3i} \tag{3.62}$$

where,

$$\beta_i(\tau) = (\eta_i^o - \frac{p_i}{m_i \omega_i^2}) f_i^1(\tau) + [\dot{\eta}_i^o + \sigma_i\, (\dot{\eta}_i^o - \frac{p_i}{m_i \omega_i^2})] \frac{f_i^2(\tau)}{\mu_i} + \frac{p_i}{m_i \omega_i^2}$$

$$\gamma_{3i-2}(\tau) = 1 - f_i^1(\tau) - \frac{\sigma_i}{\mu_i} f_i^2(\tau)$$

$$\gamma_{3i-1}(\tau) = \tau - \tau_o - \frac{f_i^2(\tau)}{\mu_i}$$

$$\gamma_{3i}(\tau) = (\tau - \tau_o)^2$$

$$\varphi_i(\tau) = (\eta_i^o - \frac{p_i}{m_i\omega_i^2})f_i^3(\tau) + [\dot{\eta}_i^o + \sigma_i(\dot{\eta}_i^o - \frac{p_i}{m_i\omega_i^2})] \frac{f_i^4(\tau)}{\mu_i} \qquad (3.63)$$

$$\psi_{3i-2}(\tau) = - f_i^3(\tau) - \frac{\sigma_i f_i^4(\tau)}{\mu_i}$$

$$\psi_{3i-1}(\tau) = 1 - \frac{f_i^4(\tau)}{\mu_i}$$

$$\psi_{3i}(\tau) = 2(\tau - \tau_o)$$

Substituting $\eta_i(\tau)$, $\dot{\eta}_i(\tau)$ and $\dot{\eta}_i^a(\tau)$ from eqs. (3.61), (3.62) and (3.55) in eq. (3.54), the following equation is obtained.

$$\omega_i^2 H_{3i-2} + (\tau - \tau_o + 2\xi_i\omega_i)H_{3i-1} + [(\tau - \tau_o)^2 + 4\xi_i\omega_i(\tau - \tau_o)] H_{3i}$$

$$= - \sum_{j=1}^{m} [\varepsilon_{ij} \{ \varphi_j(\tau) + \psi_{3j-2}(\tau)H_{3j-2} + \psi_{3j-1}(\tau)H_{3j-1} +$$

$$\psi_{3j}(\tau)H_{3j} \} + \nu_{ij} \{\beta_j(\tau) + \gamma_{3j-2}(\tau)H_{3j-2} + \gamma_{3j-1}(\tau)H_{3j-1}$$

$$+ \gamma_{3j}(\tau)H_{3j} \}] \qquad (3.64)$$

Since eq. (3.55) contains three unknowns, three values of τ are to be used on both sides of eq. (3.54), i.e.,

eq. (3.64) to determine these unknowns. But the eq. (3.64) is coupled and hence all the unknowns H_j, $j = 1, \ldots, 3m$ are to be found out from a set (3m in number) of simultaneous equations.

The following three values of τ are used

$$\tau^0 = \tau_0 + \frac{\Delta\tau}{3} ; \quad \tau^1 = \tau_0 + \frac{2\Delta\tau}{3} ; \quad \tau^2 = \tau_0 + \Delta\tau \tag{3.65}$$

Alternative choice of τ^0, τ^1 and τ^2 could as well be made by using Chebyshev's polynomials[61]. For each value of i, $i = 1, \ldots, m$, the above three values of τ are substituted in eq. (3.64) resulting in 3 simultaneous equations. Finally, the 3m numbers of equations, thus obtained, are rewritten in the following matrix form.

$$GH = L \tag{3.66}$$

where,

$$L_{3i-q} = - \sum_{j=1}^{m} [\varepsilon_{ij} \varphi_i(\tau^q) + \nu_{ij} \beta_i(\tau^q)]$$

$$G_{3i-q,3j-r} = \varepsilon_{ij} \psi_{3j-r}(\tau^q) + \nu_{ij} \gamma_{3j-r}(\tau^q) \qquad j \neq i \tag{3.67}$$

$$G_{3i-q,3i-2} = \omega_i^2$$

$$G_{3i-q,3i-1} = \tau^q - \tau_0 + 2\xi_i\omega_i$$

$$G_{3i-q,3i} = (\tau^q - \tau_0)^2 + 4\xi_i\omega_i(\tau^q - \tau_0)$$

$$i = 1, \ldots, m$$
$$j = 1, \ldots, m$$

q is given values 0, 1 and 2 successively for each value of i. Similarly r is given values 0, 1 and 2 successively for each value of j.

Since L and G in eq. (3.66) are known, the unknowns H are obtained by inverting the matrix G as follows:

$$H = G^{-1}L \tag{3.68}$$

Using these values of H in eqs. (3.61) and (3.62), the displacements η and velocities $\dot{\eta}$ in normal co-ordinates are obtained. The accelerations $\ddot{\eta}$ in normal co-ordinates are obtained from eq. (3.51) as follows:

$$\ddot{\eta}_i = p_i - \sum_{j=1}^{m} (\varepsilon_{ij}\,\dot{\eta}_j + \nu_{ij}\,\eta_j) - 2\xi_i\omega_i\dot{\eta}_i - \omega_i^2\eta_i \tag{3.69}$$

The displacements, velocities and accelerations are next found out in the element oriented element co-ordinates following the same procedure as explained in Chapter II.

3.4 Elastic Axial Forces

In the above sections, the pin forces P_M in eq. (3.36) were considered to be independent of the elastic behaviour of the mechanism and were evaluated from the analysis of the rigid link mechanism. In actual case, additional axial forces within a link are generated due to its own longitudinal vibrations, the foreshortening due to

its transverse vibrations and the elastic effects of other links transmitted through the pins at its ends during the interval $\Delta\tau$. In other words, the term F_x in eq. (3.36) is a function of the element displacements (represented by $\bar{u}(\tau)$) and therefore eq. (3.42) becomes non-linear. As a good estimate of the axial forces is available from the analysis of the previous interval, the iterative procedure, as described below, seems to be more suitable than the other methods available in non-linear finite element method of analysis[58,60,65].

At the beginning of the current interval, the element oriented element displacements (axial) $\bar{u}_1(\tau_o)$ and $\bar{u}_4(\tau_o)$ at the two ends of each element are known from the analysis of the previous interval. Then the average value of the axial force F_x acting on the element at that instant is found out from eq. (3.70).

$$F_x = EA \frac{\bar{u}_1(\tau_o) - \bar{u}_4(\tau_o)}{l} \qquad (3.70)$$

where E, A and l are Young's modulus, cross-sectional area and length of the element. Evaluating F_x in this way, the element geometric stiffness matrix $\bar{k}^G$ is formed from eqs. (3.29), (3.31) and (3.36). These matrices are next assembled to form the geometric stiffness matrix $\mathbf{K}^G$ for the whole mechanism and is used in eq. (3.42). After solving eq. (3.42),

the element displacements $\bar{u}_1(\tau_o + \Delta\tau)$ and $\bar{u}_4(\tau_o + \Delta\tau)$ at the end of the interval is determined as described in the previous section. Using these element displacements, the axial forces F_x for the elements are calculated from eq. (3.70). The difference ΔF_x between this value of F_x and its former value is evaluated for each element. If the maximum of these differences is less than the prescribed value, the procedures for the next interval should be started. Otherwise, a new geometric matrix for each element is found by using the latest F_x in eq. (3.36) and all such matrices are assembled to form a new geometric matrix for the whole system. Employing this new geometric stiffness matrix, eq. (3.42) is again solved for the element displacements and eventually for axial forces. The process is repeated for the same crank position until the convergence is achieved. The element displacements, velocities and accelerations at the end of the iteration process are used for the stress calculations of the current interval and as the 'initial conditions' for the next interval as mentioned in Chapter II. Since at the start of the iteration, elastic axial forces are found out from eq. (3.70) by using the values of the displacements obtained from the previous interval, the calculation for the rigid body axial forces may be omitted altogether.

Evidently, the above procedure is more time consuming than the equivalent procedure for the rigid body axial forces because eq. (3.42) (which requires the solution of the eigenvalue problem, eq. (3.45), and eq. (3.66) in particular) is to be solved for each iteration. However, if the interval of time is made smaller, very few (usually two only) iterations are needed for each interval.

It may be noted that though the matrices K and K^G in eq. (3.45) are singular, the matrix K^S is, strictly speaking, non-singular due to the presence of the non-singular matrix K^N. However, the elements of K^N are small compared to those of K and K^G (except at unusually high speeds). Thus, the matrix K is always nearly singular. For this reason, it is advisable to use the method of Section 2.5.2 for the solution of the eigenvalue problem.

CHAPTER IV

DIRECT STEADY STATE ANALYSIS

4.1 Introduction

The basic framework of the analysis presented in the Chapters II and III is based on the conventional procedures of the finite element method. Though this framework allows the designer to find the deflections and the stresses of the mechanism in very general cases, it nevertheless fails to predict the parametric instability of the mechanisms unless frequency response curves are obtained at the cost of huge computer time. Moreover, the method of analysis treats the continuous motion of the mechanism by dividing it into numerous small intervals, the vibrations at the end of each interval being incorporated in the subsequent interval as 'initial conditions'. Thus, even if steady-state deflections only are desired, the analysis has to be carried out through a large number of intervals until the steady-state conditions are reached. This method of describing the steady-state motions by recurrent use of the transient motions is certainly not efficient as it entails a heavy loss of computer time. In view of these drawbacks a new approach to the analysis of flexible mechanisms is presented in this

chapter. This method of analysis, applicable to a restricted class of mechanisms for which the rigid body harmonic analysis is available beforehand, enables the designer to find out the steady-state deflections and stresses in a straightforward manner. The analysis may be equally applied to determine the instability zones of the operating speeds of the input crank. In Section 4.2, the element oriented element co-ordinates are selected in the usual way and, starting from the harmonic analysis of the angles, the equation of motion of each element is derived. The element co-ordinates are also considered as system co-ordinates and the equation of motion for the whole mechanism is derived in these system co-ordinates. The boundary conditions are introduced in the form of a set of compatibility equations. Next, the displacements are expressed in Fourier series, the constraints expressed by the compatibility equations are eliminated and finally the differential equation of motion is reduced to a set of algebraic equations. Using this set of equations, the steady-state deflections and stresses are calculated in Section 4.3. Finally, the same set of equations are utilised in Section 4.4 to find out the various instability zones for the operating speeds.

4.2 Equation of Motion

4.2.1 Element analysis

For the method of analysis described in this chapter, it is assumed that the mechanism is planar with uniformly straight links and has only one input crank rotating with constant speed ω. The method can be easily extended to other mechanisms provided the associated rigid body harmonic analysis is already known.

In case of any element E' shown in Fig. 3.1, Fourier series expressions for sine and cosine of the angle $\theta_{E'}$, are given by eqs. (2.85) and (2.86). Similar expressions for the angular speed $\omega_{E'}$, $\omega^2_{E'}$ and the angular acceleration $\alpha_{E'}$ are given by eqs. (2.89), (2.90) and (2.91) respectively. Corresponding to the element E', the element co-ordinate axes x-y and the element oriented element co-ordinates $\bar{u}_1$ to $\bar{u}_6$ are selected in the same manner of Chapter III and are shown in Fig. 3.1. The element oriented element force vector $\bar{p}$ due to the rigid body inertia forces and other external forces (external forces having a fundamental frequency different from the crank speed will not be considered in this chapter) is given by eq. (2.100).

The series expressions for the rigid body pin force P_M, $\omega^2_{E'}$ and A_{Mx}, obtained from the rigid body analysis

(Appendix D), eq. (2.90) and (2.93) respectively, are put in the expression of the element oriented element geometric stiffness matrix $\bar{k}^G$ (Appendix B). The resulting series expression for $\bar{k}^G$ may be written in the following form:

$$\bar{k}^G = \sum_{j=1}^{h_1} [\bar{k}_j^1 \cos(j-1)\omega\tau + \bar{k}^2 \sin j\omega\tau]$$

$$+ \omega^2 \sum_{j=1}^{h_1} [\bar{k}_j^3 \cos(j-1)\omega\tau + \bar{k}_j^4 \sin j\omega\tau] \qquad (4.1)$$

where $\bar{k}_j^1$, $\bar{k}_j^2$, $\bar{k}_j^3$ and $\bar{k}_j^4$ are 6 x 6 matrices. The ω-dependent part of $\bar{k}^G$ is separately treated for the purpose of the stability analysis outlined in Section 4.4.

Upon substitution of the series expressions for $\omega_{E'}$, $\omega_{E'}^2$, $\bar{k}^G$, $\alpha_{E'}$ and $\bar{p}$ in eq. (3.41), the equation of motion for the element assumes the following form (neglecting $\bar{p}^a$ and $\bar{Q}$):

$$\bar{m}\,\ddot{\bar{u}} + 2\,\bar{c}^c\dot{\bar{u}} + (\bar{k}^c + \omega^2\bar{k}^v)\bar{u} = \bar{p} \qquad (4.2)$$

where,

$$\bar{c}^c = \sum_{j=1}^{h_1} [\bar{c}_j^1 \cos(j-1)\omega\tau + \bar{c}_j^2 \sin j\omega\tau]$$

$$\bar{c}_j^1 = vc_j\,\bar{m}^a$$

$$
\begin{aligned}
\bar{c}_j^2 &= vs_j\, \bar{m}^a \\
\bar{k}^c &= \sum_{j=1}^{h_1} [\bar{k}_j^5 \cos(j-1)\,\omega\tau + \bar{k}_j^2 \sin j\omega\tau] \\
\bar{k}^v &= \sum_{j=1}^{h_1} [\bar{k}_j^6 \cos(j-1)\,\omega\tau + \bar{k}_j^7 \sin j\omega\tau] \\
\bar{k}_1^5 &= \bar{k} + \bar{k}_1^1 \\
\bar{k}_j^5 &= \bar{k}_j^1 \quad , \qquad j = 2, \ldots, h_1 \\
\bar{k}_j^6 &= \bar{k}_j^3 - nc_j\bar{m} + tc_j\bar{m}^a \\
\bar{k}_j^7 &= \bar{k}_j^4 - ns_j\bar{m} + ts_j\bar{m}^a \qquad , \quad j = 1, \ldots, h_1
\end{aligned}
\tag{4.3}
$$

and $\bar{m}$, $\bar{k}$ and $\bar{p}$ are given by eqs. (2.24), (2.23) and (2.100) respectively. vc_j, vs_j, nc_j, ns_j, tc_j, ts_j are defined in Section 2.7 and $\bar{m}^a$ is defined in eq. (3.35).

Equations similar to eq. (4.2) are derived for all elements of the mechanism following the above procedure and it completes the element analysis.

4.2.2 Assembly of elements

Unlike the previous chapters, here the system co-ordinates selected are in the directions of the element co-ordinates associated with the respective nodes. This implies that three system co-ordinates are defined at each

intermediate mode within a link in the directions matching with the element oriented element co-ordinate system attached to that link. For nodes connecting the end points of several links, three system co-ordinates for each of the links are defined as done in case of the intermediate nodes and thus the total number of the system co-ordinates for such nodes is equal to three times the number of the links attached to that node. Examples for this kind of the system co-ordinates are shown in Fig. 4.1.

However, this special choice of the system co-ordinates does not preclude the use of the code-system of assembly described in Section 2.4. On the contrary, the effectiveness of the code-system is more apparent in this case. After performing the assembly of the element matrices $\bar{m}$, $\bar{c}$, $\bar{k}^c$, $\bar{k}^v$ and the vector $\bar{p}$ in the manner described in Section 2.4, the corresponding system matrices are formed and the equation of motion for the whole system is rewritten in n numbers (say) of the system co-ordinates as follows:

$$MU + 2C^d\dot{U} + 2\,C^c\dot{U} + (K^c + \omega^2 K^v)U = P \qquad (4.4)$$

where,

$$C^d = \sum_{j=1}^{h_1} \xi_j' \omega M$$

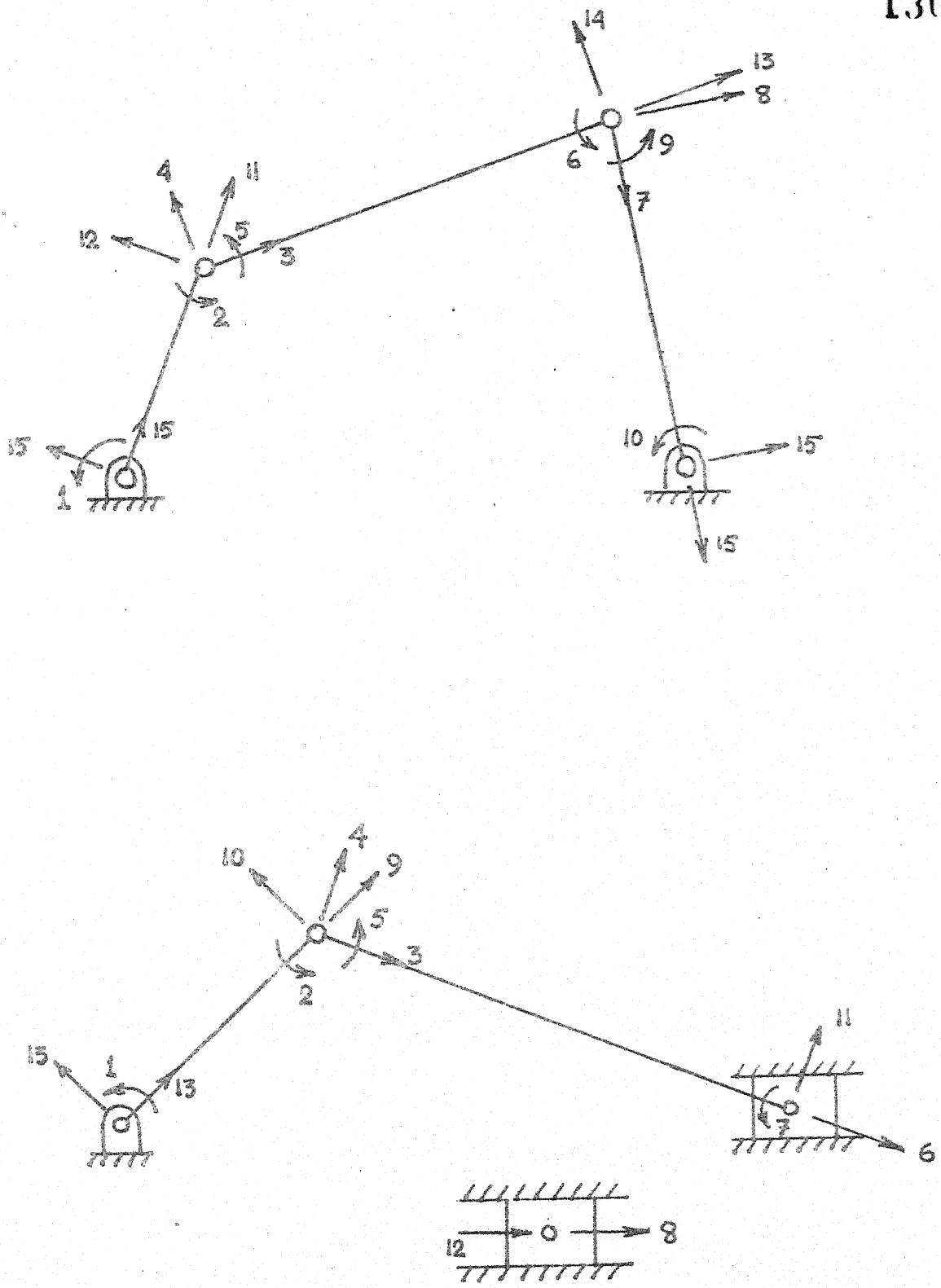

FIG 4.1 ELEMENT ORIENTED SYSTEM COORDINATES

$$C^c = \sum_{j=1}^{h_1} [C_j^1 \cos(j-1)\omega\tau + C_j^2 \sin j\omega\tau]$$

$$K^c = \sum_{j=1}^{h_1} [K_j^1 \cos(j-1)\omega\tau + K_j^2 \sin j\omega\tau] \qquad (4.5)$$

$$K^v = \sum_{j=1}^{h_1} [K_j^3 \cos(j-1)\omega\tau + K_j^4 \sin j\omega\tau]$$

$$P = \sum_{j=1}^{h_1} [P_j^1 \cos(j-1)\omega\tau + P_j^2 \sin j\omega\tau]$$

and U = nx1 displacement vector in the system co-ordinates. The nxn system matrices C_j^1, C_j^2, K_j^1, K_j^2, K_j^3, K_j^4 and nx1 system force vectors P_j^1, P_j^2 are formed from the assembly of the 6x6 element oriented element matrices $\bar{c}_j^1$, $\bar{c}_j^2$, $\bar{k}_j^5$, $\bar{k}_j^2$, $\bar{k}_j^6$, $\bar{k}_j^7$ and 6x1 element vectors $\bar{p}_j^1$, $\bar{p}_j^2$ respectively ($j = 1, \ldots, h_1$). The matrix C^d, taken as proportional to M, represents the material damping of the system. The c-oefficient ξ_j may be given suitable values for various values of j. From the rigid body force analysis, the input torque maintaining the 'static' equilibrium for the rigid body forces is determined in series form and is added to P appropriately. The 'special conditions' of the mechanism are also incorporated in eq. (4.4) in the usual way.

4.2.3 Constraint equations

The system co-ordinates selected in the previous section do not satisfy the boundary conditions existing at the joints of the links. The displacement boundary conditions at the joints are the compatibility of the displacements. Once these displacement compatibility conditions are satisfied, the compatibility conditions for the internal forces at these joints are automatically satisfied. At the hinged joints, the compatibility conditions are: the displacements of each link attached to the joint should be same in any two perpendicular directions. Since the displacements at the supported ends are zero, the corresponding boundary (or compatibility) conditions are automatically satisfied if no translational system co-ordinates are defined at these ends. It is evident that these compatibility equations depend only on the angles between the links.

The set of c numbers (say) of the compatibility equations for the whole mechanism may be written in the following matrix form:

$$SU = 0 \tag{4.6}$$

where,

$$S = \sum_{j=1}^{h_1} [S_j^1 \cos(j-1)\omega\tau + S_j^2 \sin j\omega\tau] \tag{4.7}$$

and S_j^1, S_j^2, $j = 1, \ldots, h_1$ are known cxn matrices. Explicit expressions for eq. (4.7) are shown in Appendix E for two simple mechanisms.

Equation (4.6) expresses the constraints which exist among the system displacement co-ordinates and consequently, the equation of motion given by eq. (4.4) is to be solved together with eq. (4.6). For this purpose, a set of c numbers of the dependent co-ordinates B are chosen from the total n numbers of the system co-ordinates. The numbering of the system co-ordinates should be done in such a way that these dependent co-ordinates form its last part. The corresponding partitioned form (the subscript A corresponds to the set of the independent co-ordinates) of eq. (4.6) is shown in eq. (4.8).

$$[S_A \quad S_B] \begin{bmatrix} U_A \\ U_B \end{bmatrix} = 0 \tag{4.8}$$

or,
$$U_B = S_C U_A \tag{4.9}$$

where
$$S_C = -S_B^{-1} S_A \tag{4.10}$$

Any set of c numbers of the co-ordinates from the set of the system co-ordinates may be chosen as the dependent co-ordinates provided that the sub-matrix S_B

becomes non-singular (because its inverse is used in eq. (4.10)). Furthermore, by writing the constraint equations suitably, the sub-matrix S_B can be reduced to a unit matrix.

The system co-ordinates are now transformed into a set of generalised co-ordinates (total number is n-c) in accordance with the following co-ordinate transformation:

$$U = \begin{bmatrix} U_A \\ \\ U_B \end{bmatrix} = S_D U_C \tag{4.11}$$

where $S_D = \left[\frac{I}{S_C}\right]$ (4.12)

Using the contragradient law of transformation, the equation of motion is next expressed in the generalized co-ordinate system as shown by eq. (4.13).

$$M^*\ddot{U}_C + 2\,C^*\dot{U}_C + K^*U_C = P^* \tag{4.13}$$

where,

$$\begin{aligned} M^* &= S_D^t M S_D \\ C^* &= S_D^t(C^d + C^c)S_D \\ K^* &= S_D^t(K^c + \omega^2 K^v)S_D \\ P^* &= S_D^t P \end{aligned} \tag{4.14}$$

and U_C = (n-c)x1 displacement vector in the new generalised co-ordinate system.

Since S_D depends on time, all the four co-efficients M*, C*, K* and P* in eq. (4.14) are time dependent. Therefore, eq. (4.13) belongs to a special class of the ordinary differential equations, i.e., the differential equations with periodic co-efficients.

Mathematical theories of the linear differential equations with periodic co-efficients may be found in the standard references[66-69] (detailed analysis of a very special case of this class of equations, i.e., Mathieu equation is available in Refs. (70,(71)). The method of the characteristic exponents[72-74], the averaging method[75] and a combination[76-81] of the averaging method with the variation of parameters[82] have been applied to find the steady-state response and the stability of this type of differential equations. However, when compared with the linear differential equations with periodic co-efficients treated in the literature, eq. (4.13) exhibits the following special features:

i) the co-efficient matrix of the acceleration term (i.e., the mass matrix) is time dependent.

ii) the elastic stiffness matrix is also time dependent and therefore the natural frequencies of the system vary with time.

iii) the periodic co-efficients of the velocity and displacement terms are not small.

iv) the periodic co-efficients of the velocity term is antisymmetric with strong off-diagonal(coupling) terms.

v) the co-efficient matrices of the displacement and velocity term and the force vector contain the fundamental frequency of excitation (unknown in case of stability analysis).

vi) the fundamental frequency of the parametric excitation is equal to that of the force vector.

In the context of the above characteristics, it appears that the universal method of harmonic balance[83,84] is ideally suited for finding the steady-state response as well as the instability zones of eq. (4.13). This method has already found extensive applications in the dynamic analysis of structural systems[52], and in the study of mechanisms with elastic couplings[85,86]. The description of this method, as utilised in this chapter, is given in the following sections.

4.2.4 Displacements expressed in harmonics

Since the force-vector and all other co-efficient matrices of eq. (4.13) are in the form of Fourier series with fundamental frequency ω, the steady-state response of eq. (4.13) will also vary periodically with a fundamental

frequency ω. Consequently, the displacement vector U in eq. (4.4) is an unknown function of time only and may be expressed in Fourier series.

$$U = U_o^1 + \sum_{j=1}^{h_2} (U_j^1 \cos j\omega\tau + U_j^2 \sin j\omega\tau) \qquad (4.15)$$

where U_o^1, U_j^1, U_j^2, $j = 1, \ldots, h_2$, are (unknown) amplitudes of the harmonics of U and h_2 is the total number of sine terms taken in the series of eq. (4.15). The choice of h_2 depends on the nature of the problem and the accuracy desired. In steady-state response analysis, h_2 should be made equal to the total number of the dominant cosine/sine terms present in the force vector P.

In view of the assumed expression of U, given by eq. (4.15), U will be first substituted in eqs. (4.4) and (4.6) and the constraints will be eliminated thereafter. This procedure is more advantageous than performing the matrix operations involved in eq. (4.13) and can be easily programmed.

Upon differentiation of eq. (4.15) with respect to time, the expressions for the velocity $\dot{U}$ and the acceleration $\ddot{U}$ are obtained below.

$$\dot{U} = \sum_{j=1}^{h_2} j\omega (- U_j^1 \sin j\omega\tau + U_j^2 \cos j\omega\tau) \qquad (4.16)$$

$$\ddot{U} = \sum_{j=1}^{h_2} - j^2\omega^2 (U_j^1 \cos j\omega\tau + U_j^2 \sin j\omega\tau) \qquad (4.17)$$

Substituting eqs. (4.15), (4.16) and (4.17) for $\ddot{U}$, $\dot{U}$ and U respectively in eq. (4.4), multiplying the series involved and equating the co-efficients of similar cosine and sine terms on both sides of the resulting equation, the following matrix equation is obtained.

$$(-\omega^2 M^S + K^S)U^S = P^S \qquad (4.18)$$

where,

M^S = general mass matrix with ω^2 as co-efficients.

K^S = general stiffness matrix whose terms do not contain ω.

P^S = general force vector.

U^S = general displacement vector comprising of the elements of U_j^1 and U_j^2, $j = 1, \ldots, h_2$ and U_o^1.

(The vectors and matrices in eq. (4.18) are of the order $(2h_2 + 1)n$).

Arrangement of the rows of the matrices and of the unknown elements in the unknown vector U^S may be done depending on the numerical method used in the solution of eq. (4.18).

A similar substitution of eq. (4.15) for U in eq. (4.6) yields the expanded constraint equation as shown below:

$$S^S U^S = 0 \qquad (4.19)$$

where S^s is a $(2h_2 + 1)c \times (2h_2 + 1)n$ general constraint matrix. The arrangement of the rows and columns of S^s must follow the similar arrangement of K^s and M^s in eq. (4.18).

The dependent co-ordinates B (c in numbers), chosen during the partitioning of eq. (4.6), is now expanded to $(2h_2 + 1)c$ numbers of dependent co-ordinates in the new system. Denoting them by B and the remaining $(2h_2 + 1)(n - c)$ numbers of independent co-ordinates by A, eq. (4.19) is re-written below in partitioned form:

$$[S_A^s \quad S_B^s] \begin{bmatrix} \{U_A^s\} \\ \{U_B^s\} \end{bmatrix} = \{0\} \tag{4.20}$$

$$\text{or,} \quad U_B^s = \bar{S}\, U_A^s \tag{4.21}$$

$$\text{where,} \quad \bar{S} = -(S_B^s)^{-1} S_A^s \tag{4.22}$$

In order to eliminate the constraints (given by eq. (4.19)) from the equation of motion (now expressed by eq. (4.18)), the following transformation of co-ordinates is defined:

$$U^s = S^* U^g \tag{4.23}$$

where,

$$S^* = \begin{bmatrix} I \\ \bar{S} \end{bmatrix} \tag{4.24}$$

and U^g = $(2h_2 + 1)(n - c)x1$ displacement vector in the present generalised co-ordinate system.

By the contragradient law of transformation, the mass matrix M^g, the stiffness matrix K^g and the force vector P^g, all being of order $(2h_2+1)(n-c)$, in the new generalised co-ordinate system are given below by eqs. (4.25), (4.26) and (4.27) respectively.

$$M^g = S^{*t} M^s S^* = M^s_{AA} + M^s_{AB}\bar{S} + \bar{S}^t(M^s_{BA} + M^s_{BB}\bar{S}) \qquad (4.25)$$

$$K^g = S^{*t} K^s S^* = K^s_{AA} + K^s_{AB}\bar{S} + \bar{S}^t(K^s_{BA} + K^s_{BB}\bar{S}) \qquad (4.26)$$

$$P^g = S^{*t} P^s = P^s_A + \bar{S}^t P^s_B \qquad (4.27)$$

where M^s_{AA}, M^s_{AB}, K^s_{AA}, K^s_{AB}, P^s_A etc. are the sub-matrices formed by partitioning of the parent matrices. The subscripts A and B denote the independent and the dependent co-ordinates respectively. Thus, the equation of motion in the new generalised co-ordinate system is given by eq. (4.28).

$$(-\omega^2 M^g + K^g)U^g = P^g \qquad (4.28)$$

This equation will be next used to find out the steady-state deflections and the stresses of the mechanism.

4.3 Displacement and Stress Analysis

For a given crank speed ω, the two matrices M^g and K^g in eq. (4.28) can be combined into a single matrix A^g and eq. (4.28) is reduced to

$$A^g U^g = P^g \tag{4.29}$$

where

$$A^g = -\omega^2 M^g + K^g \tag{4.30}$$

Since the rigid body degrees of freedom are not eliminated from the stiffness matrices K^c or K^s or K^g, they are singular. However, the matrix A^g is non-singular because of the addition of the non-singular matrix $-\omega^2 M^g$ to K^g. The unknown displacement vector U^g can be easily found out from eq. (4.30) by inverting the matrix A^g as follows:

$$U^g = (A^g)^{-1} P^g \tag{4.31}$$

The direct solution (shown by eq. (4.31)) of U^g by Gaussian elimination[61] is time consuming as the size of the matrix A^g is fairly large, i.e., of order $(n-c)(2h_2+1)$ and the computations in inverting a matrix increase with the cube of its size, if the band-width is not considered. For this reason, the iterative method of successive over relaxation (S.O.R.)[61] is preferred for solving eq. (4.29). In the context of eq. (4.29), this method has the following advantages over the direct method of solution, given by eq. (4.31).

i) The number of computations per iteration increases with the square of the matrix size.

ii) Since only the first few harmonics of the transverse displacement and rotational co-ordinates are dominant, they can be grouped together to form the most dominant sub-matrix of the system. It is well-known that a proper rearrangement of the dominant elements leads to a large reduction in the number of iterations required for solving the equation and the above arrangement, though immaterial in the direct method, improves the iterative scheme of solution.

iii) If desired, advantage can be taken of the considerable number of zeros present in the matrix A^g. This is not possible in the direct method of solution (because A^g does not have a regular band-width).

iv) Of each co-ordinate, the first few harmonics only are dominant; consequently greater accuracy is not needed in the values of the remaining harmonics. By using a stricter convergence criterion for the dominant co-ordinates and a less stringent criterion for the remaining co-ordinates, the number of iterations can be reduced further. This freedom in the choice of accuracy is completely absent in the direct method.

After U^g is obtained from the solution of eq. (4.29), the vector U^s is found out from eq. (4.23). As U^s is formed by the amplitudes U_o^1, U_j^1, U_j^2, $j = 1, \ldots, h_2$,

the displacement vector U and the acceleration vector $\ddot{U}$ for the whole system is known from eqs. (4.15) and (4.17) respectively. In the present method of analysis, the system co-ordinates are defined in the directions of the respective element oriented element co-ordinate systems; so the displacements $\bar{u}$ and accelerations $\ddot{\bar{u}}$ along the element oriented element co-ordinates of each element are easily found out by simply referring to the integer matrix NS.

These displacements $\bar{u}$ and accelerations $\ddot{\bar{u}}$ for all elements of the mechanism are found out in the form of a series of the harmonic functions of $\omega\tau$ and therefore can be evaluated for any position of the crank by putting the value of the crank angle in these series expressions.

As the element displacements $\bar{u}$ and accelerations $\ddot{\bar{u}}$ are known for any position of the crank, the calculation of the dynamic stresses within the links follows the same procedure as outlined in Section 2.8. The stresses in the static restrained structure are calculated during the formation of the element load vectors $\bar{p}$ as mentioned in Section 2.8.

It may be mentioned here that the mass matrices and stiffness matrices are shown separated all along only to analyse the stability of the mechanism (described in the next section). If the steady-state displacements and

stresses only are desired, the matrices $\bar{k}^c$, $\bar{k}^v$ in eq. (4.2); K^c, $\omega^2 K^v$ in eq. (4.4); $-\omega^2 M^s$, K^s in eq. (4.18) and $-\omega^2 M^g$, K^g in eq. (4.28) can be added together (as ω is known) thereby reducing the matrix operations to a large extent.

It will be shown at the end of the next section how the present method lends itself to find out the frequency response of a flexible mechanism at the cost of little additional computations.

4.4 Stability Analysis

Under dynamic loading conditions, a rod may undergo three types of instabilities: (i) the instability due to the bending resonance conditions, (ii) the parametric instability due to the time-dependent axial forces and (iii) the instability due to the longitudinal resonance conditions. In case of mechanisms, the mass and elastic stiffness vary with time as evident from eq. (4.13). Consequently, the natural frequencies also change with time and the bending resonance conditions, encountered in the ordinary elastic systems, degenerate into the parametric instability conditions. The natural frequencies of the longitudinal vibrations are usually very high; so the possibility of the existence of the longitudinal resonance conditions is remote.

From the theory of parametric vibrations[52], it is known that the instability zones corresponding to the critical (fundamental) frequency ω_a of the axial forces are separated from the stability zones by the periodic solutions having periods $\frac{2\pi}{\omega_a}$ and $\frac{4\pi}{\omega_a}$. Almost in all cases the periodic solutions themselves lie within the instability zones. Two solutions of identical periods confine the region of instability while two solutions having different periods bound the region of instability. Though unstable frequencies corresponding to all types of subharmonic and ultraharmonic solutions exist in the parametric vibrations, the harmonic solution and the subharmonic solution of order $\frac{1}{2}$ (as mentioned above) only are important from practical point of view because all other periodic solutions lie within the stability zones corresponding to these two particular periodic solutions.

In view of the above, the stability analysis of the mechanism reduces to finding out the critical frequencies of the axial forces for which the system will have the two types of periodic solutions mentioned above. Since the fundamental frequency ω_a of the rigid body axial forces is identical with the speed ω of the crank, the critical frequencies of the axial forces imply the critical speeds of the input crank.

To find out the critical frequencies corresponding to the harmonic solution having period $\frac{2\pi}{\omega}$, it is assumed that the homogeneous part of the equation of motion eq. (4.4), subject to the constraints eq. (4.6), allows a 'sustained motion'[87] given by eq. (4.15). Consequently, the desired critical frequencies are given by the solution of the homogeneous part of eq. (4.28) as shown in eq. (4.32).

$$(-\omega^2 M^g + K^g)U^g = 0$$

The eigenvalue problem of eq. (4.32) may be solved by the standard methods[64]. However, in view of the singularity of K^g, non-symmetry of M^g and the large size of these two matrices, an efficient method is described in Appendix F.

The value of h_2 to be chosen in eq. (4.15) depends on the number of instability zones to be determined corresponding to the harmonic solution of the mechanism. The effect of damping, always present in a physical system, reduces the width of the instability zones of higher order. However, due to the presence of ω, the matrices $2\omega C^c$ and $\omega^2 K^v$ will contain large off-diagonal terms and the influence of the higher harmonic terms on the lower ones may not be insignificant. For this reason, the value of h_2 should be chosen slightly higher than the number of instability zones to be determined corresponding to eq. (4.15).

To find out the periodic solutions with period $\frac{4\pi}{\omega}$, the following Fourier series expression of U is assumed in place of eq. (4.15).

$$U = \sum_{j=1,3,5}^{2h_2-1} (U_j^1 \cos \frac{j\omega\tau}{2} + U_j^2 \sin \frac{j\omega\tau}{2}) \qquad (4.33)$$

Using this series of U, an equation similar to eq. (4.32) is arrived at (following the same procedure outlined before) and is given by eq. (4.34).

$$(-\omega^2 M^{g'} + K^{g'}) U^{g'} = 0 \qquad (4.34)$$

The frequencies obtained from the solution of eq. (4.34) correspond to the periodic solutions with period $\frac{4\pi}{\omega}$. The choice of h_2 in eq. (4.33) should be governed by the factors mentioned above.

If the value of h_2 in eq. (4.15) is so chosen that it includes the dominant harmonics in the force vector P of eq. (4.4), the determination of the critical frequencies of the harmonic oscillations may also yield the frequency response of the mechanism at the cost of little additional computations. If Φ is the modal matrix, obtained from the eigenvalue solution of eq. (4.32), the following normal co-ordinate transformation may be used.

$$U^g = \Phi\eta \qquad (4.35)$$

where η is the displacement vector in the new normal co-ordinate system. As before, use of the above transformation in eq. (4.28) yields eq. (4.36).

$$(-\omega^2 M^n + K^n)\,\eta = {}_{\Phi}{}^{t}P^{g} \tag{4.36}$$

where $M^n = {}_{\Phi}{}^{t}M^{g}\,{}_{\Phi}$ and $K^n = {}_{\Phi}{}^{t}K^{g}\,{}_{\Phi}$ (4.37)

For a particular value of ω, the solution of eq. (4.36) is given by eq. (4.37).

$$\eta = (-\omega^2 M^n + K^n)^{-1}\ {}_{\Phi}{}^{t}P^{g} \tag{4.38}$$

Substitution of this η in eq. (4.35) gives the displacement vector U^g in the generalised co-ordinate system. The determination of the various harmonics of the element co-ordinates from the vector U^g follows the same procedure as outlined in Section 4.3.

Once Φ is determined from eq. (4.32), the solution of eq. (4.36) is rather simple as the order of the matrices are small. Since the matrices M^n and K^n are same for all values of the crank speed, solution of eq. (4.36) for various values of the crank speed requires only the inversion of a small order matrix in eq. (4.38) for each value of the crank speed (the vector ${}_{\Phi}{}^{t}P^{g}$ contains the crank speed, in most cases, only as a multiplication factor). If the effects of the terms due to the Coriolis components of acceleration

and the additional tangential components of acceleration are neglected, the procedure becomes particularly simple because the matrices M^n and K^n become diagonal in that case.

The advantages of the method of analysis described in this chapter over the previous method of analysis described in Chapter III are:

(i) It directly gives the steady state solution of a flexible mechanism requiring computer time much less than the other method

(ii) It enables to determine the critical speeds of the crank for the instabilities due to the subharmonic, harmonic and superharmonic oscillations of all orders. It is not possible to determine these critical speeds from the previous method.

(iii) If desired, frequency response of a flexible mechanism for a wide range of the crank speed may be obtained with a computation time less by several orders of magnitude than that required by the previous method.

(iv) In the previous method, the motion during each interval of time is described by a few modes of vibration which remain valid for that interval only. These modes continually change from one interval to another and the effects of these varying modes of vibration may be pronounced with large external forces or with high

input speeds[52]. While the previous method can not take care of the effects of the varying modes, this situation does not arise at all in the present method as it analyses the mechanism for a general configuration.

(v) In the previous method, the rigid body axial forces are considered as time independent during each interval of time which destroy the 'frequency modulation' effect of the axial forces to some extent. The present method treats the rigid body axial forces in their actual form.

(vi) The present method enables to identify the dominant harmonics of the displacements which is not possible with the previous method.

The disadvantages of the present method, when compared with the previous method, are the following:

(i) It is applicable to a restricted class of mechanisms for which the rigid body harmonic analysis is available.

(ii) It can not study the transient behaviour of the mechanism, particularly at the start of the mechanism.

(iii) The effects of the elastic axial forces can not be studied by the present method.

(iv) It may require the pheripheral storage facilities of a computer (depending on the order of the matrices).

CHAPTER V

RESULTS AND DISCUSSIONS

5.1 Introduction

To assess the merits and effectiveness of the various analytical treatments presented in Chapters II, III and IV, a number of numerical problems have been solved. For this purpose, several computer programs have been written in a sufficiently general way to accommodate various types of mechanisms. In addition, several cases, viz., effect of the number of divisions of the links, contributions of the various acceleration terms etc. may also be studied by controlling the input data only. These programs were run on IBM 7044 and IBM 370/155 computers to solve the numerical examples. In some of these numerical examples, the results obtained from the present work have been compared with those of the previous works. Only limited number of results are presented here because of space limitation.

The following mechanisms are chosen for the numerical examples:

Mechanism 1 (Fig. C-1)

Length of link 2 (assumed rigid) = 1.2";

Link 3 (connecting rod): Length = 7.2", cross-section = 0.5" X 1.0" (larger dimension in the plane of bending), sp. wt. =

0.284 Lbs./in.^{3}, Young's modulus = 30 X 10^6 Lbs./in.^{2}
Wt. of the piston = 8.1792 Lbs.; gas force on the piston and damping are considered absent.

Mechanism 2 (Fig. C-1)

Length of link 2 (assumed rigid) = 1.2";
Link 3 (connecting rod): Length = 12", cross-section = 0.5" X 1.0" (longer dimension in the plane of bending), sp. wt. = 0.284 Lbs./in.^{3}, Young's modulus = 30 X 10^6 Lbs/in.^{2}
Wt. of the piston = 0.852 Lbs.; damping ratio (ξ_i) = 0.2 for the first mode and 0.8 for the higher modes; piston force acting on the mechanism is given by eq. (D-4) of Appendix D.

Mechanism 3 (Fig. C-2)

Length of the four links are 36", 12", 36" and 30" respectively; cross-section of each link = 1.0" X 1.0"; link material is Aluminium with sp. wt. = 0.101 Lbs./in.^{3} and Young's modulus = 3 X 10^6 Lbs./in.^{2}; moment of inertia of the flywheel at the end of link 4 = 0.7 Lb. in. sec^2; damping ratio = 0.05 for each mode.
Balancing input torque at the crank end (obtained from eq. (2.57)) is assumed to be present at the crank end.

In the following, the bending stresses calculated at the extreme fibre of the links (due to the three types of factors mentioned in Section 2.8) are denoted by $\sigma_I^{bending}$, $\sigma_{II}^{bending}$ and $\sigma_{III}^{bending}$ respectively.

For the efficient representation of the various cases, the following table is used:

Table 5.1

Case	Left side of eq. (3.42)	Right side of eq. (3.42)
A	$C^a = K^N = K^G = K^T = 0$	quasi-static
B	$C^a = K^N = K^T = 0$	-Do-
C	$C^a = K^N = K^G = K^T = 0$	harmonic series ($h_1 = 20$)
D	$C^a = K^N = K^T = 0$	-Do-
E	$C^a = K^T = 0$	-Do-
F	$K^T = 0$	-Do-
G	All terms are present	-Do-
H	All terms are present but the axial forces are derived from the elastic analysis (described in Section 3.4)	-Do-

5.2 Basic Analysis

In this section, results are presented to study some of the basic features of the dynamics of flexible mechanisms. Results have been presented for the first 180 degrees of the crank rotation in most of the cases. This may not yield a complete picture but the effectiveness

of the various factors may be assessed to some extent from the transient behaviour.

Fig. 5.1 presents a comparison between the stresses ($\sigma_{II}^{bending}$) at the middle point of the follower of mechanism 3, obtained by considering the crank to be instantaneously clamped at the support end (it will be hereafter referred to as structure) and by following the method of eliminating the rigid body degrees of freedom as discussed in Section 2.5.2. It is seen from the figure that the difference in the results is appreciable and the assumption of a clamped crank does not yield the correct results. From the figure, it is apparent that the frequency of oscillation is reduced (with an apparent reduction in stiffness). The reason for the reduction in the amplitudes of the vibration may be attributed to the fact that the balancing torque applied at the crank shaft is taken up by the clamped end and does not contribute to the deformations of the mechanism. The effect of such assumption on the steady state solutions is shown in Section 5.4.

Fig. 5.2 and Fig. 5.3 show the values of $\sigma_{II}^{bending}$ at the middle point of the follower and the coupler respectively of mechanism 3 for various numbers of divisions of the follower and the coupler (the symbol i-j-k represents i, j and k numbers of divisions of the crank, coupler and follower respectively). It appears from the figures that

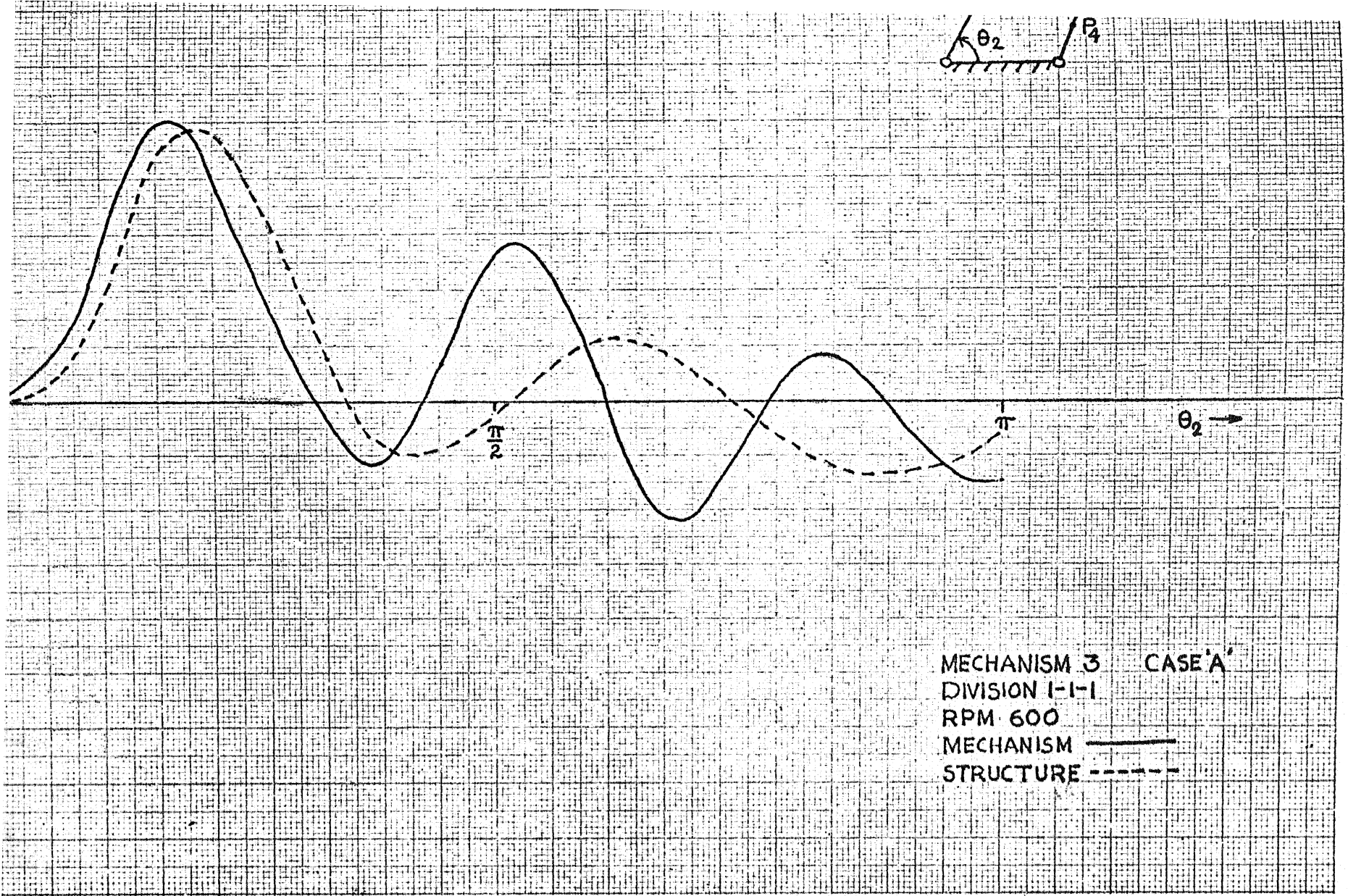

FIG 5.1 FOLLOWER STRESS OF 'MECHANISM' AND 'STRUCTURE'

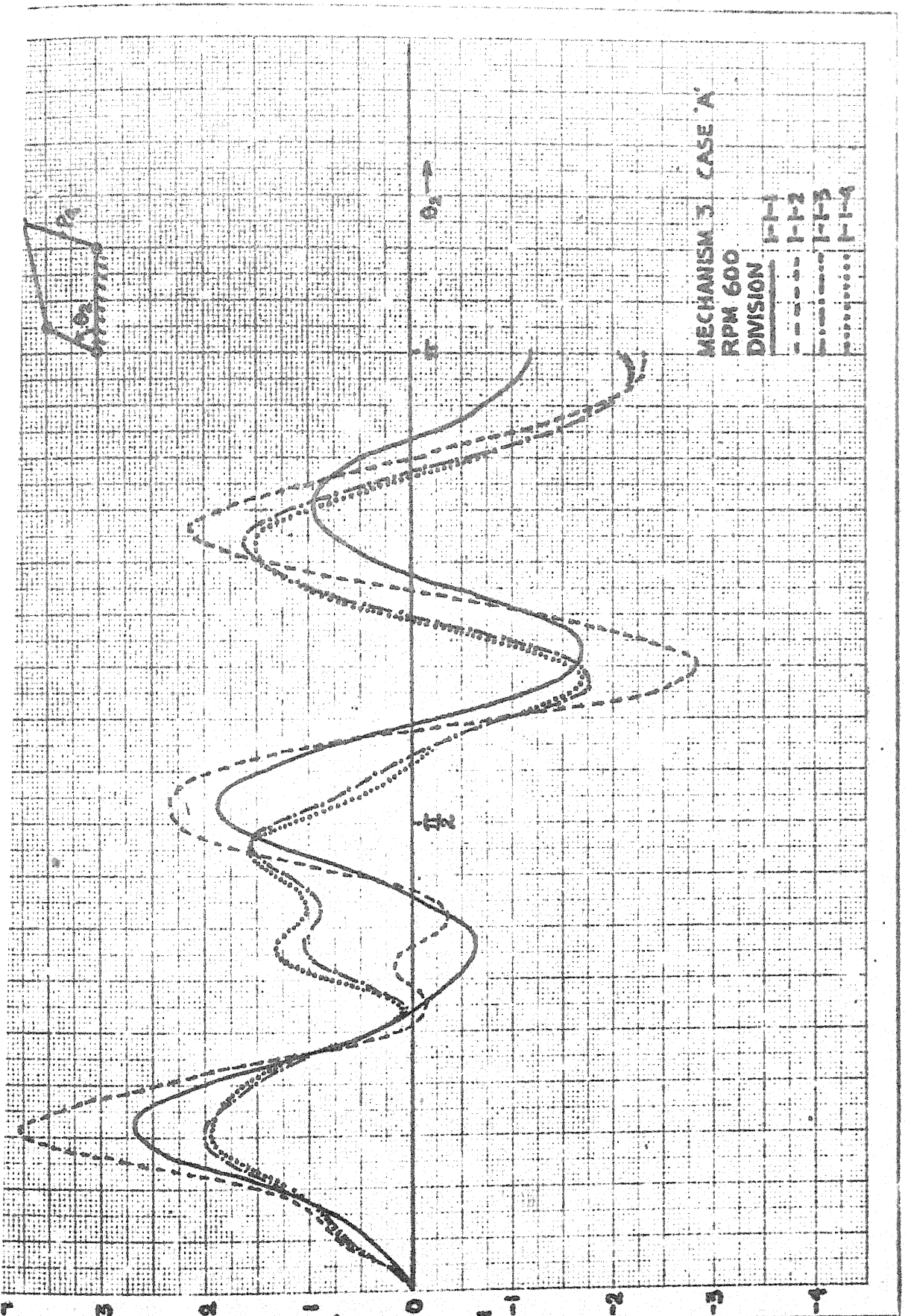

FIG 5.2 EFFECT OF DIVISION ON FOLLOWER STRESS

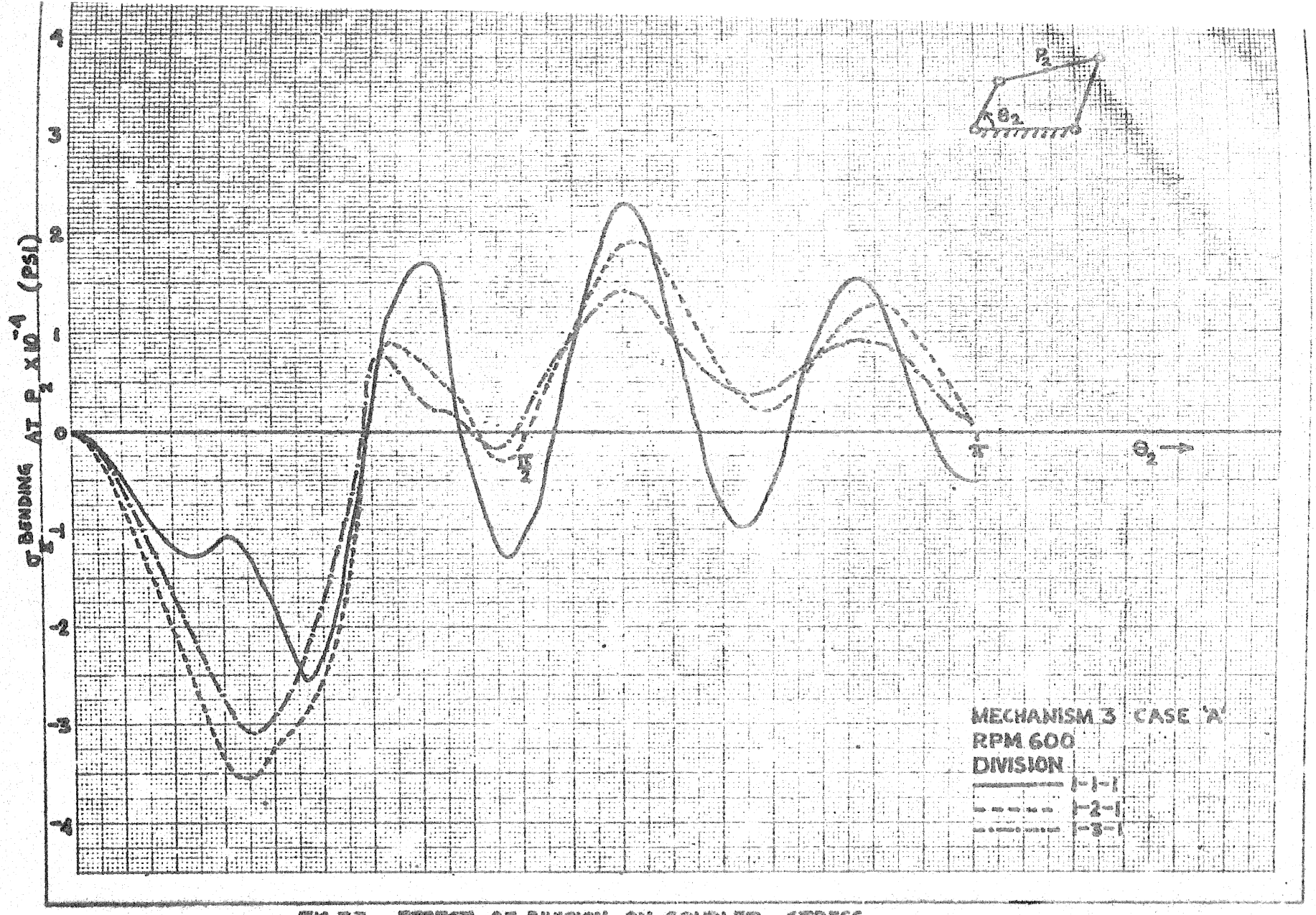

FIG 5.3 EFFECT OF DIVISION ON COUPLER STRESS

the stresses (and obviously the elastic displacements also) approach their true values when the number of divisions is three. Further increase in the number of divisions improves the results only marginally though the amount of computations increases considerably.

As explained in Section 2.5.3, an input torque acting on the crankshaft is considered to balance the rigid body inertia forces at every configuration. The nature of the variation of this input torque with the crank rotation is shown in Fig. 5.4 for mechanism 3. The variation of the torque at the rocker end is also shown in the same figure. It is clear from this figure that the fluctuation in the balancing input torque is quite large and, to obtain a reasonably uniform crank speed, a flywheel of considerable moment of inertia is needed. The effect of adding a flywheel to the crankshaft on the angular rotation of the support end of the crank and on $\sigma_{II}^{\text{bending}}$ at the middle point of the follower are shown in Fig. 5.5a and Fig. 5.5b respectively. This figures depict the sensitivity of the deformation characteristics with respect to the moment of inertia of the flywheel (denoted by I_c in the figure) at the crank end. Fig. 5.5a shows that, though the angle of rotation becomes increasingly smaller with the increase in the values of I_c, it nevertheless requires a large value of I_c to reduce the angle of rotation to zero. However, Fig. 5.5b shows that

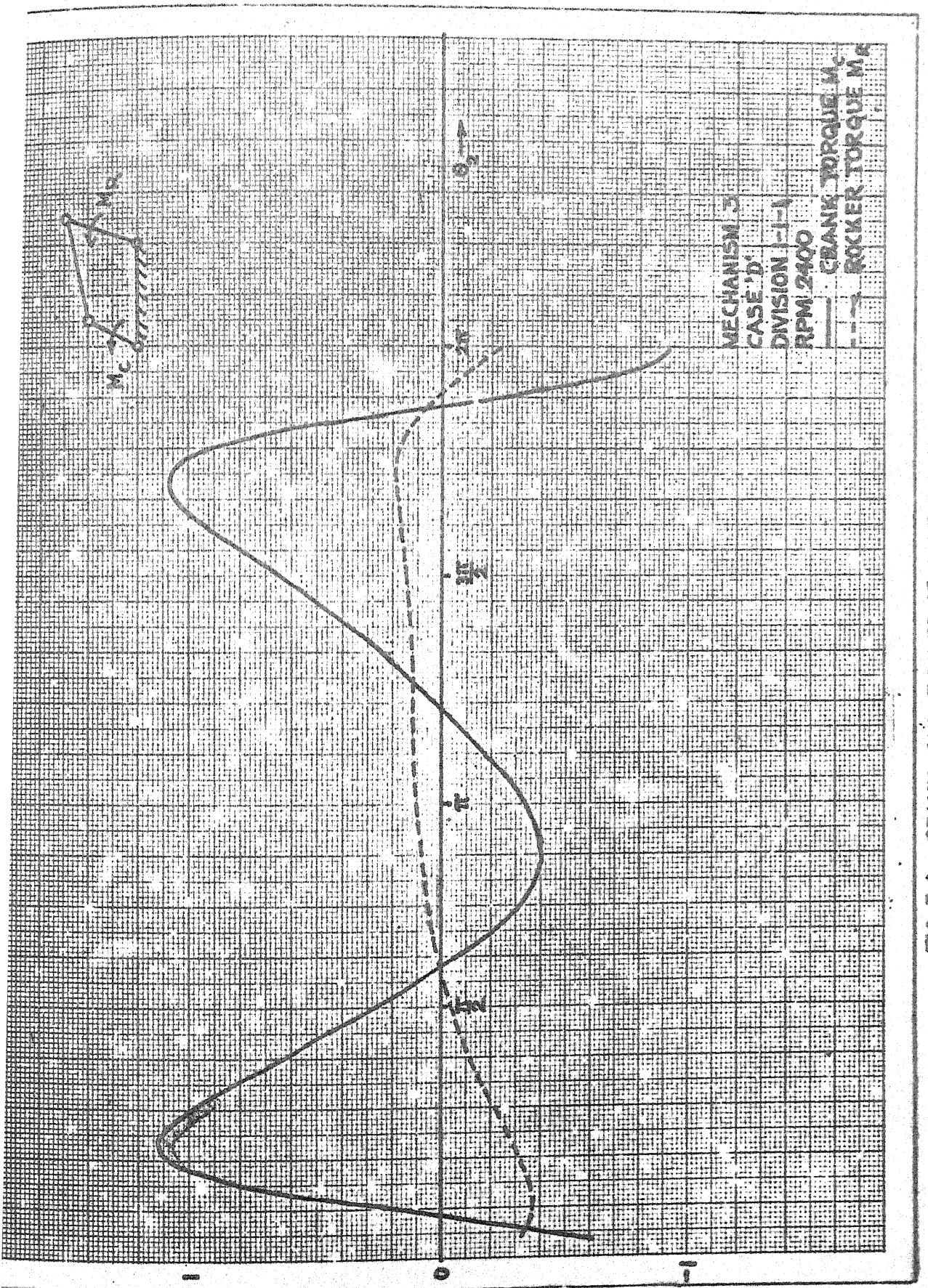

FIG 5.4 CRANK AND ROCKER TORQUE

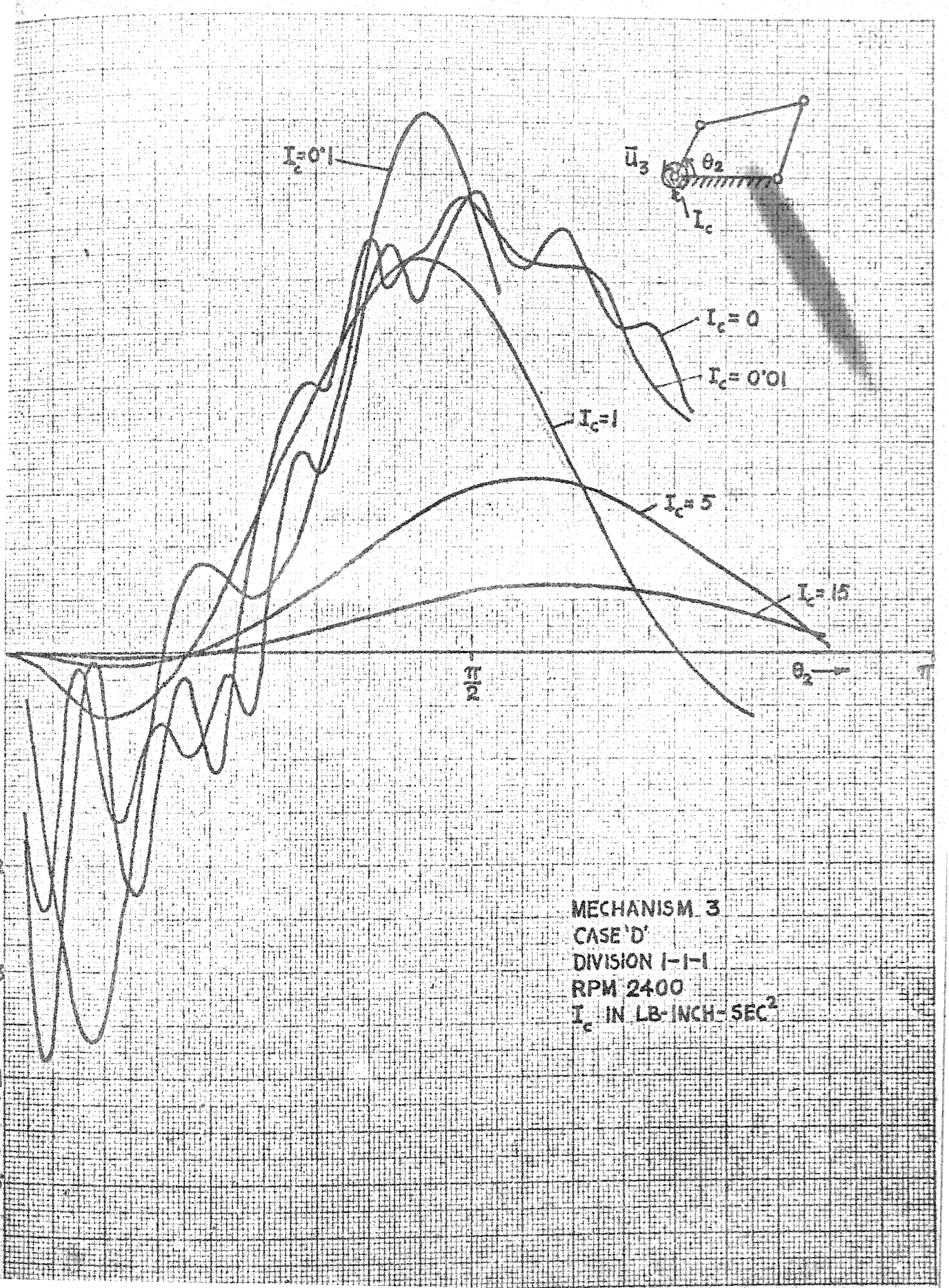
I_c=0·1
$\bar{u}_3$
θ_2
I_c
I_c= 0
I_c= 0·01
I_c=1
I_c= 5
I_c= 15
$\frac{\pi}{2}$
θ_2
π
MECHANISM 3
CASE 'D'
DIVISION 1-1-1
RPM 2400
I_c IN LB-INCH-SEC^2

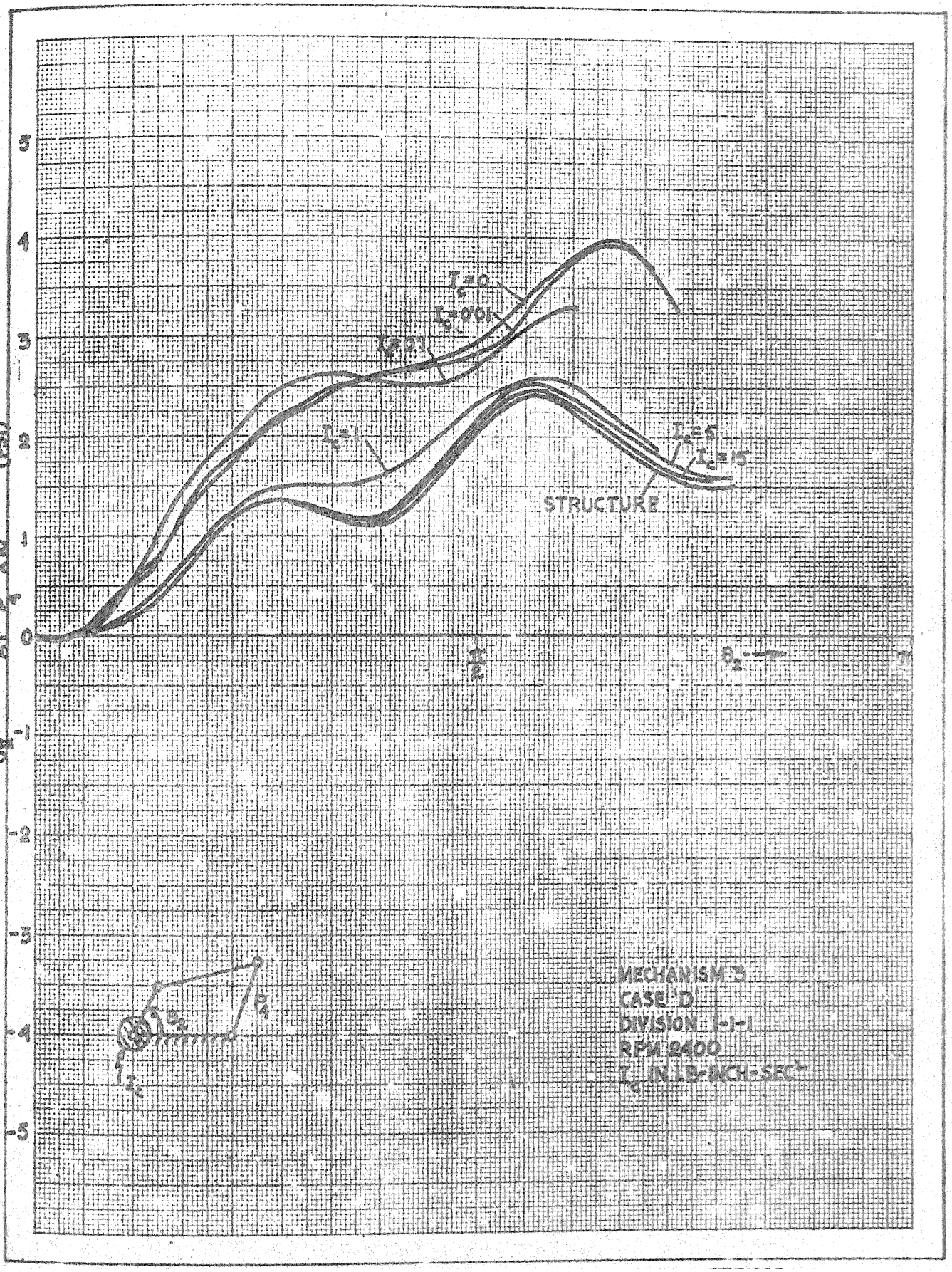
BENDING AT P_4 X 10^{-3} (PSI)
5
4
3
2
1
0
-1
-2
-3
-4
-5
$I_c=0$
$I_c=0.01$
$I_c=0.1$
$I_c=1$
$I_c=5$
$I_c=15$
STRUCTURE
$\frac{\pi}{2}$
θ_2
π
θ_{2x}
P_4
I_c
MECHANISM 3
CASE 'D'
DIVISION 1-1-1
RPM 2400
I_c IN LB-INCH-SEC^2

the transition from 'mechanism' to 'structure' is very rapidly accomplished by gradually increasing the value of I_c. This is due to the fact that the input torque is largely responsible for the vibrations of the crank and its effect on the follower is less dominant.

It is well-known that the natural frequencies of a mechanism with elastic members depend on its instantaneous configurations. Since the configuration of the mechanism changes continuously, it is interesting to observe the variations of the natural frequencies with the crank rotation. As an example, the first natural frequency of mechanism 3 for various crank positions is shown in Fig. 5.6. The first natural frequency, when the mechanism is reduced to a structure by clamping the crank end, is also shown in the same figure. It is seen that the first natural frequency is reduced by such modification. This fact is also borne out from Fig. 5.1 as mentioned earlier. It is interesting to note that no difference is noticed between the frequencies of the mechanism and the corresponding structure when the crank and the coupler lies along the same line (i.e., when the crank angle is 38 deg. and 238 deg.). It has been further observed from the obtained results (not presented here) that the higher order frequencies are more drastically reduced when the mechanism is converted into a structure.

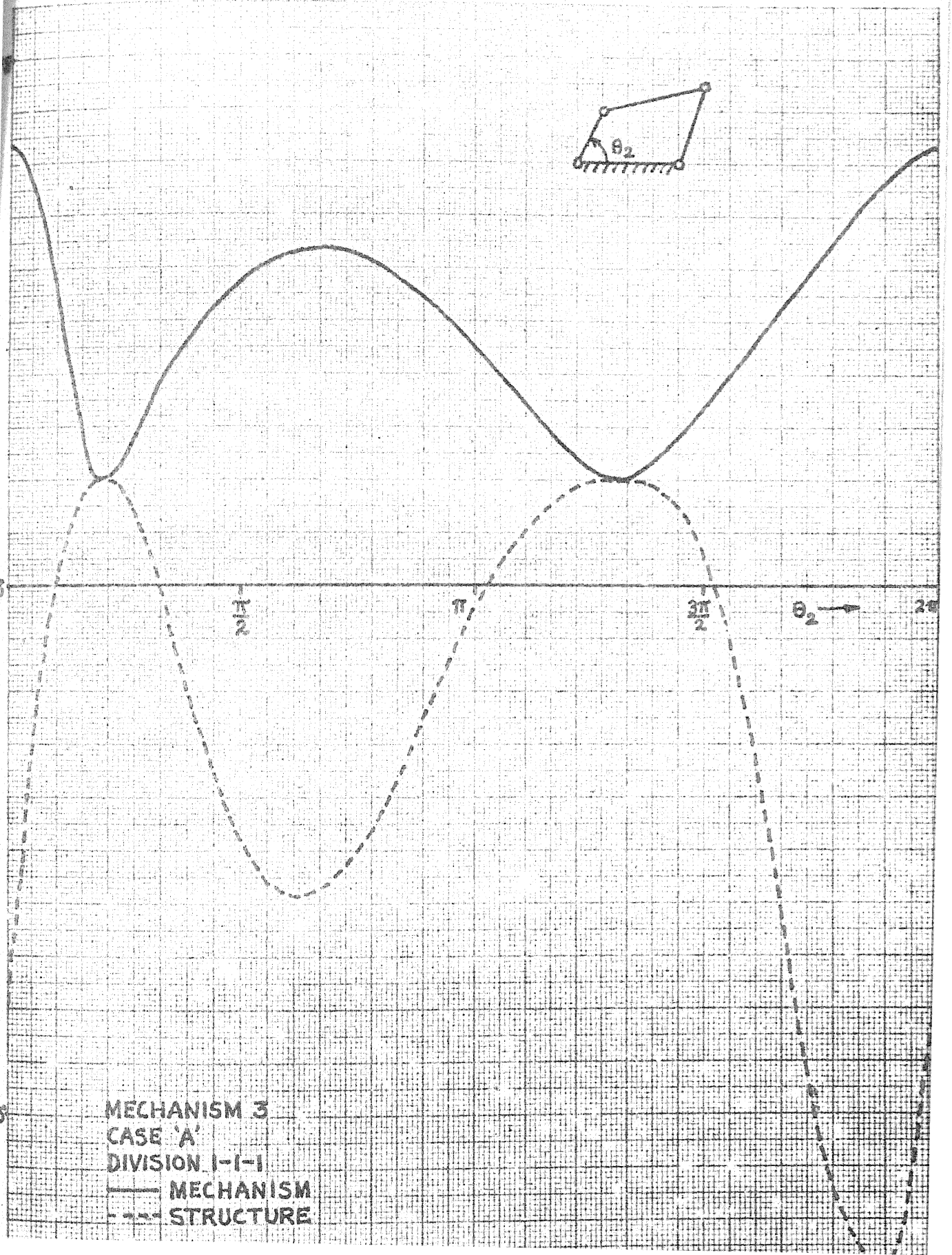
θ2
3
π/2
π
3π/2
θ2
2π
2·5
MECHANISM 3
CASE 'A'
DIVISION 1-1-1
MECHANISM
STRUCTURE

It was mentioned in Section 2.8 that the total stress (bending, shear or axial) within a link should be calculated from three considerations. These three types of stresses (for bending only) at the middle point of the follower are shown in Fig. 5.7 for mechanism 3 with no division of the links. It is seen that the stresses $\sigma_{II}^{\text{bending}}$, calculated from the displacements, are dominant over the other two. The observation made in Section 2.8 that the stresses σ_I and σ_{III} become small compared to σ_{II} when the links are subdivided is substantiated from the computed results. At higher speeds, as found in case of mechanism 1, the relative importance of σ_I and σ_{III} increases. In case of mechanism 1, with 24000 RPM of the crank, the stresses σ_I, σ_{II} and σ_{III} are found to be of the same order when no divisions of the links are taken. When computations are carried out with three divisions of the connecting rod, $\sigma_I^{\text{bending}}$ and $\sigma_{III}^{\text{bending}}$ at the middle point of the connecting rod are about $\frac{1}{10}$th (on the average) of $\sigma_{II}^{\text{bending}}$ at the same point. For four divisions of the connecting rod, this ratio reduces to about $\frac{1}{100}$.

5.3 Effects of the Dynamic Factors

This section is devoted to the discussions of the results indicating the effects of the dynamic factors

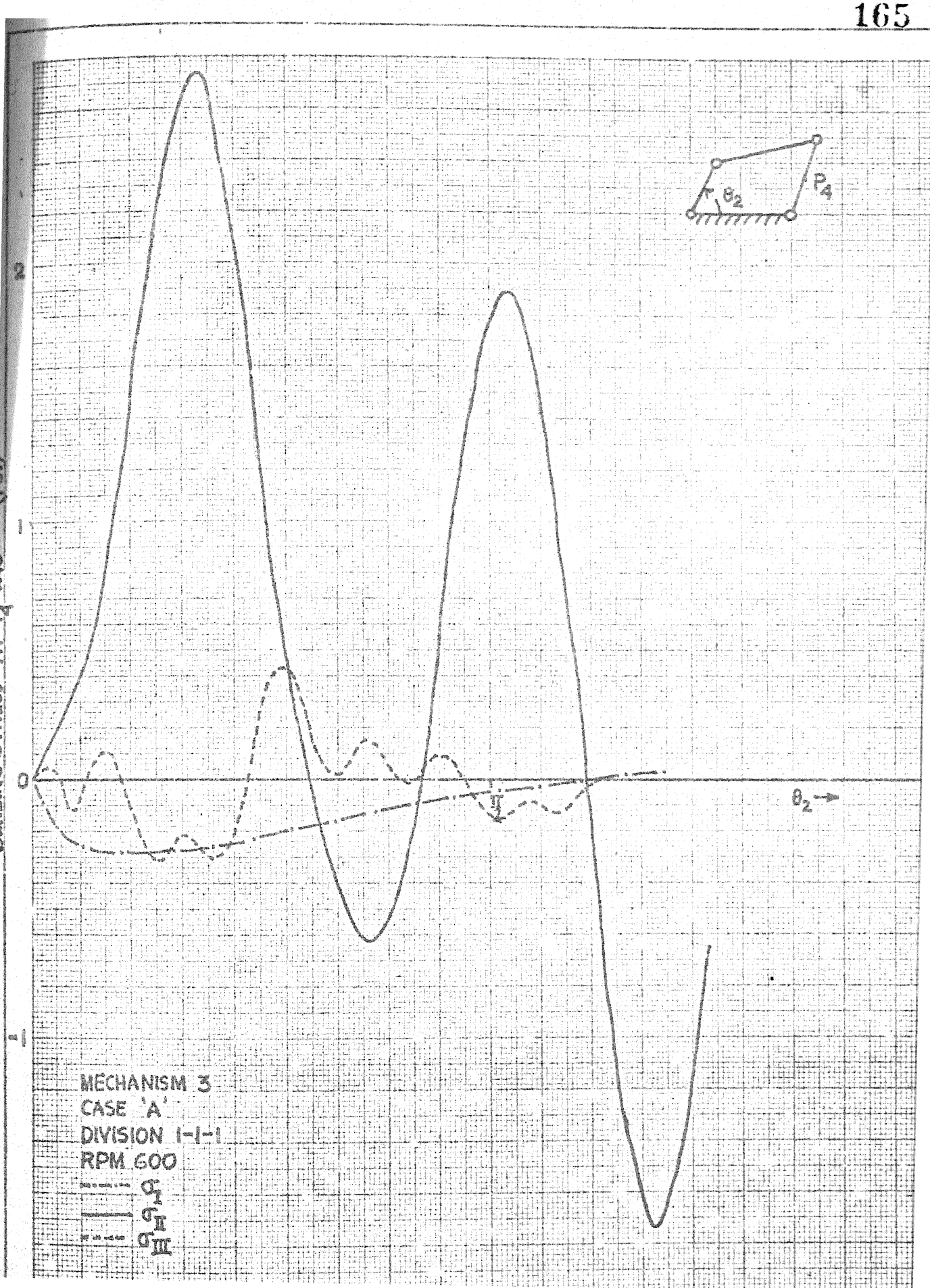
BENDING STRESS AT P4 AND VELOCITY
2
1
0
1
2
θ2
P4
θ2
MECHANISM 3
CASE 'A'
DIVISION 1-1-1
RPM 600
σI
σII
σIII

not included in the basic analysis. Again, only the initial transient portions of the characteristics are presented to study these effects.

$\sigma_{II}^{bending}$ at the middle point of the follower of mechanism 3 (with and without the effects of the rigid body axial forces) are shown in Fig. 5.8 and Fig. 5.9 for two different speeds. From both the figures, it is seen that the effects of the rigid body inertia forces are quite appreciable. The rigid body axial forces increase or decrease the deflections of the links, depending mainly on the condition whether they are in the state of compression or tension.

The contribution of the rigid body axial forces is again shown in Fig. 5.10 for the middle point of the coupler at 2400 RPM. It appears that the effect of the rigid body axial forces is more pronounced in case of the coupler. This may be due to the larger slenderness ratio of the coupler which makes it more susceptible to the axial forces. In these cases, the rigid body inertia forces acting on the instantaneous structure are considered quasi-static (i.e., independent of time during the interval $\Delta\tau$). If the forces are considered to be dynamic in nature in the interval (as discussed in Section 2.7), the results are slightly modified as indicated in Fig. 5.10.

Fig. 5.11 to Fig. 5.13 show $\sigma_{II}^{bending}$ at the middle point of the coupler for various speeds considering

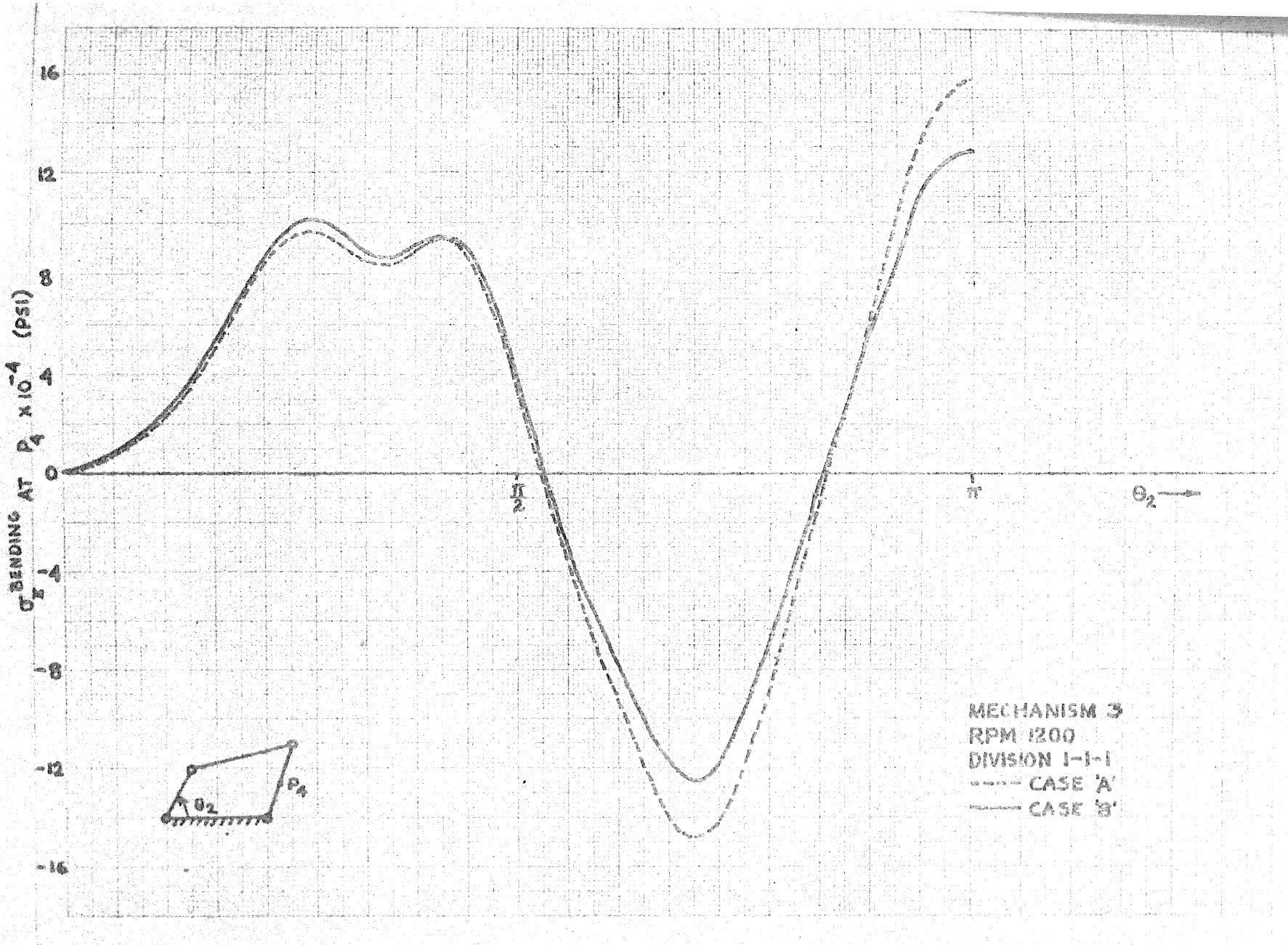

FIG 5.8 EFFECT OF RIGID BODY AXIAL FORCE ON FOLLOWER STRESS

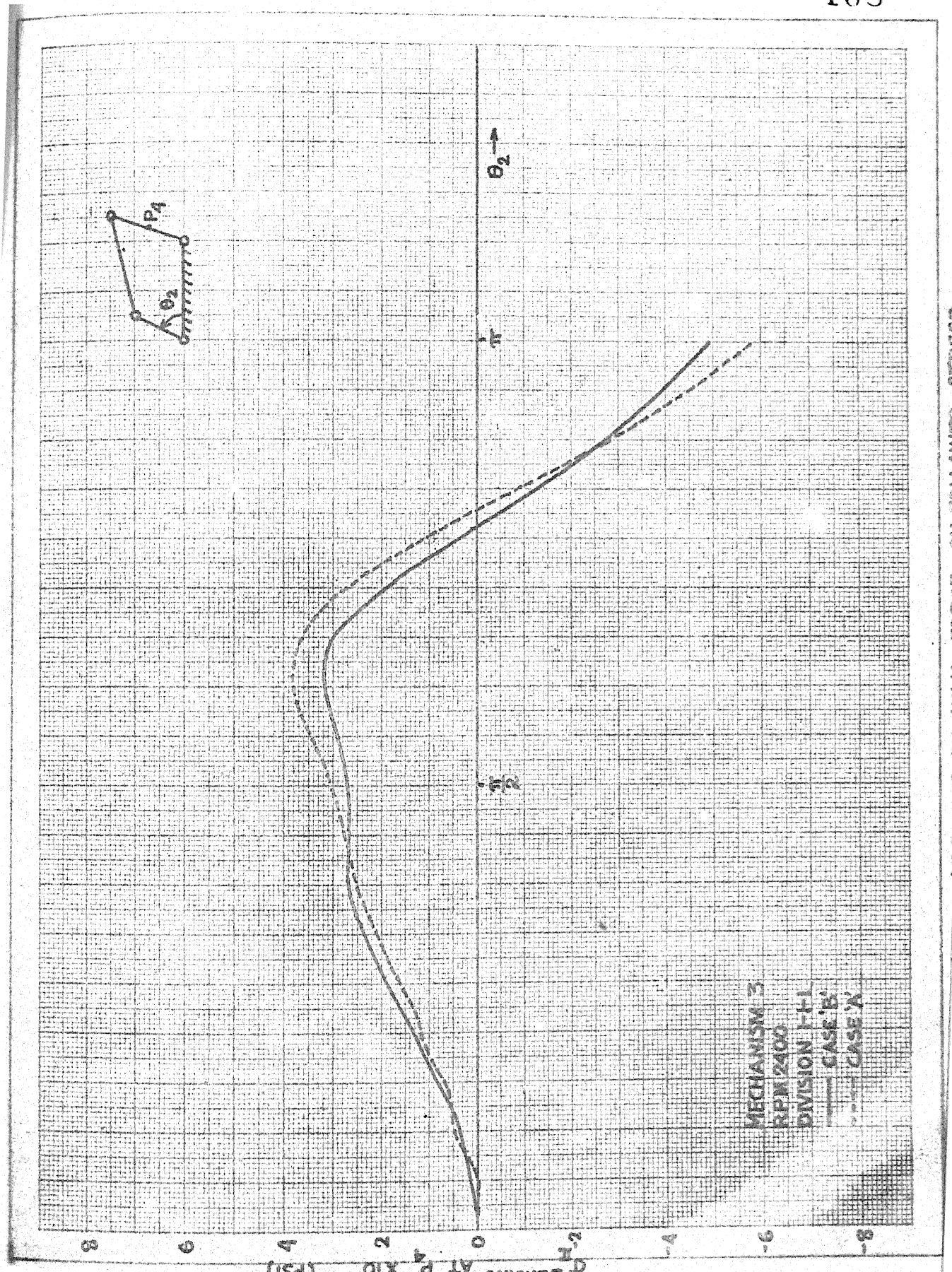

AT PIN P4 DUE TO AXIAL FORCE ON FOLLOWER STRESS

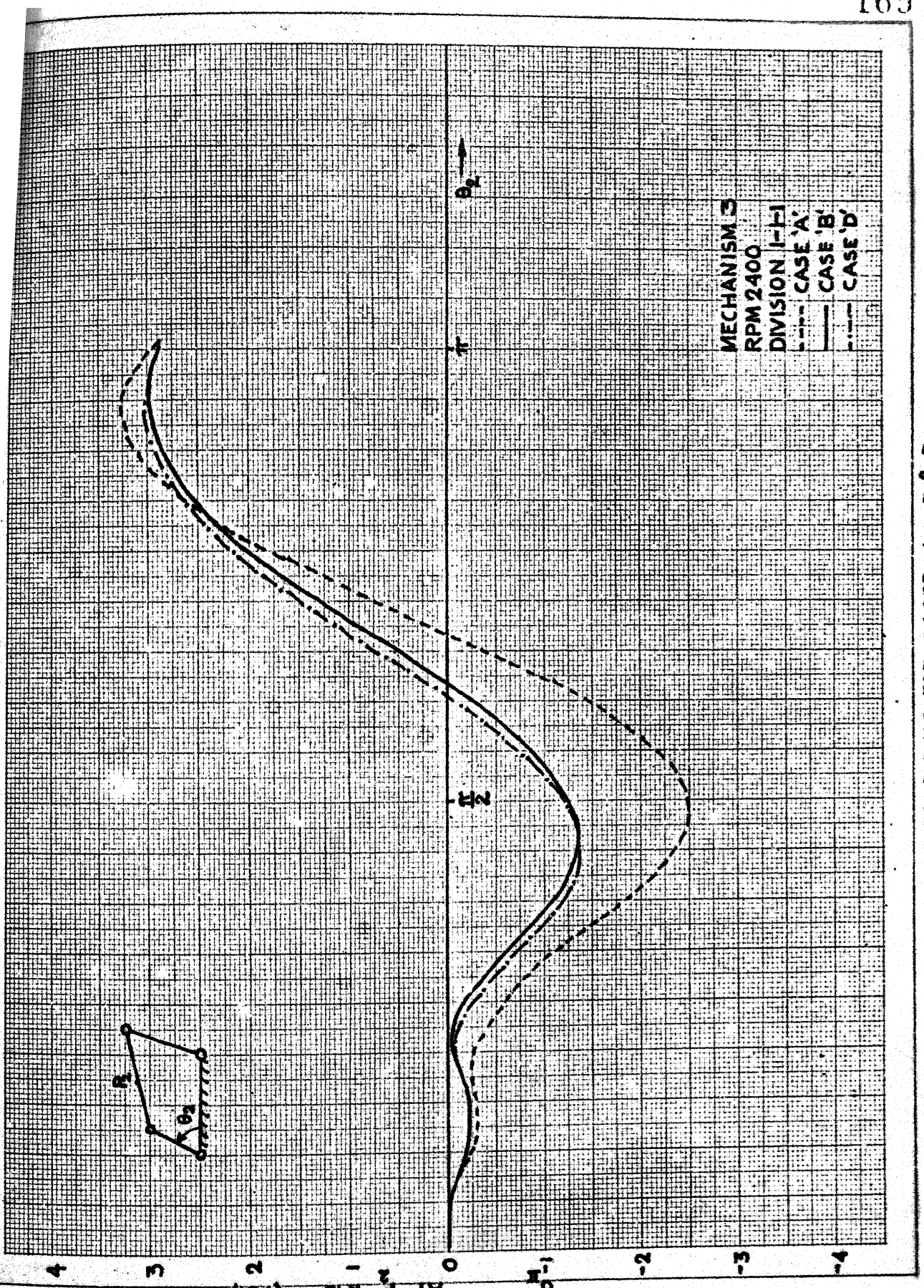

FIG 5.10 COUPLER STRESS FOR CASES A, B & D

EFFECTS OF DYNAMIC FACTORS AT 600 RPM

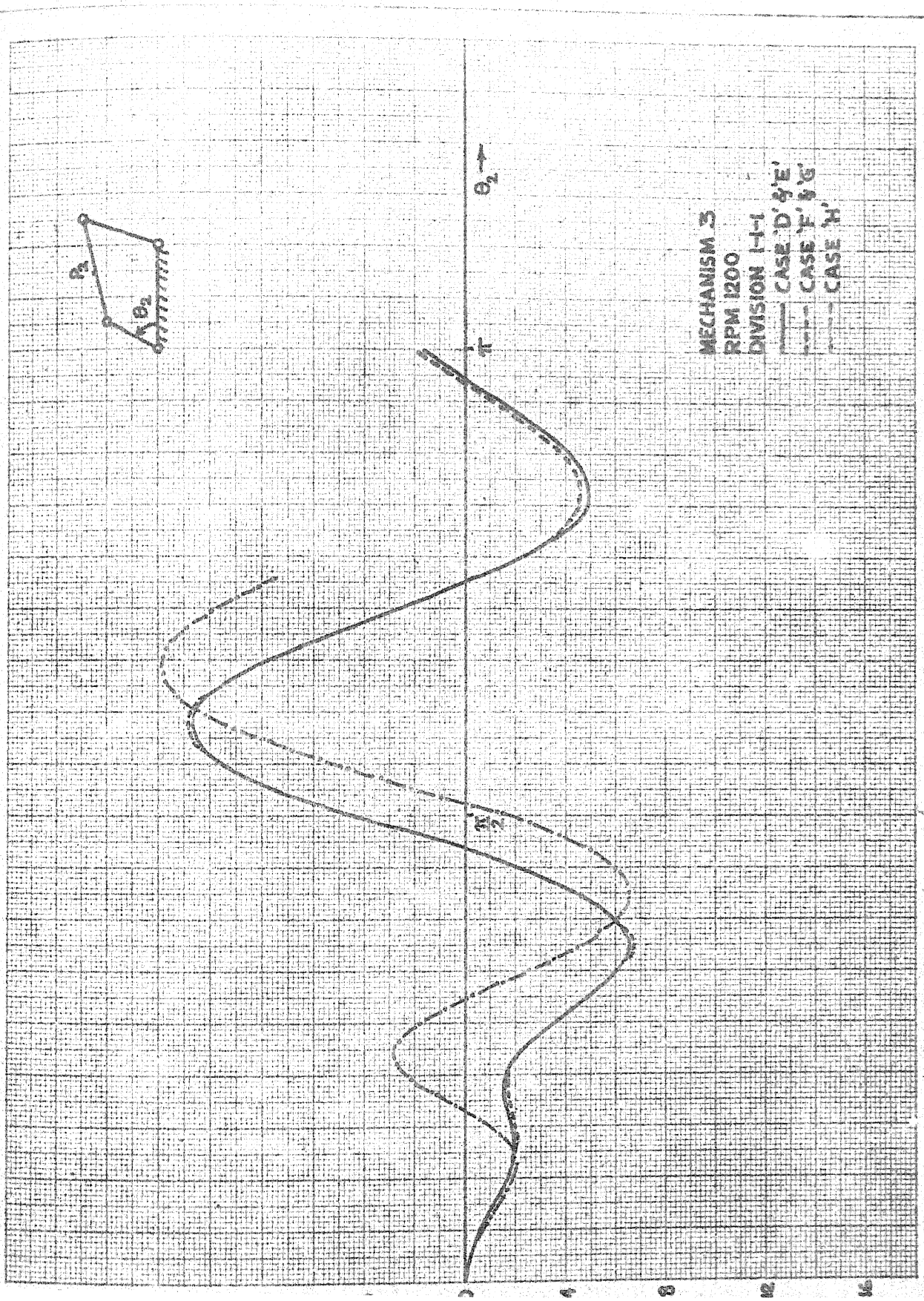

Fig. 5.12. EFFECT OF DYNAMIC FACTORS AT 1200 RPM

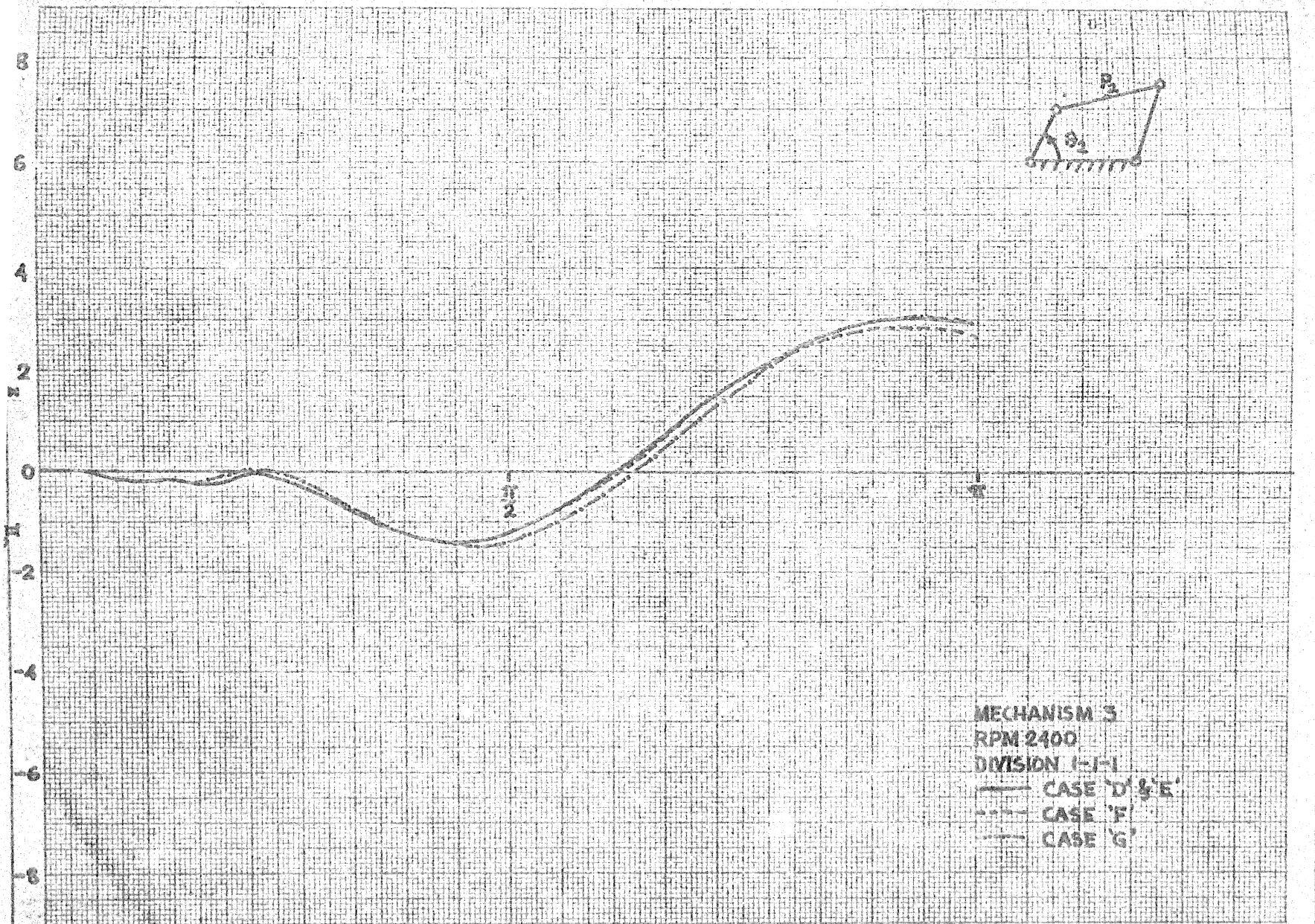

EFFECT OF DYNAMIC FACTORS AT 2400 RPM

the dynamic factors separately. Though it is apparent from the figures that the effects of the additional terms in eq. (3.42) due to the centrifugal, Coriolis and tangential accelerations increase with the speed, their orders of magnitude are quite small. The only other significant contributing factor is the consideration of the elastic axial forces as discussed in Section 3.4.

When the speed of a mechanism is increased, not only the magnitudes of the displacements change, but the nature of the variations with the crank rotation also undergoes some alterations. Fig. 5.14 to Fig. 5.17 show the variations of the stresses for different cases. The apparent large difference in the nature of the variations is due to the fact that the curves are plotted against crank rotation. If plotted against time, the difference would not be very large.

To show the effectiveness of the finite element methods considering all the aspects discussed in Chapters II and III, the problem of a slidercrank mechanism (mechanism 1) has been solved. The deflection at the middle point of the connecting rod is shown in Fig. 5.18. Comparing this with the similar results presented in References 4 and 5, it is seen that the nature of the variation of the deflections at the middle point of the connecting rod is in good agreement with those obtained in the two works mentioned above.

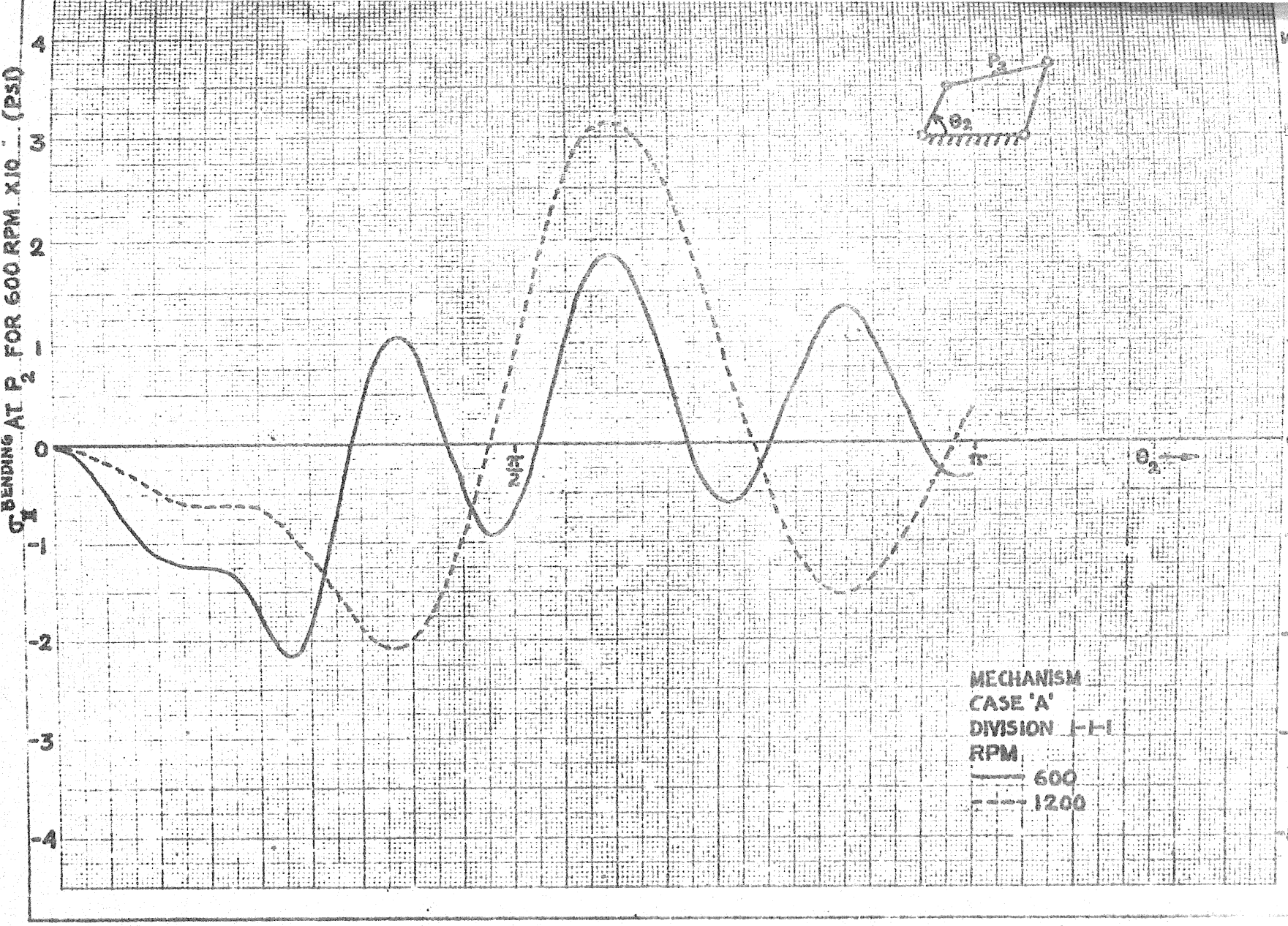

FIG 5.14 VARIATION OF COUPLER STRESS WITH CRANK SPEED CASE 'A'

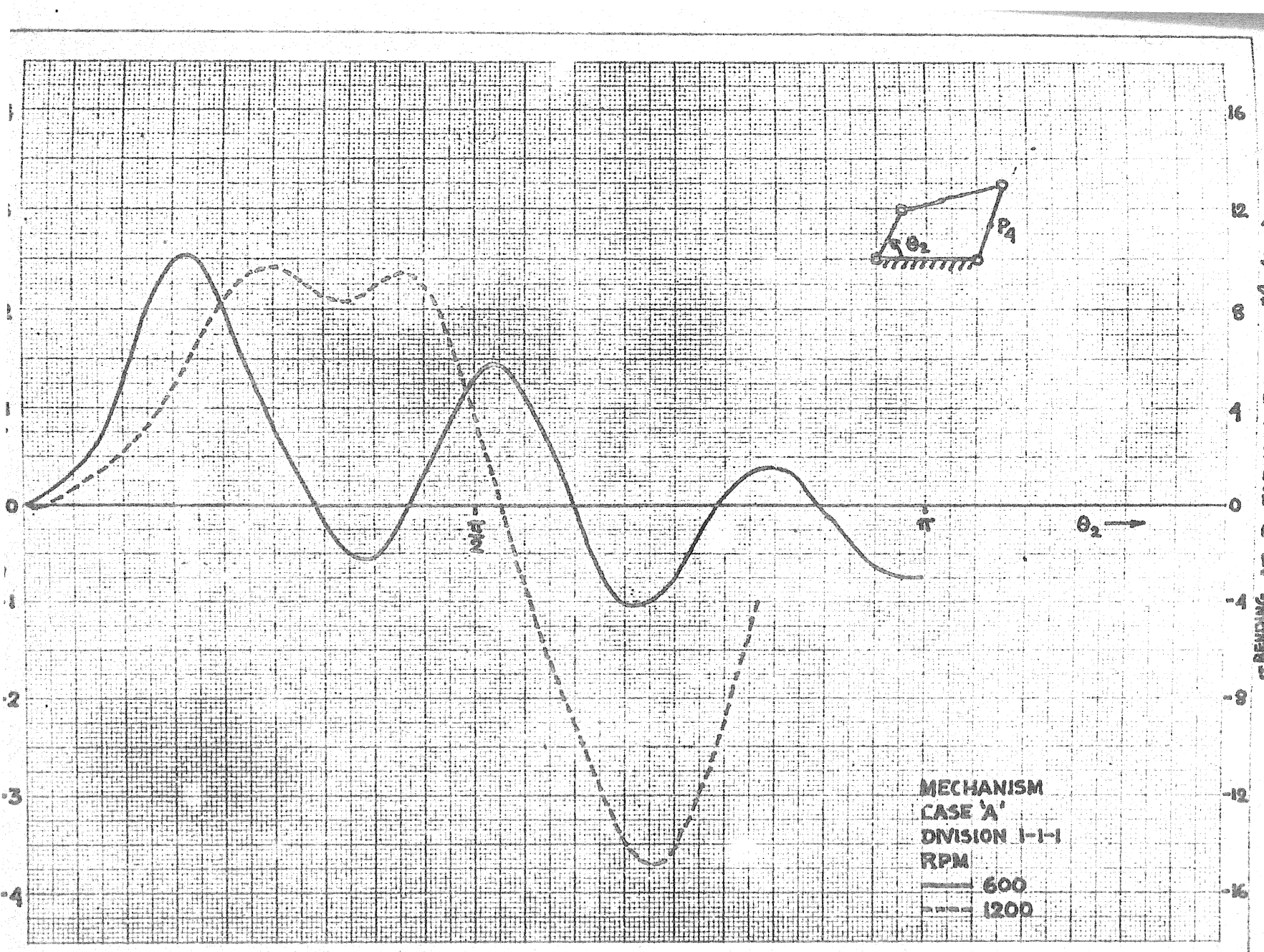

FIG 6.11 VARIATION OF FOLLOWER STRESS WITH CRANK SPEED CASE 'A'

FIG. 5.16. VARIATION OF COUPLER STRESS WITH CRANK SPEED

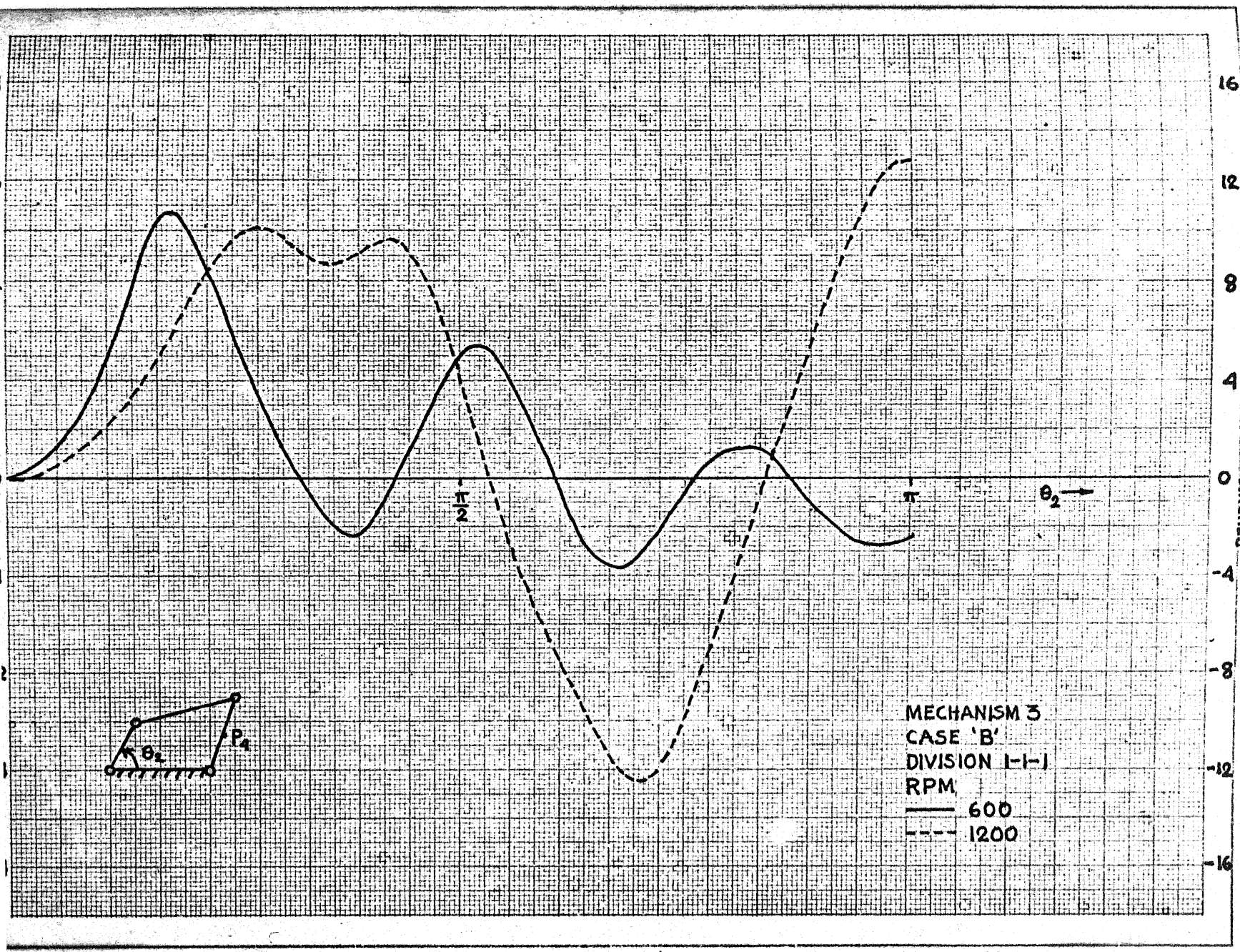

FIG 5.17 VARIATION OF FOLLOWER STRESS WITH CRANK SPEED CASE 'B'

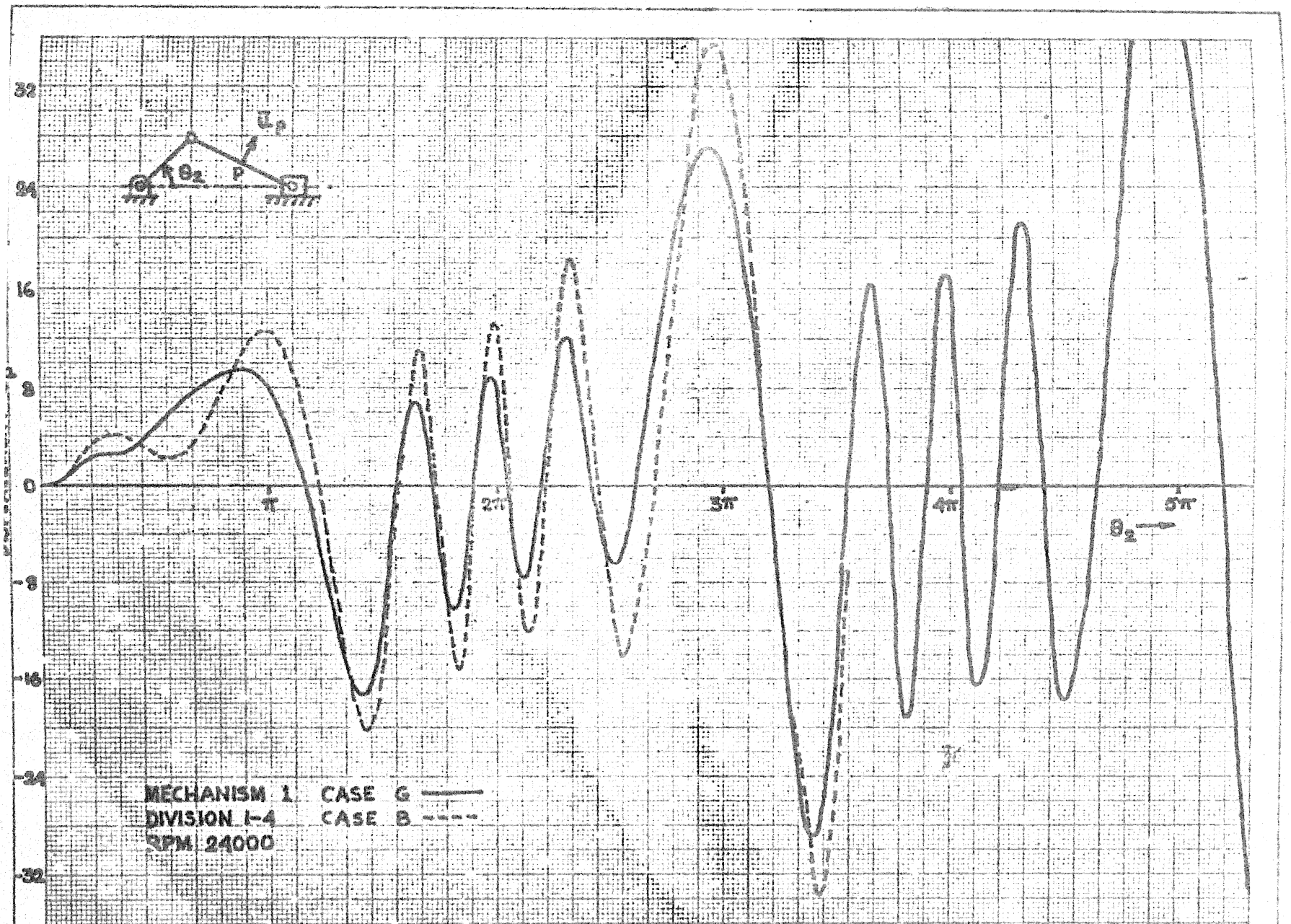
32
24
16
8
0
-8
-16
-24
-32
$\frac{1}{2}\pi$
2π
3π
4π
5π
θ_2
ω_p
θ_2
P
MECHANISM 1 CASE G
DIVISION 1-4 CASE B
RPM 24000

The discrepancies may be attributed to the difference in the methods of analysis. Transverse displacement of a point (at a distance of 4.8" from the crank end) of the connecting rod of mechanism 1 is again plotted in Fig. 5.19 at the same speed, but with case A. The importance of the different dynamic factors may be appreciated by comparing Fig. 5.18 with Fig. 5.19. It appears that when the dynamic factors are ignored, the nature of the vibratory motion is completely changed. This is due to the fact that the mechanism is running at a very high speed and the dynamic factors, particularly the rigid body axial forces, become more pronounced.

5.4 Direct Steady State Solution

Since the finite element technique is very versatile and powerful, a new approach for the direct steady state solution using the finite element techniques has been proposed in Chapter IV. In this section, the numerical results are presented and compared with those from the previous works in some cases. Both the slider crank and four-bar mechanisms have been solved using this approach.

Solving mechanism 3 with this method, the rotation $\bar{u}_9$ (in radians) at the coupler-end of the follower is found in the following form:

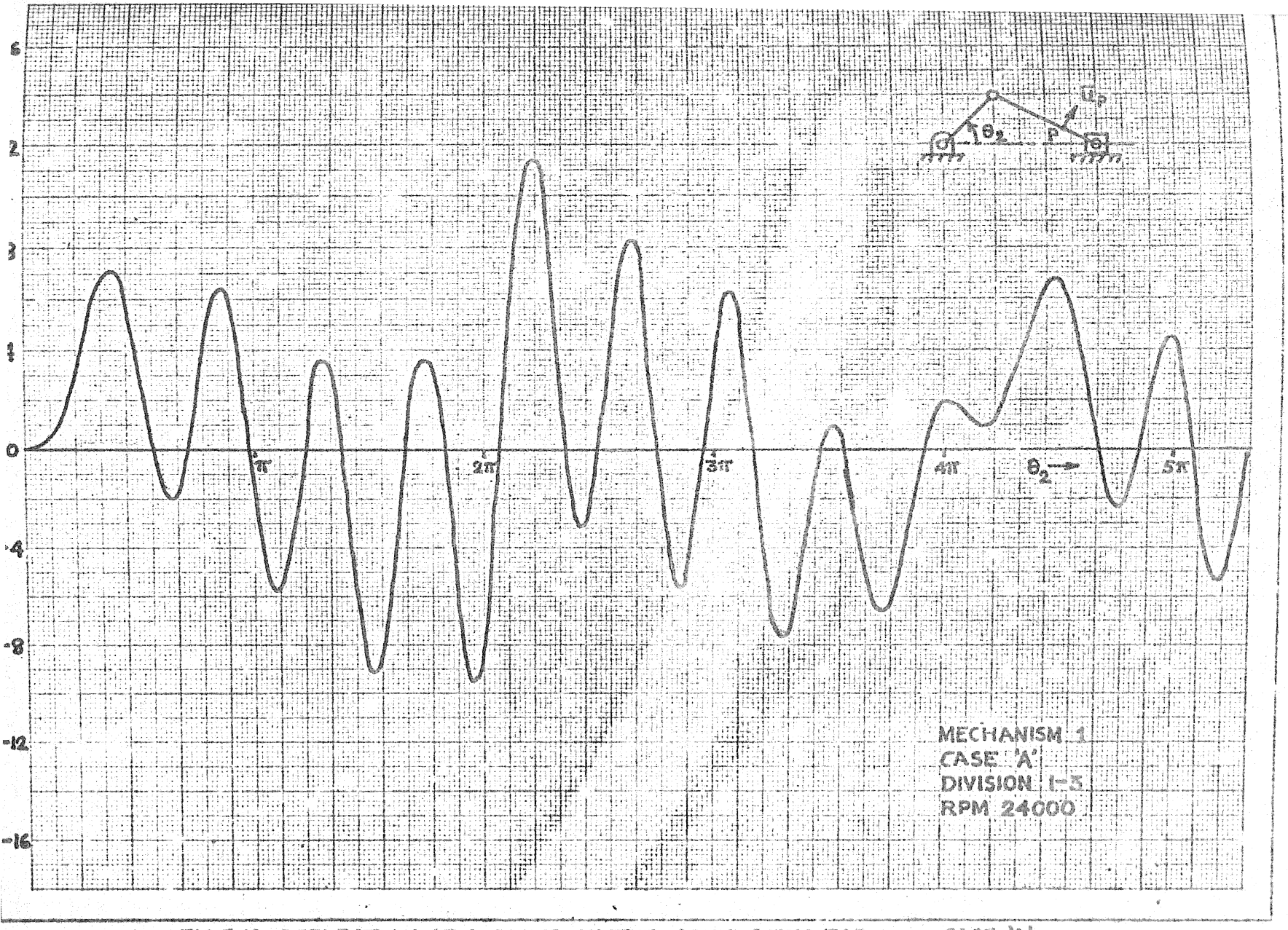

FIG 5.19 DEFLECTION OF A POINT ON THE CONNECTING ROD CASE 'A'

$$\bar{u}_9 = 10^{-3}(0.0233 + 8.12\cos\theta_2 + 3.31\cos2\theta_2 + 2.29\cos3\theta_2 + 0.0481\cos4\theta_2 - 1.59\cos6\theta_2 + 9.86\sin\theta_2 + 7.50\sin2\theta_2 + 5.81\sin3\theta_2 + 4.58\sin4\theta_2 + 1.21\sin5\theta_2 + 0.307\sin6\theta_2)$$

where θ_2 is the crank angle.

Similar expressions are also obtained for the displacements at other nodal points of the links. Fig. 5.20 to Fig. 5.22 show the variation of $\sigma_{II}^{bending}$ at the middle of the crank, follower and the coupler. Sadler and Sandor[10] have solved the same problem following the lumped parameter approach. The nature of the variation of the stresses will not be same as that of the deflections because the rigid body displacements do not take part in straining the member. However, the difference is found to be less pronounced in case of the follower. The nature of variation of the stress at the middle point of the follower shown in Fig. 5.22 is almost identical with that of the deflection at the same point found by Sadler and Sandor[10]. The same problem has been solved considering the crank to be instantaneously clamped and the results are shown in Fig. 5.21 and Fig. 5.22.

Mechanism 1 has also been solved by this approach and the deflection of the middle point of the connecting rod for one complete cycle is shown in Fig. 5.23. Comparing this with Fig. 5.18, it becomes clear that the steady state

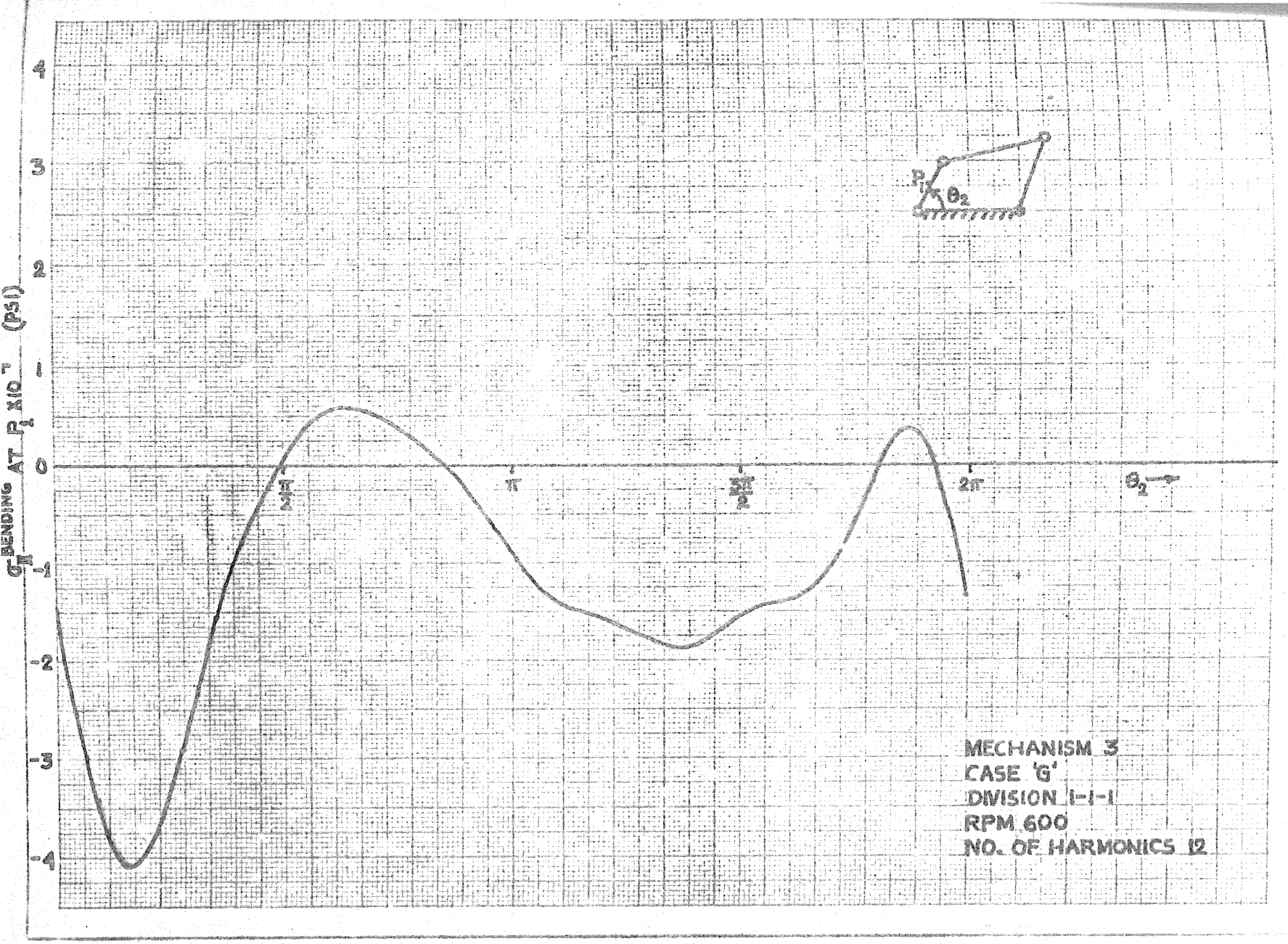

FIG 5.20 STEADY STATE CRANK STRESS OF MECHANISM 3

FIG. 5.6 STEADY STATE COUPLED STRESS FOR 'MECHANISM' AND 'STRUCTURE'

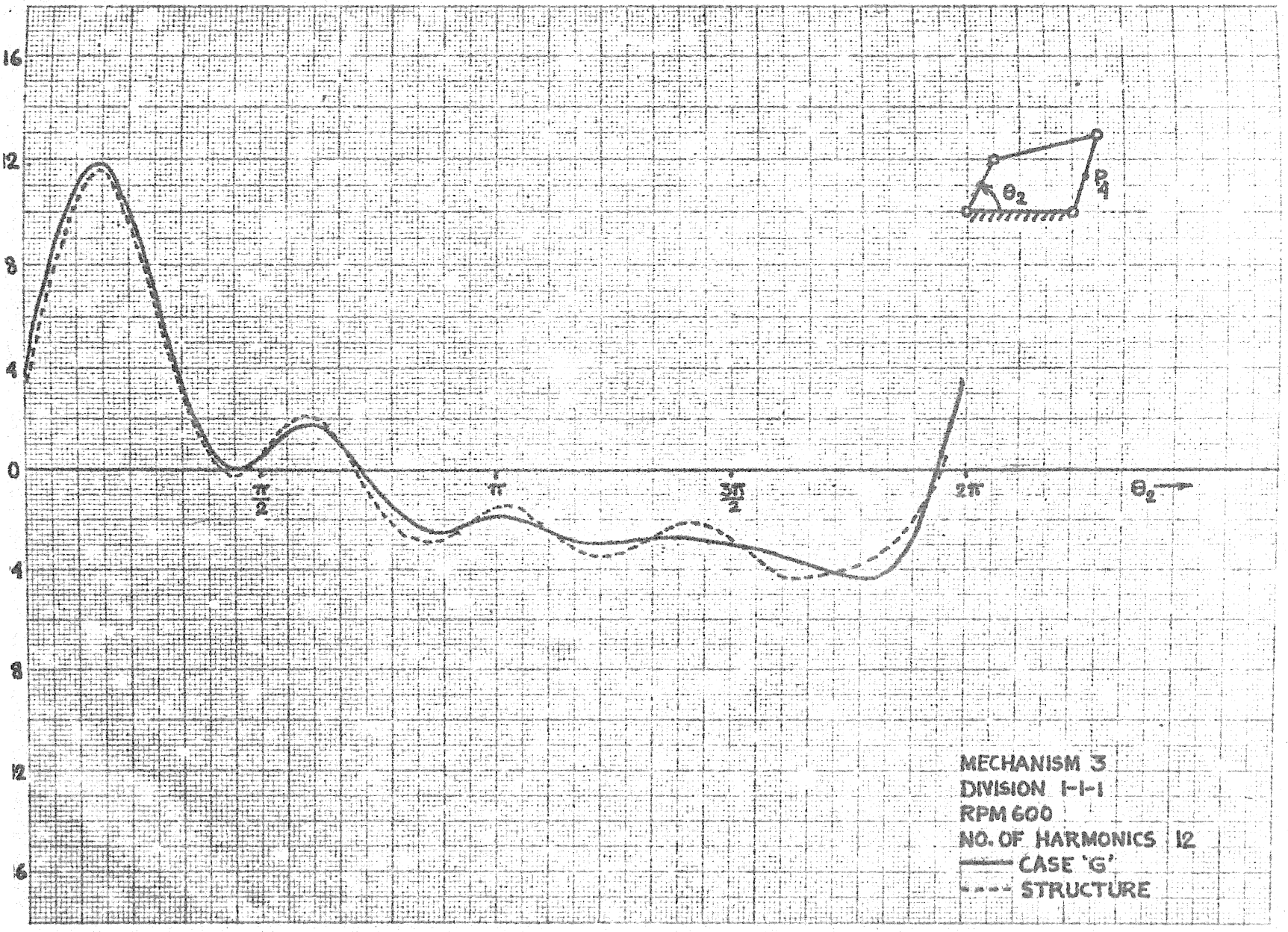
16
12
8
4
0
4
8
12
16
$\frac{\pi}{2}$
π
$\frac{3\pi}{2}$
2π
θ_2
θ_2
P_4
MECHANISM 3
DIVISION 1-1-1
RPM 600
NO. OF HARMONICS 12
CASE 'G'
STRUCTURE

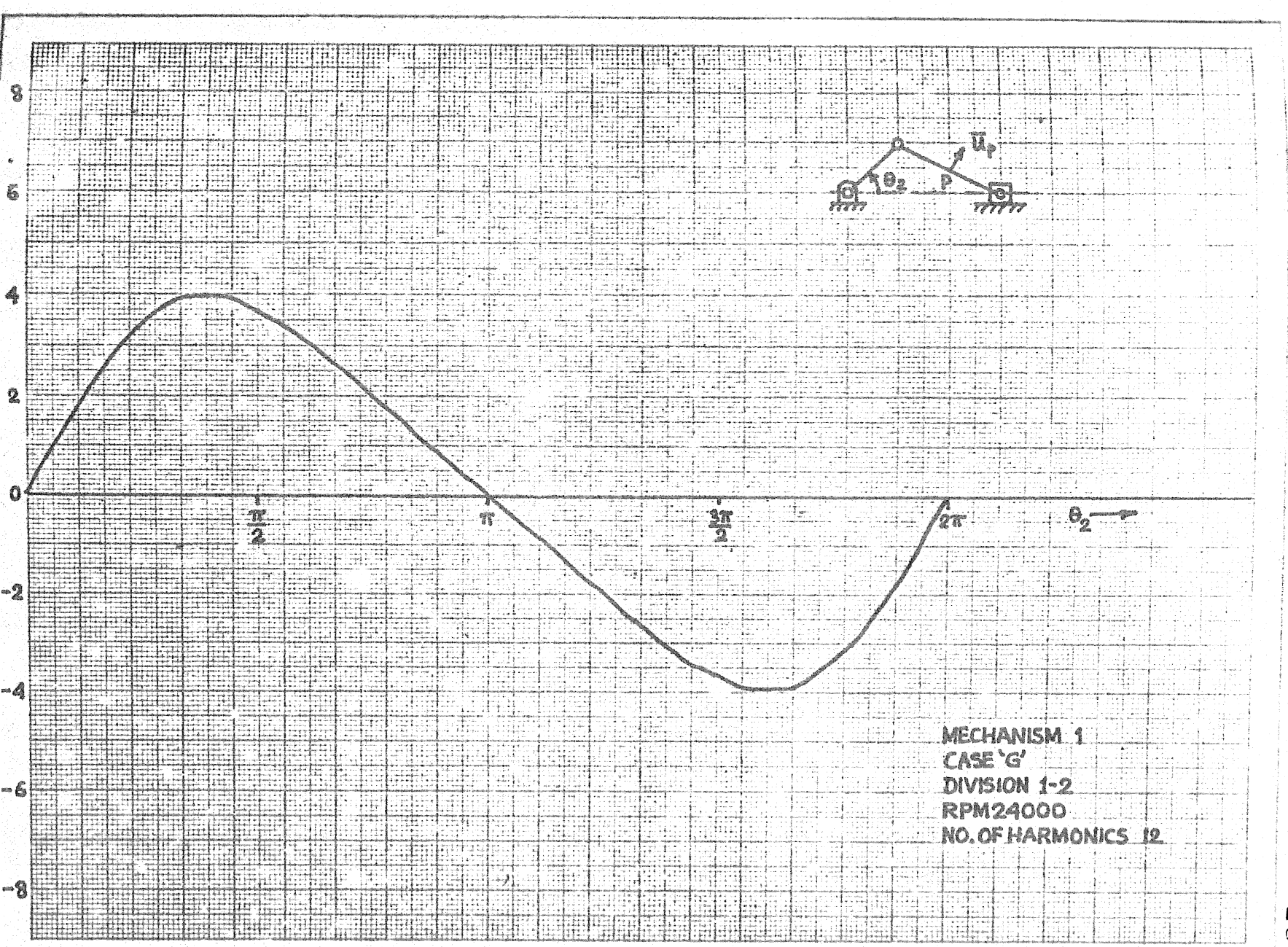

FIG 5.23 STEADY STATE DEFLECTION OF THE CONNECTING ROD

pattern can be completely different from the transient part. If the steady state solution is determined following the conventional methods (with two divisions of the connecting rod), almost 15 minutes of computer time is needed in IBM 7044 in contrast to 2 minutes taken by the new method of analysis. In complicated mechanisms where the number of co-ordinates is high, the computation time is reduced by an order of magnitude if this new method is adopted instead of the conventional finite-element approach.

Mechanism 2 has been solved for various values of the crank speeds and the normalised deflections of the middle point of the connecting rod (for one complete cycle) are shown in Fig. 5.24. The normalisation has been done to reduce the difference in the order of magnitude of the deflections for various crank speeds. Since the rigid body inertia forces increase with the square of the crank speed, the normalisation has been done by dividing the actual deflection by Ω_r^2, where Ω_r = angular velocity of the crank/ first circular natural frequency of the connecting rod, considering it to be a simply supported beam. Though mechanism 2 is not, strictly speaking, a simple degree of freedom system, its characteristics exhibit a good resemblance to those of a single degree of freedom system. When the amplitude of the deflections at the middle point of the connecting rod are plotted against the frequency ratio Ω_r,

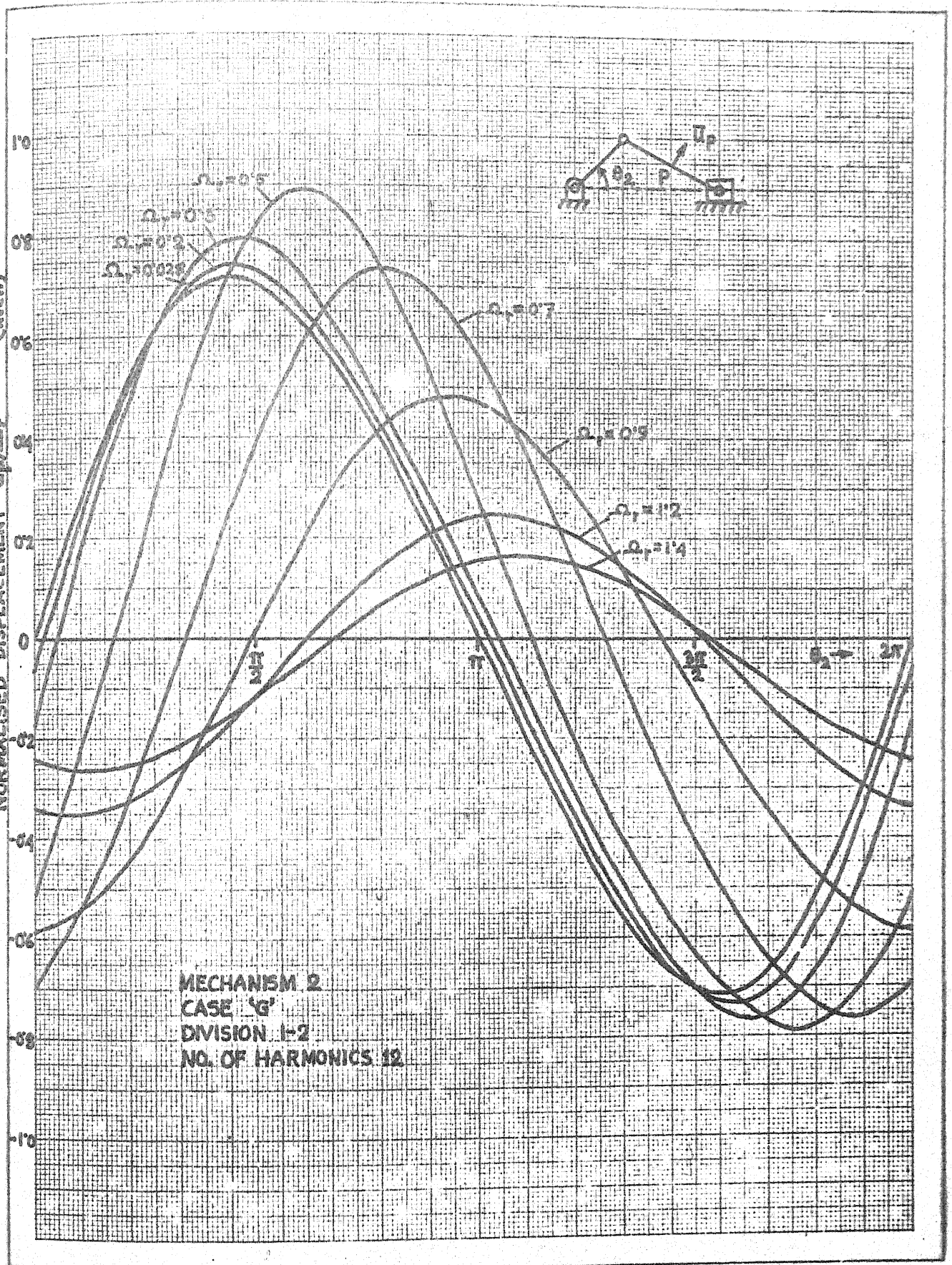

FIG 5.24 CONNECTING ROD DEFLECTION FOR VARIOUS SPEEDS

the curves obtained (Fig. 5.25) resembles the frequency response curves of a damped single degree of freedom system with excitation being proportional to the square of the forcing frequency. Fig. 5.24 also indicates a change in the phase between the excitation and deflection when the crank speed is varied. Fig. 5.26 shows the variation of phase angle with the frequency ratio Ω_r. From this figure also it is clear that the phase-shift characteristic is not much different from that of a damped single degree of freedom system. Viscomi and Ayre[5] solved the same mechanism for the steady state deflections with $\Omega_r = 0.3$ and found the steady-state amplitude to be about 0.72 in. Following the method of Chapter IV, the steady-state amplitude is found to be 0.79 in. The study of the speed-response characteristics of mechanisms is very much facilitated when the present method is adopted. Otherwise, considerable amount of computation time is required in the conventional methods.

In this chapter (except Fig. 5.5) comparisons between a 'mechanism' and 'structure' have been made by assuming that no flywheel exists at the crank-shaft of the mechanism. This has been done only to demonstrate the difference between the results obtained from the two extreme cases. It is evident that the results for a mechanism with a flywheel at the crank-shaft will lie between these two cases as shown in Fig. 5.5.

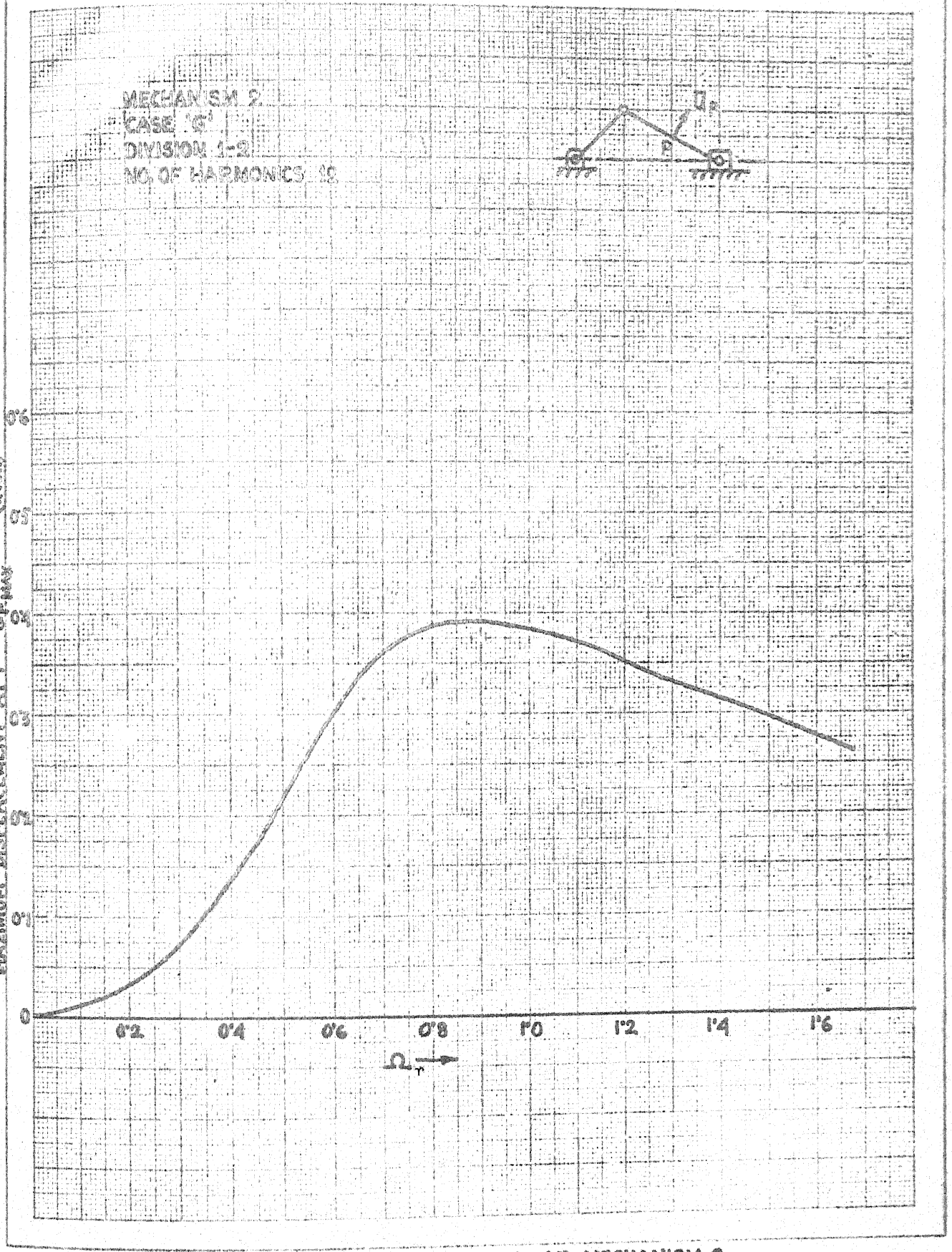

FIG 5.25 FREQUENCY RESPONSE OF MECHANISM 2

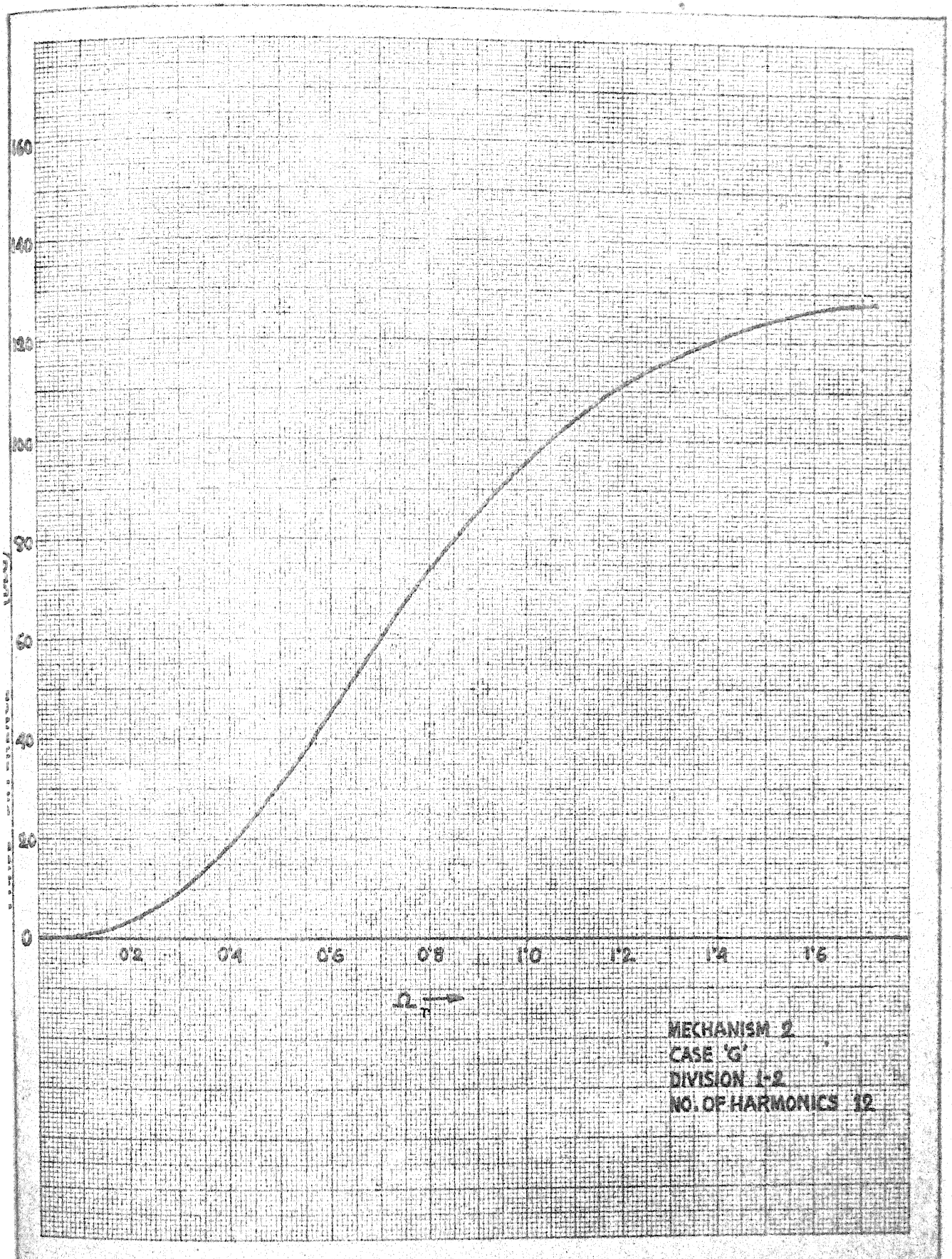

FIG 5.26 PHASE SHIFT FOR VARIOUS CRANK SPEEDS

Only a few numerical examples have been solved in this chapter as the major objective of the present work is to introduce the methods of analyses and demonstrate their efficacies rather than to study a few specific mechanisms exhaustively.

Since the numerical values of the examples solved in the previous works are in F.P.S. units, the same system of units is chosen in the examples cited in this chapter to facilitate direct comparison.

CHAPTER VI

CONCLUSIONS

Several important conclusions may be drawn following the numerical results presented in Section 2.9 and Chapter V. These may be listed as follows:

(i) When a mechanism is converted into a structure by imposing an aritifical constraint (viz., clamping the support-end of the crank), the vibration characteristics including the natural frequencies are altered. The natural frequencies of a mechanism are reduced as a consequence of such transformation. Therefore it should not be included in the analysis of flexible mechanisms.

(ii) To obtain even moderately accurate results, it is necessary to divide the links into more than one element. The optimum choice of the number of divisions of a link depends on its relative flexibility.

(iii) The stresses obtained from the analysis of 'static' and 'dynamic' restrained structures are less than those obtained from the displacement analysis alone. The relative magnitudes of the former with respect to the later type of stresses depend on the speed of the mechanism. With increase in the number of

divisions of a link, the stresses obtained from the restrained structures gradually decrease.

(iv) The general method for the rigid body analysis described in Section 2.9 takes computer time less by an order of magnitude than that taken by the existing matrix procedures.

(v) The effects of the rigid body axial forces on the transverse vibrations of the links are appreciable and in the kineto-elastodynamic analysis of high-speed mechanisms these effects should be taken into account.

(vi) The dynamic nature of the rigid body inertia forces (instead of considering them to be quasi-static) should be taken into consideration for better accuracy of the analysis.

(vii) When the axial forces are obtained from elastic deformations of the links, their effects on the transverse vibrations of the links are even more pronounced.

(viii) The effects of Coriolis components of accelerations, the additional normal and tangential components of accelerations on the vibrations of the links are not significant, at least in the transient part of a four-bar mechanism.

(ix) Computer time taken by the new method of analysis presented in Chapter IV to obtain the steady state solution is less by an order of magnitude when compared with the conventional methods.

(x) The total number of harmonics to be taken in the new method of analysis depends on the number of dominant harmonics present in the force vector. Sufficiently accurate results have been obtained with eight harmonics in a case of a slider crank mechanism described in Chapter V.

REFERENCES

1. Lowen G.G. and Jandrasits W.G., Survey of Investigations into the Dynamic Behaviour of Mechanisms Containing Links with Distributed Mass and Elasticity, Mechanism and Machine Theory, Vol. 17, No. 1, 1972, pp. 3-17.

2. Erdman A.G. and Sandor G.N., Kineto-elastodynamics – A Review of the State of the Art and Trends, Mechanism and Machine Theory, Vol. 17, No. 1, 1972, pp. 19-33.

3. Kozhevnsikov S.N., Dynamics of Machines with Elastic Links and Distributed Parameters (in Russian), Trudy II Vsesoyuznogo S'ezda po Teoreticheskoi i Prikladnoi Mekhanike, Izdatel'stvo "Nauka", Moscow, 1965, pp. 231-246.

4. Neubauer A.H. Jr., Cohen R. and Hall A.S. Jr., An Analytical Study of the Dynamics of an Elastic Linkage, Trans. ASME, J. Engng. Ind., Vol. 88, No. 3, Aug. 1966, pp. 311-317.

5. Viscomi B.V. and Ayre R.S., Nonlinear Dynamic Response of Elastic Slider Crank Mechanism, Trans. ASME, J. Engng. Ind., Vol. 93, 1971, pp. 251-262.

6. Jasinski P.W., Lee H.C. and Sandor G.N., Vibrations of Elastic Connecting Rod of a High-Speed Slider-crank Mechanism, Trans. ASME, J. Engng. Ind., Vol. 93, 1971, pp. 636-644.

7. Jasinski P.W., Lee H.C. and Sandor G.N., Stability and Steady-state Vibrations in a High-speed Slider-crank Mechanism, Trans. ASME, J. Appl. Mech., Vol. 37, 1970, p. 1069.

8. Meyer Zur Capellen W., Biegungsschwingungen in der Koppel einer Kurbelschwinge, Österreichisches Ingenieur-Archiv 16(4), 1962, pp. 341-348.

9. Sadler J.P. and Sandor G.N., A Lumped Parameter Approach to Vibration and Stress Analysis of Elastic Systems, Trans. ASME, J. Engng. Ind., Vol. 95, 1973, pp. 549-557.

10. Sadler J.P. and Sandor G.N., Non-linear Vibration Analysis of Elastic Four-Bar Linkages, Trans. ASME, J. Engng. Ind., Vol. 96, 1974, pp. 549-557.

11. Winfrey R.C., Dynamics of Mechanisms with Elastic Links, Ph.D. Dissertation, Univ. of California at Los Angeles, 1969.

12. Winfrey R.C., Elastic Link Mechanism Dynamics, Trans. ASME, J. Engng. Ind., Vol. 93, 1971, pp. 268-272.

13. Uicker J.J. Jr., Denavit J. and Hartenberg R.S., An Iterative Method for the Displacement Analysis of Spatial Mechanisms, Trans. ASME, J. Appl. Mech., Vol. 31, 1964, pp. 309-314.

14. Denavit J., Hartenberg R.S., Razi R. and Uicker J.J. Jr., Velocity, Acceleration and Static-Force Analyses of Spatial Linkages, Trans. ASME, J. Engng. Ind., Vol. 32, 1965, pp. 903-910.

15. Erdman A.G., Sandor G.N. and Oakberg R.C., A General Method for Kineto-elastodynamic Analysis and Synthesis of Mechanisms, Trans. ASME, J. Engng. Ind., Vol. 94, 1972, pp. 1193-1205.

16. Erdman A.G., Imam I. and Sandor G.N., Applied Kineto-elastodynamics, Proceedings of the Second OSU Applied Mechanisms Conference, Stillwater, Oklahoma, 1971.

17. Imam I., Sandor G.N. and Kramer S.N., Deflection and Stress Analysis in High Speed Planar Mechanisms with Elastic Links, Trans. ASME, J. Engng. Ind., Vol. 95, 1973, pp. 541-548.

18. Fox R.L. and Kapoor M.P., Rate of Change of Eigenvalues and Eigenvectors, J. AIAA, Vol. 6, 1968, pp. 2426-2429.

19. Ogawa K. and Funabashi H., On the Balancing of the Fluctuating Input Torques Caused by Inertia Forces in the Crank and Rocker Mechanisms, Trans. ASME, J. Engng. Ind., Vol. 91, 1969, pp. 97-102.

20. Berkof R.S. and Lowen G.G., Theory of Shaking Moment Optimization of Force-balanced Four-bar Linkages, Trans. ASME, J. Engng. Ind., Vol. 93, 1971, pp. 53-60.

21. Habiger E., Das dynamische Verhatten des Drehstrom-Asynchronmotors bei kleinen periodischen Drehmomen-tänderungen, Maschinenbautechnik, 16(11), 579-583 (1967).

22. Müller D., Das Verhatten einer Klasse schwingungsfähiger linearer mechanischer Systeme bei Beachtung der elektrischen Ausgleichvorgange im Antrieb (Asynchronmaschine. Maschinenbautechnik 16(11), 575-578, 588 (1967).

23. Houben H., Das Verhatten von Asynchronmotoren in Maschinen mit periodish veränderlicher reduzierter Masse, Industrie-Anzeiger 90(78), 1767-1768 (1968).

24. Houben H., Schurngungen und Belastungen in Maschinengruppen, Proceedings of the 2nd International Conference on the theory of Machines and Mechanisms, Vol. 2, pp. 78-85, Zakopane, Poland (1969).

25. Houben H., Drehschwingungen unter Berucksichtigüng der Getrieberückwirkungen auf die Antriebsmachine, VDI-Berichte No. 127, 43-50 (1969).

26. Houben H., Erzwungene und freie Drehschwingungen sowie ihre Instabilitäten erster und zweiter Art in Maschinensätzen mit antreibendem Asynchronmotor, Fortschritt Berichte, VDI-Zeitschrift, Series 9, No. 8 (March 1970).

27. Benedict C.E., Dynamic Response Analysis of Real Mechanical Systems Using Kinematic Influence Coefficients, Master's thesis, Univ. of Florida, Gainesville, 1969.

28. Benedick C.E. and Tesar D., Dynamic Response Analysis of Quasi-Rigid Mechanical System Using Kinematic Influence Coefficients, J. Mechanisms, Vol. 6, 1971, pp. 383-403.

29. Biezeno C.B. and Grammel R., Engineering Dynamics, Vol. 4, Blackie and Son, Ltd., London, England, 1954.

30. Meyer zur Capellen W., Harmonische Analyse bei der Kurbelschleife, Z. Angew. Math. Mech., Vol. 36, 1956, p. 151.

31. Meyer zur Capellen W., Kinematic und Dynamik der Kurbelschleife, Werkstatt und Betrieb, 1956, part 1, No. 10, pp. 581-588; part 2, No. 12, pp. 677-683.

32. Meyer zur Capellen W., Die Kurbelschleife zweiter Art, Werkstatt und Betrieb, 1957, No. 5, pp. 306-308.

33. Freudenstein F., Harmonic Analysis of Crank and Rocker Mechanisms with Applications, Trans. ASME, J. Appl. Mech., Vol. 81, 1959, pp. 673-675.

34. Flory J.F. and Wollford J.C., Harmonic Analysis of Kinematic Linkages, ASME Paper No. 64-Mech-38 (1964).

35. Bogden R.C. and Huncher T.V., General Systematization and Unified Calculation of Five and Four-bar Plane Basic Mechanisms, ASME Paper No. 66-Mech-11 (1966).

36. Markus L. and Tomas J., Harmonic Analysis of Planar Mechanisms – Kinematics, J. Mechanisms, Vol. 3, 1968, pp. 171-185.

37. Sherwood A.A., The Dynamics of the Harmonic Space Slider-crank Mechanism, J. Mechanisms, Vol. 1, 1966, pp. 203-208.

38. Meyer zur Capellen W., Kinematik der Spharischen Zchubkurbel, Forschungsberichte des Wirtschafts und Verkehrsministeriums Nordrhein-Westfalen, Westdeutscher Verlag Cologne, Germany, No. 873, 1960.

39. Yang A.T., Harmonic Analysis of Spherical Four-bar Mechanisms, Trans. ASME, J. Appl. Mech., Vol. 84, 1962, pp. 683-688.

40. Sadler J.P. and Sandor G.N., Kineto-elastodynamic Harmonic Analysis of Four-Bar Path Generating Mechanisms, presented at the 11-th ASME Conference on Mechanisms, Columbus, Ohio, Nov. 1-4, 1970, ASME Paper No. 70-Mech-61.

41. Sadler J.P. and Sandor G.N., Kineto-elastodynamic Harmonic Analysis of Four-bar Path Generating Mechanisms Including Centrifugal Stiffening, Mech. Engng. News.

42. Sadler J.P., On the Analytical Lumped Mass Model of an Elastic Four-Bar Mechanism, Trans. ASME, J. Engng. Ind., Vol. 97, 1975, pp. 561-565.

43. Hurty W.C. and Rubinstein M.F., Dynamics of Structure, Prentice-Hall, Inc., Englewood Cliffs, 1966.

44. Beggs J.S., Stresses in Redundant Mechanisms, Trans. ASME, J. Appl. Mech., Vol. 37, 1970, pp. 223-228.

45. Seevers J.A., Dynamic Stability of Linkages with Elastic Members, M.S. thesis, Univ. of California, Davis, California (1969).

46. Seevers J.A. and Yang A.T., Dynamic Stability Analysis of Linkages with Elastic Members via Analog Simulation, ASME Paper No. 70-Mech-48.

47. Houben H., Untersuchungen Über die Stabilität elastischer Bewegungen in der Koppel eines Viergelenkgetriebes, Ph.D. Dissertation, TH Aachen (1965).

48. Houben H., Über die Stabilität von Schwingungen in Gelenkgetrieben, Forsch Ber Landes NRhein-Westf. No. 1959, Westodeutscher Verlag, Koln und Opladen (1968).

49. Houben H., Stabilität von Biegeschwingungen in der Koppel von Kurbeltrieben, Industrie-Anzeiger 90(25), 1968, pp. 485-489.

50. Witfeld H., Zur Spannungs und Stabilitätsberechnung der Koppel eines schnellaufenden Gelenkgetriebes, Fortschritt Berichte, VDI-Zeitschrift, Series 1, No. 19, 1970.

51. Tobias J.R., The Design of Planar Mechanisms with Distributed Flexibility and Inertia, Ph.D. Dissertation, Univ. of Minnesota, 1970.

52. Bolotin V.V., The Dynamic Stability of Elastic Systems, Holden-Day, Inc., San Francisco, London, Amsterdam, 1964.

53. Evanston H.A. and Evan-Iwanowski R.M., Effects of Longitudinal Inertia Upon the Parametric Response of Elastic Columns, Trans. ASME, J. Appl. Mech., Vol. 33, 1966, pp. 141-148.

54. Mayer zur Capellen W., Torsional Vibrations in the Shafts of Linkage Mechanisms, Trans. ASME, J. Engng. Ind., Vol. 89, 1967, p. 126.

55. Eringen A.C., On the Nonlinear Vibration of Elastic Bars, Quarterly of Applied Mathematics, 9, 1952, pp. 361-368.

56. Lubkin S. and Stoker J.J., Stability of Columns and Strings Under Periodically Varying Forces, Quart. Appl. Math., Vol. 1, 1943, pp. 215-217.

57. Broniarek C.A. and Sandor G.N., Dynamic Stability of an Elastic Parallelogram Linkage, Non-linear Vibration Problems, No. 12, 1971, pp. 315-325.

58. Przemieniecki J.S., Theory of Matrix Structural Analysis, McGraw-Hill Book Co., New York, 1968.

59. Rubinstein M.F., Matrix Computer Analysis of Structures, Prentice Hall, Inc., 1966.

60. Zienkiewicz O.C., The Finite Element Method in Engineering Science, 2nd ed., McGraw-Hill, New York, 1971.

61. Ralston A., A First Course in Numerical Analysis, McGraw-Hill Book Co., N.Y., 1965.

62. Uicker J.J. Jr., Dynamic Force Analysis of Spatial Linkages, Trans. ASME, J. Appl. Mech., Vol. 34, 1967, pp. 418-424.

63. Archer J.S., Consistent Matrix Formulations for Structural Analysis Using Finite Element Techniques, J. AIAA, Vol. 3, 1965, pp. 1910-1918.

64. Wilkinson J.H., The Algebraic Eigenvalue Problem, Clarendon Press, Oxford, 1965.

65. Desai C.S. and Abel J.F., Introduction to the Finite Element Method: A Numerical Method for Engineering Analysis, Van Nostrand Reinhold Co., New York, 1972.

66. Cesari L., Asymptotic Behaviour and Stability Problems in Ordinary Differential Equations, Springer-Verlag, Berlin, 1963.

67. Coddington E.A. and Levinson N.L., Theory of Ordinary Differential Equations, McGraw-Hill Book Co., New York, 1955.

68. Leftschetz S., Differential Equations: Geometric Theory, 2nd ed., Interscience Publishers, New York, 1963.

69. Whittaker E.T. and Watson G.N., A Course of Modern Analysis, Cambridge Univ. Press, 1963.

70. McLachlan N.W., Theory and Application of Mathieu Functions, Dover Publications, New York, 1964.

71. Stoker J.J., Nonlinear Vibrations in Mechanical and Electrical Systems, Interscience Publishers, 1950.

72. Valeev K.G., On the Solution and Characteristic Exponents of Solutions of Some Systems of Linear Differential Equations with Periodic Coefficients, J. Appl. Math. Mech., Vol. 24, 1960, pp. 877-902.

73. Valeev K.G., On Hill's Method in the Theory of Linear Differential Equations with Periodic Coefficients, J. Appl. Math. Mech., Vol. 24, 1960, pp. 1493-1505.

74. Valeev K.G., On Hill's Method in the Theory of Linear Differential Equations with Periodic Coefficients. Determination of the Characteristic Exponents, J. Appl. Math. Mech., Vol. 25, 1961, pp. 460-466.

75. Yamamoto T. and Saito A., On the Vibrations of 'Summed and Differential Types' Under Parametric Excitation, Memoirs of the Faculty of Engineering, Nagoya Univ., (Japan), Vol. 22, No. 1, 1970, pp. 54-123.

76. Hsu C.S., On the Parametric Excitation of a Dynamic System Having Multiple Degrees of Freedom, Trans. ASME, J. Appl. Mech., Vol. 30, 1963, pp. 367-372.

77. Hsu,C.S., Further Results on Parametric Excitation of a Dynamical System, Trans. ASME, J. Appl. Mech., Vol. 32, 1965, pp. 373-377.

78. Hsu C.S., Impulsive Parametric Excitation: Theory, Trans. ASME, J. Appl. Mech., Vol. 39, 1972, pp. 551-558.

79. Hsu C.S. and Cheng W.H., Applications of the Theory of Impulsive Parametric Excitation and New Treatments of General Parametric Excitation Problems, Trans. ASME, J. Appl. Mech., Vol. 40, 1973, pp. 78-86.

80. Hsu C.S. and Cheng W.H., Steady State Response of a Dynamical System Under Combined Parametric and Forcing Excitations, Trans. ASME, J. Appl. Mech., Vol. 41, 1974, pp. 371-378.

81. Tani J., Dynamic Instability of Truncated Conical Shells under Periodic Axial Load, Int. J. Solids Struct., Vol. 10, No. 2, 1974, pp. 169-176.

82. Struble R.A., Nonlinear Differential Equations, McGraw-Hill Book Co., New York, 1962.

83. Hayashi C., Nonlinear Oscillations in Physical Systems, McGraw-Hill Book Co., New York, 1964.

84. Cunningham W.J., Introduction to Nonlinear Analysis, McGraw-Hill Book Co., New York, 1958.

85. Kobrinskii A.Ye., Mechanisms with Elastic Couplings – Dynamics and Stability, Nauka Press, Moscow, 1964, NASA Technical Translation, NASA TT F-534, June 1969.

86. Kobrinskii A.Ye., Dynamics of Mechanisms with Elastic Connections and Impact Systems, ILIFE Books Ltd., London, 1969.

87. Rayleigh J.W.S., The Theory of Sound, 2nd ed., Dover Publications, New York, 1945.

88. Green W.G., Theory of Machines, Blackie & Sons, London, 1958.

89. Hobson E.W., A Treatise on Plane and Advanced Trigonometry, seventh ed., Dover Publications, New York, 1957.

90. Bathe K.J. and Wilson E.L., Large Eigenvalue Problems in Dynamic Analysis, J. Engng. Mech. Div., ASCE, Vol. 98, No. EM6, Dec. 1972, pp. 1471-1485.

91. Osborne E.E., On Acceleration and Matrix Deflation Processes with Power Method, J. Soc. Industr. Appl. Math., Vol. 6, 1958, pp. 279-287.

Appendix - A

Description of Computer Programs

In order to solve the numerical examples in Chapter V, several computer programs have been written. Of them, only two major programs are described below. These programs are sufficiently general in the sense that these can analyse (i) a mechanism or a structure (having no rigid body degrees of freedom), (ii) with arbitrary number of divisions of any link, (iii) with or without axial deformations of the links, (iv) with or without the effects of rotary inertia and shear deflection,(v) a quasi-static or a complete dynamic problem of a mechanism etc.

Program I

The purpose of this program is to solve eq. (3.42) for the types of mechanisms cited in Chapter V. All cases described in Chapter II (with the exception of Sections 2.6 and 2.9) and Chapter III are included in this program. The major steps of computations are:

(i) Read the input data (consisting of geometrical, material properties etc. special conditions like damping, external loading etc. and the necessary codes).

(ii) Find the angles, angular velocities, square of the angular velocities, angular accelerations and the absolute longitudinal and transverse accelerations of the left end of each link, all in series of harmonics of the crank angle.

(iii) Find the element oriented element matrices $\bar{m}$, $\bar{k}$ and $\bar{m}^a$ for each link.

(iv) Starting with a crank angle, find the quantities calculated in step (ii) by summing up all harmonics for the current crank angle.

(v) From the rigid body analysis, find the total rigid body axial pin forces acting at the left end of each link. For the analysis described in Section 3.4, this step may be omitted.

(vi) Transform the element matrices of eq. (3.41), the initial displacement vector and velocity vector into the system oriented element co-ordinates by use of the rotation matrix R in eq. (2.26).

(vii) Find the stresses for all elements in the 'static' restrained structure. Also find the element load vector and the element geometric stiffness matrix for all elements in the system oriented element co-ordinates.

(viii) Assemble the element matrices and vectors to form the system matrices M, C^a, $K+K^N+K^G$ and K^T and the vector P (expressed in harmonics) of eq. (3.42). Also form the initial displacement and velocity vectors for the whole system from the assembly of the corresponding terms found in step (vi).

(ix) Add 'special conditions' of the mechanism to the relevant terms of the system matrices.

(x) Find the transformation matrix T defined in eq. (2.41). Also find the input torque from eq. (2.57) and add it to P.

(xi) Solve the eigenvalue problem of eq. (3.45) to find the spectral and the modal matrices for the whole system.

(xii) Transform the system matrices, vectors and 'initial conditions' into the normal co-ordinate system.

(xiii) Solve the equation of motion, eq. (3.42) (using the method of Section 3.3).

(xiv) Transform back the displacements, velocities and accelerations from normal co-ordinate system obtained in step (xiii) to the system co-ordinates.

(xv) Transforming the above quantities in element oriented element co-ordinates, find the stresses σ_{II} and σ_{III} within the elements and the nodal displacement and

velocity vectors in element oriented element co-ordinates to be used in step (vi)as 'initial conditions' for the subsequent crank position.

(xvi) If the analysis of Section 3.4 is used, find the increment in the axial forces of the elements and test the convergence criterion. If the convergence is achieved, go to the next step. Otherwise, form the incremental geometric stiffness matrix, add it to the previous stiffness matrix and go back to step (xi).

(xvii) Find the new crank position by adding the prescribed increment to the current crank angle and go back to step (iv).

Program II

The purpose of this program is to solve eq. (4.29) for the types of mechanisms cited in Chapter V. The program may be divided into the following major steps:

(i) Read the input data (consisting of geometrical, material properties etc.,'special conditions' like external loading, damping etc. and the necessary codes).

(ii) Find the angles, absolute angular velocities, square of the absolute angular velocities, absolute angular

accelerations, the absolute longitudinal and transverse accelerations of the left end of each link, all in series of harmonics of the crank angle.

(iii) Find the element matrices $\bar{m}$, $\bar{c}^a$, $\bar{k}^{\ddot{\theta}}$ and $\bar{k}^v$ (excluding the contributions of the element geometric stiffness matrix) of eq. (4.2) for each link.

(iv) From the rigid body analysis, find the harmonics of the torque at the crank end and the rigid body axial pin forces acting at the left end of each link.

(v) Find the stresses for all elements in the 'static' restrained structure. Also find the element load vector and the element geometric stiffness matrix for all elements in the element co-ordinates.

(vi) Assemble the element matrices and vectors to form the system matrices M, C^c and $(K^c + \omega^2 K^v)$ and vector P of eq. (4.4).

(vii) Add 'special conditions' of the mechanism to the relevant terms of the system matrices.

(viii) Find the constraint matrix S of eq. (4.6).

(ix) Construct the matrix $(-\omega^2 M^s + K^s)$ and the vector P^s of eq. (4.18) from eqs. (4.4) and (4.15).to (4.17).

(x) Construct the matrix S^s of eq. (4.19) from eqs. (4.6) and (4.15).

(xi) Eliminate the constraints to form the matrix A^g of eq. (4.29).

(xii) Solve eq. (4.29) for the displacement vector U^g.

(xiii) Rearrange the elements of U^g to find the displacement at each co-ordinate, expressed in series of harmonics.

(xiv) For any position of the crank, find the displacements (and accelerations) at the element co-ordinates.

(xv) Find the stresses σ_{II} and σ_{III} within the elements.

The special subroutines used by the above two programs are described here very briefly.

Routine SCSKNW

In the above programs I and II, multiplications of the harmonic series of the following kind are required very frequently.

$$\sum_{i=1}^{h_1} [a_i \cos(i-1)\theta + b_i \sin i\theta] \sum_{j=1}^{h_2} [c_j \cos(j-1)\theta + d_j \sin j\theta]$$

$$= \sum_{l=1}^{h_3} [e_l \cos(l-1)\theta + f_l \sin l\theta] \qquad (A-1)$$

where the scalars h_1, h_2, a_i, b_i ($i = 1, \ldots, h_1$) and c_j, d_j ($j = 1, \ldots, h_2$) are known. For a given value of h_3, the scalars e_l, f_l ($l = 1, \ldots, h_3$) are to be found out from the multiplication of the two harmonic series at the left side of eq. (A-1). For this purpose, a routine SCSKNW has been written which returnsthe coefficients e_l, f_l ($l = 1, \ldots, h_3$) as output after performing the indicated series multiplications (for any value of θ).

Routine SCALUN

In step (iv) of Program II, it is necessary to solve eq. (A-1) for the unknown scalars a_i, b_i ($i = 1, \ldots, h_1$) when the scalars c_j, d_j ($j = 1, \ldots, h_1$), e_l, f_l ($l = 1, \ldots, h_1$) and h_1 ($= h_2 = h_3$) are known. A routine SCALUN has been written which returns the coefficients a_i, b_i ($i = 1, \ldots, h_1$) as output (for any value of θ) after equating the coefficients of the similar harmonic terms on both sides of eq. (A-1).

Routine UNKNOW

This routine has been written to obtain the matrices M^s and K^s respectively of eq. (4.18) as output when the matrices M, C^d, C^c, K^c, K^v of eq. (4.4) and the scalar h_2 of eq. (4.15) are supplied as input. The same routine also returns the combined value of $(-\omega^2 M^s + K^s)$ of eq. (4.18 if the value of ω is supplied. For the assumed series of U in eq. (4.15), the output matrices are non-symmetric. However, by using a multiplication factor $\frac{1}{2}$ suitably, these matrices are rendered a symmetric form so that they may be used more efficiently in the numerical procedures. Needless to say that the final solution should be modified accordingly to obtain the correct results. The special features of the routine are:

(i) The routine is equally applicable if the unknown displacement vector U is expressed in the form of eq. (4.33) instead of eq. (4.15). With little alterations, the routine may be used for the stability analysis of the subharmonic and superharmonic oscillations of all orders.

(ii) The columns of the output matrices may be separated, if desired, into the following six different groups. The elements of these groups are associated with

(a) the preferred co-ordinates (these co-ordinates should form the first part of the system co-ordinates) and the preferred harmonics (i.e., a few pre-selected dominant harmonics)

(b) the preferred co-ordinates and non-preferred harmonics

(c) the non-preferred co-ordinates (excluding the preferred co-ordinates and the dependent co-ordinates) and preferred harmonics

(d) the non-preferred co-ordinates and the non-preferred harmonics

(e) the dependent co-ordinates and the preferred harmonics

(f) the dependent co-ordinates and the non-preferred harmonics.

The second feature of the routine enables to use certain numerical procedures (for example, Gauss-Seidel iteration procedure[61]) very efficiently. As this routine uses the peripheral storage facilities of a computer, it can handle very large matrices. However, in spite of large size matrices, the routine takes very little computer time as no multiplication is involved (in the real sense).

Routine UNTSTR

This routine has been written to find the matrix S^s of eq. (4.19) from eq. (4.6) by using the assumed harmonic expression eq. (4.15). With the same routine, similar matrix may be obtained corresponding to the assumed relation eq. (4.33) for the system displacement U or for other assumed relations of U corresponding to the subharmonic and super-harmonic oscillations of various orders. This routine is very similar to the routine UNKNOW and possesses the same two features. Like UNKNOW, it also takes very little computer time (as no multiplication is involved) and uses the pheripheral storage facilities.

Appendix - B

Explicit Expressions of the Element Matrices

The explicit expressions for the element stiffness matrix $\bar{k}$, element mass matrix $\bar{m}$, element force vector $\bar{p}$ and the element geometric stiffness matrix $\bar{k}^G$, given by eqs. (2.23), (2.24), (2.25) and (3.36) respectively, in the element oriented element co-ordinate system are shown in eqs. (B-1) to (B-4) respectively.

F_{Mx} in eq. (B-4) is the axial force (+ve along +ve x-direction) acting at the left-end of the element E' and $\omega_{E'}$ is its angular velocity. It may be noted that when the links are subdivided into several elements, the matrix $\bar{k}^G$ and the vector $\bar{p}$ are different for these elements even when the links are uniform.

The explicit form of the matrix $\bar{m}^a$ given by eq. (3.35), is shown in eq. (B-5).

$$\bar{m}^a = \frac{\rho A l}{120(1+\varphi)} \begin{bmatrix} 0 & & & & & \\ 72+40\varphi & 0 & & \text{antisymmetric} & & \\ (6+5\varphi)l & 0 & 0 & & & \\ 0 & -(18+20\varphi) & -(4+3\varphi)l & 0 & & \\ 18+20\varphi & 0 & 0 & 42+40\varphi & 0 & \\ -(4+5\varphi)l & 0 & 0 & -(6+5\varphi)l & 0 & 0 \end{bmatrix} \tag{B-5}$$

$$= \frac{1}{l^3(1+\varphi)} \begin{bmatrix} EAl^2 & & & & & \\ 0 & 12EI & & & \text{Symmetric} & \\ 0 & 6EIl & (4+\varphi)EIl^2 & & & \\ -EAl^2 & 0 & 0 & EAl^2 & & \\ 0 & -12EI & -6EIl & 0 & 12EI & \\ 0 & 6EIl & (2-\varphi)EI^2 & 0 & -6EIl & (4+\varphi)EIl^2 \end{bmatrix} \qquad \text{(B-1)}$$

$$= \frac{\rho Al}{840(1+\varphi)^2} \begin{bmatrix} 280(1+\varphi)^2 & & & & & \\ 0 & (312+588\varphi+280\varphi^2) & & & & \\ 0 & (44+77\varphi+35\varphi^2)l & (8+140\varphi+7\varphi^2)l^2 & & & \\ 140(1+\varphi)^2 & 0 & 0 & 280(1+\varphi)^2 & & \\ 0 & (108+252\varphi+140\varphi^2) & (26+63\varphi+35\varphi^2)l & 0 & (312+588\varphi+280\varphi^2) & \\ 0 & -(26+63\varphi+35\varphi^2)l & -(6+14\varphi+7\varphi^2)l^2 & 0 & -(44+77\varphi+35\varphi^2)l & (8+140\varphi+7\varphi^2)l^2 \end{bmatrix}$$

$$+ \frac{\rho I}{60l(1+\varphi)^2} \begin{bmatrix} 0 & & & & & \\ 0 & 72 & & & & \\ 0 & (6-30\varphi)l & (8+10\varphi+20\varphi^2)l^2 & & & \\ 0 & 0 & 0 & 0 & & \\ 0 & -72 & (-6+30\varphi)l & 0 & 72 & \\ 0 & (6-30\varphi)l & (-2-10\varphi+10\varphi^2)l^2 & 0 & (-6+30\varphi)l & (8+10\varphi+20\varphi^2)l^2 \end{bmatrix} \qquad \text{(B-2)}$$

$$\bar{p} = -\frac{\rho A l}{120(1+\varphi)} \begin{bmatrix} 20(1+\varphi)(2A_{Mx} + A_{Nx}) \\ (42+80\varphi)A_{My} + (18+20\varphi)A_{Ny} \\ (6+5\varphi)l\, A_{My} + (4+5\varphi)l\, A_{Ny} \\ 20(1+\varphi)(A_{Mx} + 2A_{Nx}) \\ (18+20\varphi)A_{My} + (42+40\varphi)A_{Ny} \\ -(4+5\varphi)l\, A_{My} - (6+5\varphi)l\, A_{Ny} \end{bmatrix} \qquad \text{(B-3)}$$

$$\bar{k}^G = \frac{-F_{Mx}}{60l(1+\varphi)^2} \begin{bmatrix} 0 & & & & & \\ 0 & (72+120\varphi+60\varphi^2) & & & & \\ 0 & 6l & (8+10\varphi+5\varphi^2)l^2 & & \text{Symmetric} & \\ 0 & 0 & 0 & 0 & & \\ 0 & -(72+120\varphi+60\varphi^2) & -6l & 0 & (72+120\varphi+60\varphi^2) & \\ 0 & 6l & -(2+10\varphi+5\varphi^2)l^2 & 0 & -6l & (8+10\varphi+5\varphi^2)l^2 \end{bmatrix}$$

$$\frac{\rho A\, A_{Mx}}{420(1+\varphi)^2}$$

$$\begin{bmatrix}
0 & & & & & \\
 & (72+120\varphi+60\varphi^2) & & & & \\
0 & (12+16\varphi+10\varphi^2)l & (4+6\varphi+5\varphi^2)l^2 & & \text{Symmetric} & \\
0 & 0 & 0 & 0 & & \\
0 & -(72+120\varphi+60\varphi^2) & -(12+16\varphi+10\varphi^2)l & 0 & (72+120\varphi+60\varphi^2) & \\
0 & -(16\varphi-10\varphi^2)l & (-2+10\varphi-5\varphi^2) & 0 & (16\varphi-10\varphi^2)l & (12+14\varphi+5\varphi^2)l^2
\end{bmatrix}$$

$$\frac{\rho Al\ \omega_{E_1}^2}{840(1+\varphi)^2}$$

$$\begin{bmatrix}
0 & & & & & \\
0 & (144+252\varphi+140\varphi^2) & & & & \\
0 & (30+49\varphi+35\varphi^2)l & (2+14\varphi+14\varphi^2)l^2 & & \text{Symmetric} & \\
0 & 0 & 0 & 0 & & \\
0 & -(144+252\varphi+140\varphi^2) & -(30+49\varphi+35\varphi^2)l & 0 & (144+252\varphi+140\varphi^2) & \\
0 & -(12+63\varphi+35\varphi^2)l & -(6+28\varphi+14\varphi^2)l^2 & 0 & (12+63\varphi+35\varphi^2)l & (36+42\varphi+14\varphi^2)l^2
\end{bmatrix}$$

(B-4)

Appendix - C

Direct Calculation of the Transformation Matrix

Introduction

A general procedure for calculating the rigid body transformation matrix of a mechanism has been outlined in Section 2.5.2. For some mechanisms, the transformation matrix may also be determined directly from the geometry. Two illustrative examples are given below for a(plane.) slider-crank and a crank-rocker mechanism.

Slider-crank mechanism

For the ν-th division of the link2(crank) of the slider-crank mechanism shown in Fig. C-1, the co-ordinates X_A,Y_A of its right-end A in the system co-ordinates X-Y are:

$$X_A = \nu \frac{L_2}{d_2} \cos\theta_2 \; ; \qquad Y_A = \nu \frac{L_2}{d_2} \sin\theta_2 \qquad (C-1)$$

where,

L_2 = length of the link 2

d_2 = total number of divisions of the link 2

ν = division number of the element

and θ_2 = angle made by the link 2 with X-axis.

Let the rotational co-ordinate of the support-end of the crank be chosen as dependent co-ordinate. Corresponding to a small increment $\delta\theta_2$ in the angle θ_2, the variations δX_A

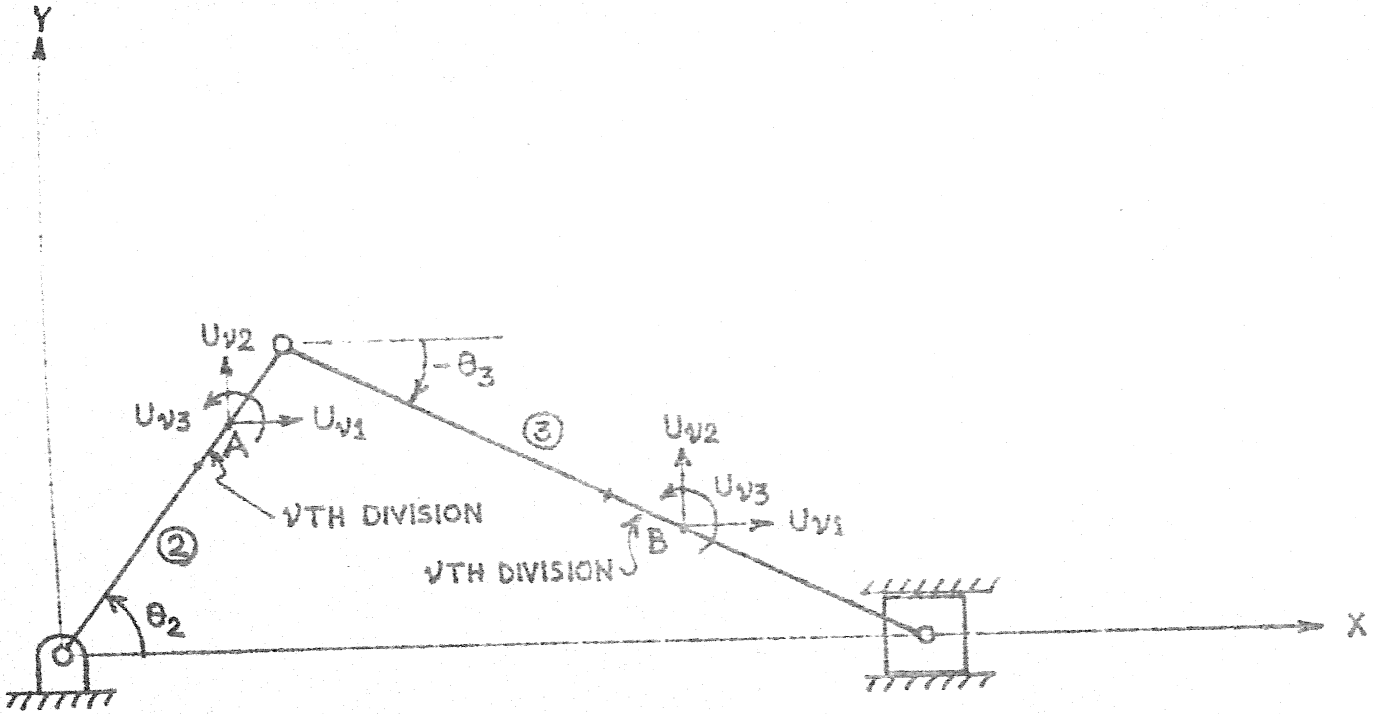

FIG C-1 SLIDER CRANK MECHANISM

and δY_A in the co-ordinates X_A, Y_A are obtained from eq. (C-1) as follows:

$$\delta X_A = - \nu \frac{L_2}{d_2} \sin\theta_2 \, \delta\theta_2 \; ; \qquad \delta Y_A = \nu \frac{L_2}{d_2} \cos\theta_2 \, \delta\theta_2 \tag{C-2}$$

For the ν-th division of the link 3 (connecting rod) shown in Fig. C-1, the co-ordinates X_B, Y_B of its right-end B in the system co-ordinates X-Y are:

$$X_B = L_2 \cos\theta_2 + \nu \frac{L_3}{d_3} \cos\theta_3 \; ; \tag{C-3}$$

$$Y_B = L_2 \sin\theta_2 + \nu \frac{L_3}{d_3} \sin\theta_3$$

where,

L_3 = length of the link 3

d_3 = total number of divisions of the link 3

and θ_3 = angle made by the link 3 with the X-axis.

Corresponding to a small increment $\delta\theta_2$ in the angle θ_2, the variations δX_B, δY_B and $\delta\theta_3$ in the co-ordinates X_B, Y_B and the angle θ_3 are obtained from eq. (C-3) as follows:

$$\delta X_B = - L_2 \sin\theta_2 \, \delta\theta_2 - \nu \frac{L_3}{d_3} \sin\theta_3 \, \delta\theta_3 \tag{C-4}$$

and

$$\delta Y_B = L_2 \cos\theta_2 \, \delta\theta_2 + \nu \frac{L_3}{d_3} \cos\theta_3 \, \delta\theta_3 \tag{C-5}$$

For the slider-crank mechanism, the following relation holds:

$$\sin\theta_3 = - \frac{L_2}{L_3} \sin\theta_2 \tag{C-6}$$

$$\text{or,} \qquad \delta\theta_3 = -\frac{L_2}{L_3}\frac{\cos\theta_2}{\cos\theta_3}\,\delta\theta_2 \tag{C-7}$$

Replacement of $\delta\theta_3$ from eqs. (C-4) and (C-5) by eq. (C-7) yields:

$$\delta X_B = \left(-L_2 \sin\theta_2 + \nu \frac{L_2}{d_3}\frac{\sin\theta_3}{\cos\theta_3}\cos\theta_2\right)\delta\theta_2 \tag{C-8}$$

$$\delta Y_B = \left(L_2 \cos\theta_2 - \nu \frac{L_2}{d_3}\cos\theta_2\right)\delta\theta_2 \tag{C-9}$$

Therefore, the elements of the transformation matrix T (defined in eq. (2.41)) corresponding to the co-ordinates $U\nu_1$, $U\nu_2$ and $U\nu_3$ at the point A are obtained from eq. (C-2) as:

$$T\nu_1 = -\nu\frac{L_2}{d_2}\sin\theta_2\,; \qquad T\nu_2 = \nu\frac{L_2}{d_2}\cos\theta_2\,; \qquad T\nu_3 = 1 \tag{C-10}$$

Similar elements of the matrix T corresponding to the co-ordinates $U\nu_1$, $U\nu_2$ and $U\nu_3$ at the point B are obtained from eqs. (C-8), (C-9) and (C-7) as follows:

$$\begin{aligned} T\nu_1 &= -L_2 \sin\theta_2 + \nu\frac{L_2}{d_3}\frac{\sin\theta_3}{\cos\theta_3}\cos\theta_2 \\ T\nu_2 &= L_2 \cos\theta_2 - \nu\frac{L_2}{d_3}\cos\theta_2 \\ T\nu_3 &= -\frac{L_2}{L_3}\frac{\cos\theta_2}{\cos\theta_3} \end{aligned} \tag{C-11}$$

Crank-rocker Mechanism

For the crank-rocker mechanism shown in Fig. C-2, the co-ordinates X_C, Y_C of the right-end C of the ν-th division of the link 4 (rocker) are:

$$X_C = L_4(-1 + \frac{\nu}{d_4})\cos\theta_4 \tag{C-12}$$

$$Y_C = L_4(-1 + \frac{\nu}{d_4})\sin\theta_4 \tag{C-13}$$

where,

L_4 = length of the link 4

d_4 = total number of divisions of the link 4

and θ_4 = angle made by the link 4 with the X-axis.

For a crank-rocker mechanism, the following relations hold(40):

$$\cos\theta_3 = \frac{(1-c_3'\cos\theta_2)(c_4'-c_5'\cos\theta_2)+c_3'c_6'\sin\theta_2\sqrt{1-(c_1'+c_2'\cos\theta_2)^2}}{(c_3')^2-2c_3'\cos\theta_2+1} \tag{C-14}$$

$$\sin\theta_3 = \frac{(1-c_3'\cos\theta_2)c_6'\sqrt{1-(c_1'+c_2'\cos\theta_2)^2}-c_3'\sin\theta_2(c_4'-c_5'\cos\theta_2)}{(c_3')^2-2c_3'\cos\theta_2+1} \tag{C-15}$$

$$\cos\theta_4 = -\cos\theta_3(c_1'+c_2'\cos\theta_2)+\sin\theta_3\sqrt{1-(c_1'+c_2'\cos\theta_2)^2} \tag{C-16}$$

$$\sin\theta_4 = -\sin\theta_3(c_1'+c_2'\cos\theta_2) - \cos\theta_3\sqrt{1-(c_1'+c_2'\cos\theta_2)^2} \tag{C-17}$$

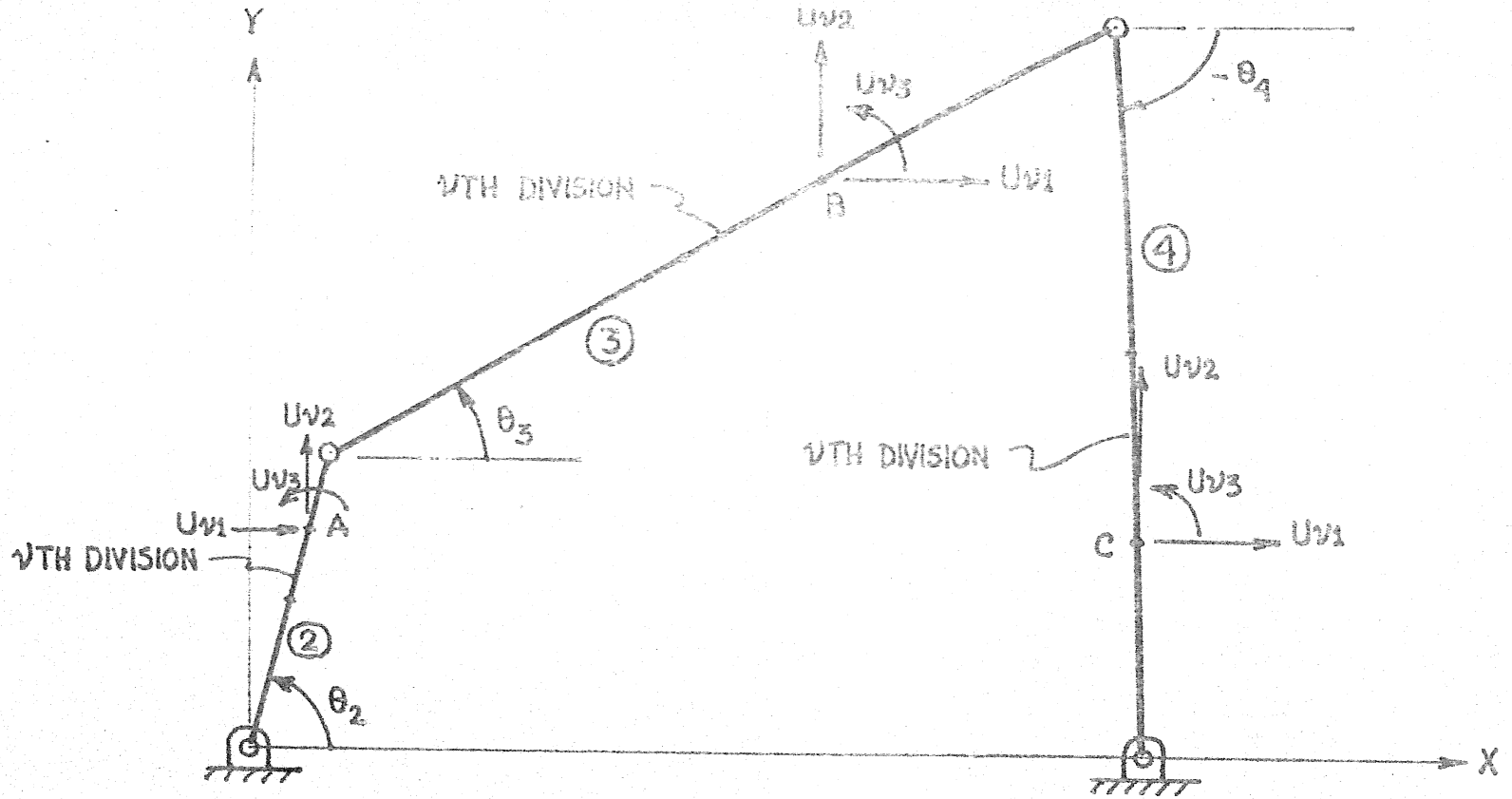

FIG C-2 CRANK-ROCKER MECHANISM

$$L_2 \sin\theta_2 + L_3 \sin\theta_3 + L_4 \sin\theta_4 = 0 \qquad \text{(C-18)}$$

$$L_2 \cos\theta_2 + L_3 \cos\theta_3 + L_4 \cos\theta_4 = L_1 \qquad \text{(C-19)}$$

where,

$$c_1' = \frac{L_3^2 + L_4^2 - L_2^2 - L_1^2}{2L_3L_4}$$

$$c_2' = \frac{L_1L_2}{L_3L_4}$$

$$c_3' = \frac{L_2}{L_1} \qquad \text{(C-20)}$$

$$c_4' = \frac{L_2^2 + L_3^2 - L_4^2 + L_1^2}{2L_1L_3}$$

$$c_5' = \frac{L_2}{L_3}$$

$$c_6' = \frac{L_4}{L_1}$$

Corresponding to a small increment $\delta\theta_2$ in θ_2, variations $\delta\theta_3$ and $\delta\theta_4$ in the angles θ_3 and θ_4 respectively are obtained from eqs. (C-18) and (C-19) as follows:

$$\delta\theta_3 = -\frac{L_2}{L_3}\frac{\sin(\theta_2 - \theta_4)}{\sin(\theta_3 - \theta_4)}\delta\theta_2 \qquad \text{(C-21)}$$

$$\delta\theta_4 = \frac{L_2}{L_4}\frac{\sin(\theta_2 - \theta_3)}{\sin(\theta_3 - \theta_4)}\delta\theta_2 \qquad \text{(C-22)}$$

Substitution of $\delta\theta_3$, obtained from eq. (C-21), in eqs. (C-4) and (C-5) yields

$$\delta X_B = (- L_2 \sin\theta_2 - \nu \frac{L_3}{d_3} \sin\theta_3 \gamma') \delta\theta_2 \qquad (C-23)$$

$$\delta Y_B = (L_2 \cos\theta_2 + \nu \frac{L_3}{d_3} \cos\theta_3 \gamma') \delta\theta_2 \qquad (C-24)$$

where $$\gamma' = - \frac{L_2}{L_3} \frac{\sin(\theta_2 - \theta_4)}{\sin(\theta_3 - \theta_4)} \qquad (C-25)$$

Corresponding to a small increment $\delta\theta_2$ in the crank angle θ_2, the variations δX_C and δY_C in X_C and Y_C respectively are obtained from eqs. (C-12), (C-13) and (C-22) as follows:

$$\delta X_C = - L_4(- 1 + \frac{\nu}{d_4}) \sin\theta_4 \gamma'' \delta\theta_2 \qquad (C-26)$$

$$\delta Y_C = L_4(- 1 + \frac{\nu}{d_4}) \cos\theta_4 \gamma'' \delta\theta_2 \qquad (C-27)$$

where $$\gamma'' = \frac{L_2}{L_4} \frac{\sin(\theta_2 - \theta_3)}{\sin(\theta_3 - \theta_4)} \qquad (C-28)$$

Thus, the elements of the transformation matrix T corresponding to the co-ordinates at the points A, B, and C are given by eqs. (C-10), (C-29) and (C-30) respectively.

$$T_{\nu 1} = - L_2 \sin\theta_2 - \nu \frac{L_3}{d_3} \sin\theta_3 \gamma'$$

$$T_{\nu 2} = L_2 \cos\theta_2 + \nu \frac{L_3}{d_3} \cos\theta_3 \gamma' \qquad (C-29)$$

$$T_{\nu 3} = \gamma'$$

$$T\nu_1 = -L_4\left(-1 + \frac{\nu}{d_4}\right) \sin\theta_4 \; \gamma''$$

$$T\nu_2 = L_4\left(-1 + \frac{\nu}{d_4}\right) \cos\theta_4 \; \gamma'' \qquad \text{(C-30)}$$

$$T\nu_3 = \gamma''$$

The arrangement of these elements in the matrix T in accordance with the numbering of the system co-ordinates may be conveniently done by using the integer matrix NS.

Appendix - D

Rigid Body Analysis

Procedures for direct kinematic analysis as well as static-force analysis of a slider-crank mechanism and a crank-rocker mechanism are outlined below. Since the mechanisms are considered to be composed of rigid links only, it is convenient to use minimum number of co-ordinates for each link, i.e., to treat each hinge-joined link as a truss member.

Slider-crank Mechanism

For the slider-crank mechanism shown in Fig. C-1, the absolute angular velocity $\dot{\theta}_3$ and angular acceleration $\ddot{\theta}_3$ of the connecting rod are determined by differentiating eq. (C-6) with respect to time:

$$\dot{\theta}_3 = -\frac{L_2}{L_3}\frac{\cos\theta_2}{\cos\theta_3}\dot{\theta}_2 \tag{D-1}$$

$$\ddot{\theta}_3 = \frac{L_2 \sin\theta_2 \dot{\theta}_2^2 + L_3 \sin\theta_3 \dot{\theta}_3^2}{L_3 \cos\theta_3} \tag{D-2}$$

where $\dot{\theta}_2$ is the uniform angular velocity of the crank.

The piston acceleration α_4 is[88]

$$\alpha_4 = -\dot{\theta}_2^2 L_2 \left[\cos\theta_2 + \frac{\underline{n}^2 \cos 2\theta_2 + \sin^4\theta_2}{(\underline{n}^2 - \sin^2\theta_2)^{3/2}}\right] \tag{D-3}$$

where $\underline{n} = \frac{L_3}{L_2}$.

The following analytical expression(5) for the gas force F_G (acting on the position) may be assumed:

$$F_G = -\dot{\theta}_2^2 M_3 L_2 (3.75 - 1.25 \cos\theta_2 - 5 \cos\theta_3) \qquad (D-4)$$

where M_3 is the mass of the link 3 (connecting rod).

The standard shape function for a truss member E' (Fig. D-1a) is

$$a = \begin{bmatrix} 1-\xi & \zeta & \xi & -\zeta \\ 0 & 1-\xi & 0 & \xi \end{bmatrix} \qquad (D-5)$$

where ξ and ζ are as defined in eq. (2.13).

Using this shape function in eq. (2.25), the statically equivalent modal forces due to the rigid body inertia forces acting on the member E' are:

$$\begin{bmatrix} \bar{p}_1 \\ \bar{p}_2 \\ \bar{p}_3 \\ \bar{p}_4 \end{bmatrix} = -\frac{M_{E'}}{6} \begin{bmatrix} 2A_{Mx} + A_{Nx} \\ 2A_{My} + A_{Ny} \\ A_{Mx} + 2A_{Nx} \\ A_{My} + 2A_{Ny} \end{bmatrix} \qquad (D-6)$$

where $M_{E'}$ is the mass of the member E' and A_{Mx}, A_{Nx}, A_{My} and A_{Ny} are as defined in Section 2.3.

For the uniformly rotating crank:

$$A_{Mx} = A_{My} = A_{Ny} = 0 \quad \text{and} \quad A_{Nx} = -\dot{\theta}_2^2 L_2$$

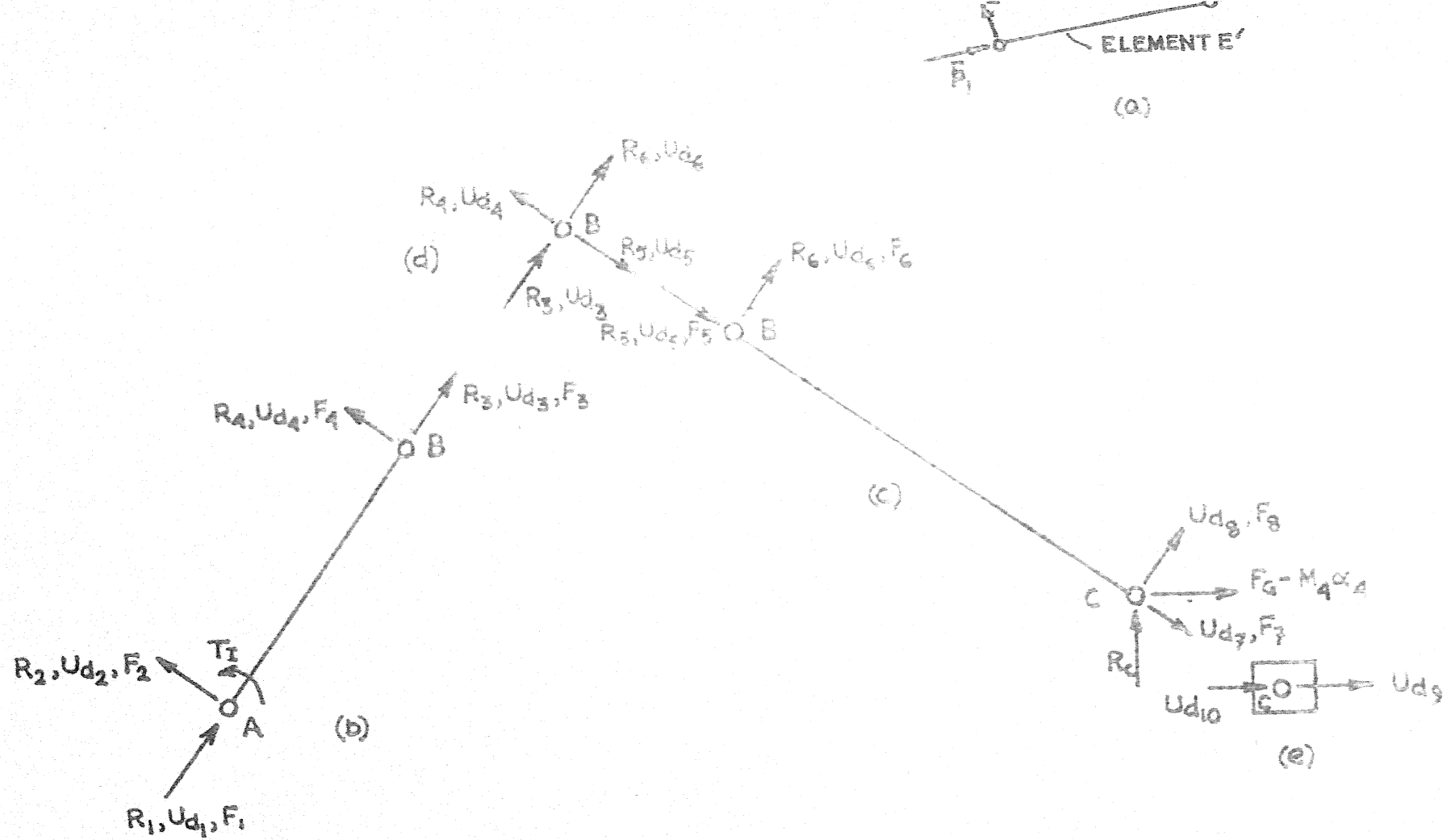

FIG D-1 FORCES IN A SLIDER CRANK MECHANISM

For the connecting rod:

$$A_{Mx} = -\dot{\theta}_2^2 L_2 \cos(\theta_2 - \theta_3) \; ; \qquad A_{Nx} = \alpha_4 \cos\theta_3$$
$$A_{My} = -\dot{\theta}_2^2 L_2 \sin(\theta_2 - \theta_3) \; ; \qquad A_{Ny} = -\alpha_4 \sin\theta_3 \qquad \text{(D-8)}$$

Using eqs. (D-7) and (D-8) in eq. (D-6), the nodal forces F_1 to F_8 (shown in Fig. D-1) are obtained. From the free-body diagrams of the crank (Fig. D-1b) and the connecting rod together with the piston (Fig. D-1c), the following equations result:

$$\begin{aligned} F_1 + F_3 + R_1 + R_3 &= 0 \\ F_2 + F_4 + R_2 + R_4 &= 0 \\ T_I + (R_4 + F_4)L_2 &= 0 \\ F_6 + R_6 &= 0 \end{aligned} \qquad \text{(D-9)}$$

and $$R_5 \cos\theta_3 = -F_G + M_4\alpha_4 - (F_5 + F_7)\cos\theta_3 + F_8 \sin\theta_3$$

where T_I is the output torque at the crank end and R_1 to R_6 are pin reactions on the links as shown in Fig. D-1b and c. From the compatibility of the internal forces at the hinged joint B (Fig. D-1d), the following relations are

$$\begin{aligned} R_3 &= -R_5 \cos(\theta_2 - \theta_3) - R_6 \sin(\theta_2 - \theta_3) \\ R_4 &= R_5 \sin(\theta_2 - \theta_3) - R_6 \cos(\theta_2 - \theta_3) \end{aligned} \qquad \text{(D-10)}$$

After elimination of the unknowns R_2, R_3, R_4 and R_6 from the eqs. (D-9) and (D-10), the desired axial rigid

body pin forces R_1, R_5 and the torque T_I are finally obtained.

Crank-rocker mechanism.

The absolute angular velocities $\dot{\theta}_3$ and $\dot{\theta}_4$ of the coupler and the rocker respectively of the mechanism shown in Fig. C-2 are obtained in eqs. (D-11) and (D-12), after dividing eqs. (C-21) and (C-22) by $\delta\tau$.

$$\dot{\theta}_3 = \gamma' \dot{\theta}_2 \qquad \text{(D-11)}$$

$$\dot{\theta}_4 = \gamma'' \dot{\theta}_2 \qquad \text{(D-12)}$$

where γ', γ'' are defined in eqs. (C-25), (C-28) and $\dot{\theta}_2$ is the uniform angular velocity of the crank.

Upon differentiation of eqs. (D-11) and (D-12) with respect to time, the absolute angular accelerations $\ddot{\theta}_3$ and $\ddot{\theta}_4$ of the coupler and the rocker respectively are given by eqs. (D-13) and (D-14).

$$\ddot{\theta}_3 = -\frac{L_2\dot{\theta}_2^2 \cos(\theta_2-\theta_4) + L_3\dot{\theta}_3^2 \cos(\theta_3-\theta_4) - L_4\dot{\theta}_4^2}{L_3 \sin(\theta_3-\theta_4)} \qquad \text{(D-13)}$$

$$\ddot{\theta}_4 = -\frac{L_2\dot{\theta}_2^2 \cos(\theta_2-\theta_3) - L_4\dot{\theta}_4^2 \cos(\theta_3-\theta_4) + L_3\dot{\theta}_3^2}{L_4 \sin(\theta_3-\theta_4)} \qquad \text{(D-14)}$$

The nodal forces F_1 to F_{12} (Fig. D-2) may be obtained from eq. (D-6) when the following relations are used.

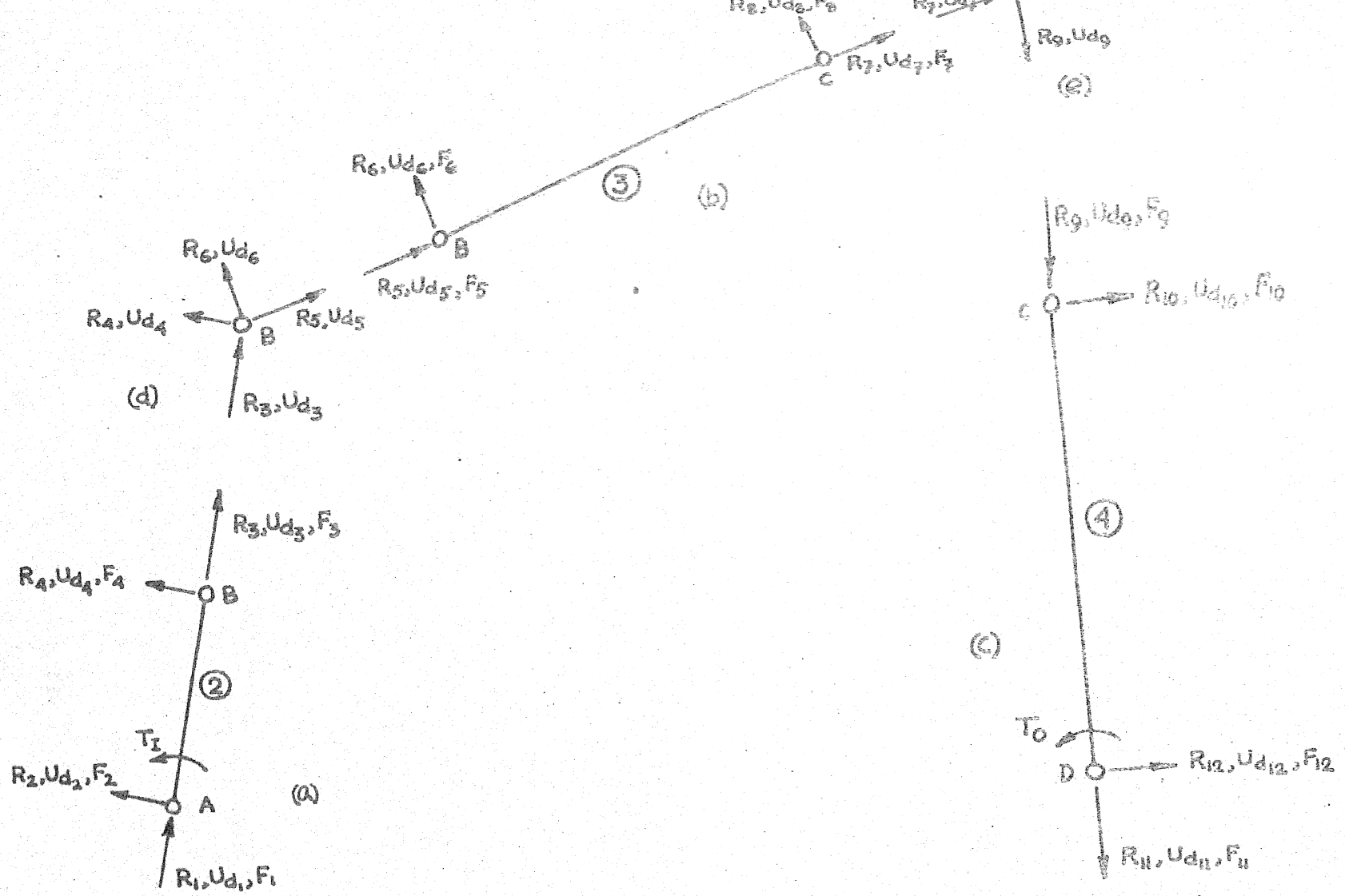

FIG D-2 FORCES IN A CRANK-ROCKER MECHANISM

For the crank: $A_{Mx} = A_{My} = A_{Ny} = 0$ and $A_{Nx} = -\dot{\theta}_2^2 L_2$ (D-15)

For the coupler:

$$A_{Mx} = -\dot{\theta}_2^2 L_2 \cos(\theta_2 - \theta_3); \quad A_{Nx} = A_{Mx} - \dot{\theta}_3^2 L_3$$

$$A_{My} = -\dot{\theta}_2^2 L_2 \sin(\theta_2 - \theta_3); \quad A_{Ny} = A_{My} + \ddot{\theta}_3 L_3 \qquad \text{(D-16)}$$

For the rocker: $A_{Mx} = \dot{\theta}_4^2 L_4$; $A_{My} = -\ddot{\theta}_4 L_4$; $A_{Nx} = A_{Ny} = 0$ (D-17)

From the free-body diagrams of the links 2, 3 and 4 (Fig. D-2a to c), the following equations are obtained:

$$\begin{aligned}
R_1 + R_3 + F_1 + F_3 &= 0 \\
R_2 + R_4 + F_2 + F_4 &= 0 \\
T_I + (R_4 + F_4)L_2 &= 0 \\
R_5 + R_7 + F_5 + F_7 &= 0 \\
R_8 + F_8 &= 0 \\
R_6 + F_6 &= 0 \\
T_O - (R_{10} + F_{10})L_4 &= 0
\end{aligned} \qquad \text{(D-18)}$$

where R_1 to R_8 are the pin reactions on the links and T_I, T_O are the torques at the crank and rocker ends as shown in Fig. D-2. The compatibility equations for the internal forces at the hinged joints may be written from Fig. D-2d and Fig. D-2e

$$
\begin{aligned}
R_3 &= -R_5 \cos(\theta_2-\theta_3) - R_6 \sin(\theta_2-\theta_3) \\
R_4 &= R_5 \sin(\theta_2-\theta_3) - R_6 \cos(\theta_2-\theta_3) \\
R_7 &= -R_9 \cos(\theta_3-\theta_4) - R_{10} \sin(\theta_3-\theta_4) \\
R_8 &= R_9 \sin(\theta_3-\theta_4) - R_{10} \cos(\theta_3-\theta_4)
\end{aligned}
\qquad \text{(D-19)}
$$

Assuming that T_0 is known, the desired pin forces R_1, R_5, R_9 and the torque T_I may be obtained by solving eqs. (D-18) and (D-19).

Appendix - E

Expressions for Harmonic Analysis and Constraint Equations

Slider-crank mechanism

Using the same symbols of Appendix C, the relevant harmonic expressions, correct up to $\frac{1}{n^{10}}$, are:

$$\cos\theta_3 = (1-a_1-3a_2-35a_4-126a_5) + (a_1+4a_2+15a_3+56a_4+210a_5)\cos2\theta_2 - (a_2+6a_3+28a_4+120a_5)\cos 4\theta_2 + (a_3+8a_4+45a_5)\cos6\theta_2 - (a_4+10a_5)\cos8\theta_2 + a_5\cos10\theta_2 \qquad (E-1)$$

$$\dot{\theta}_3^2 = \dot{\theta}_2^2 [(2a_1+8a_2+32a_3+128a_4+512a_5) + (2a_1-16a_3-102.4a_4-512a_5)\cos2\theta_2 - (8a_2+32a_3+102.4a_4+292.5714a_5)\cos4\theta_2$$

where $a_1 = \frac{1}{4\underline{n}^2}$; $a_2 = \frac{1}{64\underline{n}^4}$; $a_3 = \frac{1}{512\underline{n}^6}$; $a_4 = \frac{5}{(128)^2\underline{n}^8}$ and

$$a_5 = \frac{14}{(512)^2\underline{n}^{10}} \qquad \text{(E-5)}$$

Constraint equations for a slider crank mechanism

From the compatibility of the displacements at the hinged joint B (Fig. D-1d) and at the piston position C (Fig. D-1e), the following equations result:

$$U_{d_3} - U_{d_5}\cos(\theta_2-\theta_3) - U_{d_6}\sin(\theta_2-\theta_3) = 0 \qquad \text{(E-6)}$$

$$U_{d_4} + U_{d_5}\sin(\theta_2-\theta_3) - U_{d_6}\cos(\theta_2-\theta_3) = 0 \qquad \text{(E-7)}$$

$$U_{d_6} + U_{d_5}\frac{\sin\theta_3}{\cos\theta_3} = 0 \qquad \text{(E-8)}$$

$$
\begin{array}{cccccccc}
\cdot\ d_5 & \cdots & d_6 & \cdots\ d_7 & \cdots & d_3\ d_4 & d_8 & d_{10} \\
\cdot\cos(\theta_3-\theta_3) & -\sin(\theta_2-\theta_3) & 0 & & & 1\ 0 & 0 & 0 \\
\sin(\theta_2-\theta_3) & -\cos(\theta_2-\theta_3) & 0 & & & 0\ 1 & 0 & 0 \\
0 & 0 & \frac{\sin\theta_3}{\cos\theta_3} & & & 0\ 0 & 1 & 0 \\
- \quad 0 & 0 & -\frac{1}{\cos\theta_3} & & & 0\ 0 & 0 & 1
\end{array}
\begin{bmatrix} \\ \\ U_X \\ \\ \end{bmatrix} = 0 \qquad \text{(E-11)}
$$

where $U_X = \{..U_{d_5}..U_{d_6}..U_{d_7}..U_{d_3}, U_{d_4}, U_{d_8}, U_{d_{10}}\}$.

$$
\begin{array}{cccccccc}
.. \ U_{d_5} & \cdots & U_{d_6} & \cdots & U_{d_9} & \cdots & U_{d_{10}} \cdots & U_{d_3}\ U_{d_4}\ U_{d_7}\ U_{d_8} \\
-\cos(\theta_2-\theta_3) & -\sin(\theta_2-\theta_3) & 0 & & 0 & & & 1\ 0\ 0\ 0 \\
\sin(\theta_2-\theta_3) & -\cos(\theta_2-\theta_3) & 0 & & 0 & & & 0\ 1\ 0\ 0 \\
0 & 0 & -\cos(\theta_3-\theta_4) & & -\sin(\theta_3-\theta_4) & & & 0\ 0\ 1\ 0 \\
0 & 0 & \sin(\theta_3-\theta_4) & & -\cos(\theta_3-\theta_4) & & & 0\ 0\ 0\ 1
\end{array}
\begin{bmatrix} \\ \\ U_Y \\ \\ \end{bmatrix} = 0
$$

(E-21)

where $U_Y = \{..U_{d_5}..U_{d_6}..U_{d_9}..U_{d_{10}}..U_{d_3}, U_{d_4}, U_{d_7}, U_{d_8}\}$.

Fourier series expressions for the fractional terms in eq. (E-11) are:

$$\frac{\sin\theta_3}{\cos\theta_3} = \frac{1}{n}\left[(1+1.5a_1+15a_2+87.5a_3+401a_4)\sin\theta_2 - (0.5a_1+7.5a_2 +52.5a_3+294a_4)\sin3\theta_2 + (1.5a_2+17.5a_3+126a_4)\sin5\theta_2 - (2.5a_3+31.5a_4)\sin7\theta_2 + 3.5a_4 \sin9\theta_2\right] \quad \text{(E-12)}$$

$$\frac{1}{\cos\theta_3} = (1+a_1+9a_2+50a_3+245a_4+1134a_5) - (a_1+12a_2+75a_3+392a_4+1890a_5)\cos2\theta_2 + (3a_2+30a_3+196a_4+1080a_5)\cos4\theta_2 - (5a_3+56a_4+405a_5)\cos6\theta_2 + (7a_4+90a_5)\cos8\theta_2 - 9a_5 \cos10\theta_2 \quad \text{(E-13)}$$

where a_1 to a_5 are as defined in eq. (E-5).

Crank-rocker mechanism

The following series expressions result[33] from the theory of complex variables:

$$\frac{\cos\theta_2 + C_3'}{(C_3')^2 + 2C_3'\cos\theta_2 + 1} = \sum_{i=1}^{\infty} (-C_3')^{i-1} \cos i\theta_2), \quad (C_3'^2 < 1)$$

$$\frac{\sin\theta_2}{(C_3')^2 + 2C_3'\cos\theta_2 + 1} = \sum_{i=1}^{\infty} (-C_3')^{i-1} \sin i\theta_2 \quad (C_3'^2 < 1) \quad \text{(E-14)}$$

Since $\frac{C_2'}{1+C_1'}$ and $\frac{C_2'}{1-C_1'}$ are less than unity, the following equation is obtained from binomial expansions.

$$\sqrt{1-(C_1'+C_2'\cos\theta_2)^2} = \sqrt{1-C_1'^2}\,(1+\frac{C_2'}{C_1'+1}\cos\theta_2)^{\frac{1}{2}}\,(1+\frac{C_2'}{C_1'-1}\cos\theta_2)^{\frac{1}{2}}$$

$$= \sqrt{1-C_1'^2}\sum_{i=1}^{h_1}\sum_{j=1}^{h_1} d_i^1 d_j^2 \cos^{i+j-2}\theta_2 \qquad (E\text{-}15)$$

where,

$$d_1^1 = d_1^2 = 1$$

$$d_i^1 = (\tfrac{1}{2}\cdot\tfrac{-\frac{1}{2}}{2!}\cdots \text{ up to } i-1 \text{ terms})\,(\frac{C_2'}{C_1'+1})^{i-1}, \quad i>1 \qquad (E\text{-}16)$$

$$d_j^2 = (\tfrac{1}{2}\cdot\tfrac{-\frac{1}{2}}{2!}\cdots \text{ up to } j-1 \text{ terms})\,(\frac{C_2'}{C_1'-1})^{j-1}, \quad j>1$$

and h_1 is as defined in eq. (2.87).

Using the following trigonometrical identity[89]

$$2^{n-1}\cos^n\theta = \cos n\theta + n\cos(n-2)\theta + \frac{n(n-1)}{2!}\cos(n-4)\theta + \cdots$$

$$\cdots + \frac{\lfloor n\ \cos\theta}{\lfloor\frac{1}{2}(n-1)\ \lfloor\frac{1}{2}(n+1)} \quad \text{for } n = \text{odd}$$

$$\cdots + \tfrac{1}{2}\frac{\lfloor n}{(\lfloor\frac{n}{2})^2} \quad \text{for } n = \text{even} \qquad (E\text{-}17)$$

in eq. (E-15), the following Fourier series expression is obtained:

$$\sqrt{1 - (C_1' + C_2' \cos\theta_2)^2} = \sum_{j=1}^{h_1} d_j^3 \cos(j-1)\theta_2 \qquad \text{(E-18)}$$

where d_j^3, $j = 1, \ldots h_1$ are known functions of C_1' and C_2'.

Use of eqs. (E-14) and (E-18) in eqs. (C-14) to (C-17) and multiplications of the series yield the harmonic expressions[40] for the angles in the following forms:

$$\cos\theta_3 = \sum_{j=1}^{h_1} [d_j^4 \cos(j-1)\theta_2 + d_j^5 \sin j\theta_2]$$

$$\sin\theta_3 = \sum_{j=1}^{h_1} [d_j^6 \cos(j-1)\theta_2 + d_j^7 \sin j\theta_2] \qquad \text{(E-19)}$$

$$\cos\theta_4 = \sum_{j=1}^{h_1} [d_j^8 \cos(j-1)\theta_2 + d_j^9 \sin j\theta_2]$$

$$\sin\theta_4 = \sum_{j=1}^{h_1} [d_j^{10} \cos(j-1)\theta_2 + d_j^{11} \sin j\theta_2]$$

where d_j^4 to d_j^{11}, $j = 1, \ldots h_1$ are known co-efficients.

Constraint equations for a crank-rocker mechanism

Compatibility of the displacements at the hinged joints B and C (Fig. D-2d and D-2e) yields the following equations:

$$U_{d_3} - U_{d_5} \cos(\theta_2 - \theta_3) - U_{d_6} \sin(\theta_2 - \theta_3) = 0$$

$$
\begin{aligned}
U_{d_4} + U_{d_5} \sin(\theta_2-\theta_3) - U_{d_6} \cos(\theta_2-\theta_3) &= 0 \\
U_{d_7} - U_{d_9} \cos(\theta_3-\theta_4) - U_{d_{10}} \sin(\theta_3-\theta_4) &= 0 \\
U_{d_8} + U_{d_9} \sin(\theta_3-\theta_4) - U_{d_{10}} \cos(\theta_3-\theta_4) &= 0
\end{aligned}
\qquad \text{(E-20)}
$$

where U_{d_1} to $U_{d_{10}}$ are nodal displacements as shown in Fig. D-2. Considering U_{d_3}, U_{d_4}, U_{d_7} and U_{d_8} as displacements at the dependent co-ordinates, the constaint equation for a crank-rocker mechanism, obtained from eq. (E-20), is written in eq. (E-21) (shown just after eq. (E-11)).

The harmonic series expressions for the rigid body axial forces and the balancing torque at the crank end may be obtained from the rigid body analysis of these two mechanisms as described in Appendix D. For this purpose, the special routine SCSKNW, described in Appendix A, has to be extensively used for the multiplications of the harmonic series involved in the calculations. In the process of eliminating the unknowns, it is further necessary to use another special routine SCALUN described in Appendix A (for example, to find out the harmonic series expression for the reaction R_5 from the last equation of eq. (D-9)).

It may be noted that it is also necessary to use the same routine SCSKNW repeatedly in the analysis procedures described in Section 2.7, and in Subsections 4.2.1, eqs. (E-11) and (E-21).

Appendix - F

Solution of Large Eigenvalue Problems

An efficient iterative procedure for large generalised eigenvalue problems has been outlined in Ref. (90) which uses generalised Ritz method along with subspace iterations. Without going into the theories involved, the necessary steps of the procedure are given below.

Let the undamped generalised eigenvalue problem be given by eq. (F-1)

$$K \Phi = M \Phi \Omega^2 \qquad (F-1)$$

where,

K = stiffness matrix of size n X n (say)

M = mass matrix of size n X n

Ω^2 = m X m a diagonal spectral matrix whose principal diagonals are squares of the lowest eigen-frequencies (m numbers)

and Φ = n X m modal matrix whose columns are the eigen-vectors of the system.

Starting with an initial modal matrix Φ_o, the iteration scheme is:

i) Find $\overline{\Phi}_i$ by solving eq. (F-2)

$$K\overline{\Phi}_i = M\Phi_{i-1} \Omega^2_{i-1} \qquad (F-2)$$

$$(i = 1,2,3,....)$$

ii) Calculate

$$K_i = \bar{\Phi}_i^t K \bar{\Phi}_i \; ; \qquad M_i = \bar{\Phi}_i^t M \bar{\Phi}_i \tag{F-3}$$

iii) Solve for the following reduced eigensystem

$$K_i Q_i = M_i Q_i \Omega_i^2 \tag{F-4}$$

(where Q_i is the modal matrix corresponding to the reduced eigenvalue problem in eq. (F-4))to find Q_i and Ω_i^2.

iv) Find an improved approximation to the eigenvectors

$$\Phi_i = \bar{\Phi}_i Q_i \tag{F-5}$$

v) Stop if the convergence is achieved; otherwise replace i by i+1 and go back to step (i).

For efficient calculation of step (i), the matrix K is decomposed in two triangular matrices by Choleski's metho of decomposition[61]. Moreover, the eigenvalue problem defined by eq. (F-4) is to be solved for all eigenvalues and eigenvectors. For this purpose, direct methods (i.e., generalised Jacobi's method, Rutishauser's method etc.) are suitable compared to the iterative Power method.

The procedure of choosing a good modal matrix Φ_o and a suitable convergence criterion is mentioned in Ref. (90 and therefore is not repeated here.

It may be noted that, by virtue of the application of Ritz's analysis[64], the iterations converge very rapidly (usually within eight iterations) for the lowest frequencies if the eigenvectors are orthogonal. When K and M are both symmetric, the eigenvectors are mutually orthogonal with respect to K or M. However, following the method of analysis presented in Chapter IV, the mass matrix M^g in eq. (4.32) becomes asymmetric and the stiffness matrix K^g in the same equation, though still remains symmetric, is singular due to the presence of the rigid body degrees of freedom. In view of these special features of the matrices M^g and K^g, the above iterative procedure should be implemented along with the following modifications.

Assuming a single degree of freedom mechanism, the total number of the dependent rows (or columns) in K^g of eq. (4.32) is $w_1 = 2h_2 + 1$, h_2 being already defined in eq. (4.15). Let eq. (4.32) be partitioned in the following way.

$$-\omega^2 \begin{bmatrix} M^g_{AA} & M^g_{AB} \\ M^g_{BA} & M^g_{BB} \end{bmatrix} \begin{bmatrix} U^g_A \\ U^g_B \end{bmatrix} + \begin{bmatrix} K^g_{AA} & K^g_{AB} \\ K^g_{BA} & K^g_{BB} \end{bmatrix} \begin{bmatrix} U^g_A \\ U^g_B \end{bmatrix} = 0 \qquad (F-6)$$

Denoting the number of elements present in U^g of eq. (4.32) by $n_1 = (2h_2 + 1)(n-c)$, the number of elements in U^g_A and U^g_B are equal to $n_2 = n_1 - w_1$ and w_1 respectively (h_2, n and c are defined in Chapter IV). The matrices

M^g_{AA}, K^g_{AA} etc. are the partioned blocks of M^g and K^g whose dimensions ensure the matrix multiplications in eq. (F-6). Following the procedure described in Section 2.5.2, the eigenvalue problem, defined in eq. (4.32), may be reduced to eq. (F-7).

$$(-\omega^2 M^x + K^x)U^x = 0 \tag{F-7}$$

where,

$$\begin{aligned} K^x &= K^g_{AA} \\ M^x &= M^g_{AA} + (M^g_{AA}T_g + M^g_{AB})(I - T^*_g T_g)^{-1} T^*_g \\ T^*_g &= -(T^t_g M^g_{AB} + M^g_{BB})^{-1} (T^t_g M^g_{AA} + M^g_{BA}) \\ U^x &= U^g_A - T_g U^g_B \end{aligned} \tag{F-8}$$

and the rigid body transformation matrix T_g is defined by the following relation:

$$K^g_{AA}T_g + K^g_{AB} = 0 \tag{F-9}$$

The matrix K^x in eq. (F-7) is non-singular and therefore may be decomposed into two triangular matrices. Since the above mentioned iterative procedure performs iterations for the m numbers of eigenvalues and eigenvectors simultaneously, eq. (F-7) is rewritten in the form of eq. (F-1) as follows:

$$K^x \phi = M^x \phi \Omega^2$$

where Φ is the n_2 X m modal matrix and Ω^2 is the m X m (diagonal) spectral matrix as defined in eq. (F-1).

Since the matrix M^X in eq. (F-10) is asymmetric, the eigenvectors in the modal matrix Φ may not be orthogonal with respect to K^X or M^X. Consequently, the convergence may be slow if the iterative procedure is directly applied to eq. (F-10). To overcome this difficulty, the iteration procedure should be carried out in two different phases.

In the first phase, the iteration may be started by considering only the upper half of the matrix M^X and then making its lower half equal to this upper half. This modification renders the matrix M^X a symmetric form. Next, steps (i) to (v) of the iteration procedure should be carried out until a moderate convergence criterion is satisfied. Since the factors contributing to the asymmetry of M^X are small compared to the basic symmetric property of M^X, it is expected that the eigenvalues and eigenvectors thus obtained are fairly close to the desired actual quantities.

The second phase of iterations begins with the actual form of the matrix M^X in eq. (F-10) together with the eigenvalues and eigenvectors obtained at the end of the first phase of iterations. Instead of using subspace iterations, the second phase consists of inverse iteration in the original space of dimension n_2 and evaluation of

Rayleigh's quotients in each iteration. The relevant steps of the second phase of iterations are:

(vi) Find Φ_i by solving eq. (F-11)

$$K^x \Phi_i = M^x \Phi_{i-1} \Omega^2_{i-1} \tag{F-11}$$

vii) Calculate Rayleigh's quotients

$$\Omega^2_{i,j} = \frac{\Phi^t_{i,j} K \Phi_{i,j}}{\Phi^t_{i,j} M \Phi_{i,j}} \tag{F-12}$$

where $\Phi_{i,j}$ and $\Omega^2_{i,j}$ denote the j-th column of Φ_i and j-th diagonal of Ω^2_i respectively, j = 1, ... m.

viii) Stop if convergence is achieved; otherwise replace i by i+1 and go back to step (vi).

ix) Find the modal matrix for eq. (F-6) by applying the last relation of eq. (F-8) to the modal matrix obtained at the end of the second phase of iteration. (an equation similar to eq. (2.53) may be easily deduced for this purpose).

While the rapidity of the convergence rate in the first phase of iteration largely depends on the orthogonality of the modes obtained from step (iii), similar rapidity in the second phase depends only on the good estimates of Φ_i and Ω^2_i (it does not require any orthogonality between the modes for rapid convergence). As a good estimate of Φ_i and

ω_i^2 is obtained from the first phase of iteration, the inverse iteration in step (vi) converges very quickly (usually in 3 to 4 iterations[64]). The faster rate of convergence in step (vi) is further enhanced by the quadratic rate of convergence of the method of Rayleigh's quotients in step (vii).

The size of the matrices K^g and M^g being fairly large, peripheral storage facilities of a computer may have to be used if the high speed storage capacity is very limited. In that case, the change-over of M^x from symmetry to asymmetry in the two phases of iteration does not demand any extra location in the core memory.

In the context of the specialities of the matrices involved, the above scheme appears to be more efficient than the popular practice adopted for asymmetric matrices, i.e., successive applications of Power method, inverse iteration of Wielandt and deflation procedure[91].